Effect of nanoclay addition on the mechanical properties of glass fibre reinforced epoxy nanocomposites processed through VARIM

A Dissertation submitted

in partial fulfillment of the requirements

for the degree of

Master of Engineering

in

Production Engineering

by

Daksh Shelly

Regd. No. 801482005

Under the supervision of:

Dr. Tarun Nanda
Assistant Professor, MED,
Thapar University, Patiala

Dr. Rajeev Mehta
Professor, CHED
Thapar University, Patiala

MECHANICAL ENGINEERING DEPARTMENT

THAPAR UNIVERSITY, PATIALA-147004, PUNJAB, INDIA

July, 2016

Dedicated to my Parents

Declaration

I hereby declare that the thesis entitled **"Effect of nanoclay addition on the mechanical properties of glass fibre reinforced epoxy nanocomposites processed through VARIM"** is an authentic record of my study carried out as requirements for the award of the degree of Master of Engineering in Production Engineering at Thapar University, Patiala under the supervision of **Dr. Tarun Nanda**, Assistant Professor, Mechanical Engineering Department and **Dr. Rajeev Mehta**, Professor, Chemical Engineering Department, Thapar University, Patiala.

Place: Patiala

Date: 15/7/16

Daksh Shelly

Daksh Shelly

It is certified that the above statement made by the student is correct to the best of my/our knowledge and belief.

Dr. Tarun Nanda
Assistant Professor
Mechanical Engineering Department
Thapar University, Patiala
147004

Dr. Rajeev Mehta
Professor
Chemical Engineering Department
Thapar University Patiala
147004

Counter signed by

Dr. S.K. Mohapatra
Sr. Professor and Head
Mechanical Engineering Department
Thapar University, Patiala
147004

Dr. S.S. Bhatia
Dean
Academic Affairs
Thapar University, Patiala
147004

Acknowledgement

On the keynote, I would like to thank Dr. Tarun Nanda, Assistant Professor, MED for all the unconditional love, care, support, enthusiasm, positive energy, and inspiration given, without which I would have never developed my keen interest in glass fibre reinforced epoxy based nanocomposites. He is the best academician I have ever met in my life and I do believe he would be the last because no one could ever be like him. My thanks also go to Dr. Rajeev Mehta, Professor, CED, a man of ideas and positive hope, for all his support, patience and sharing experience. He is the backbone of my complete research work, with his limits ranging from giving appreciation for good work to even positive criticism. My both mentors are the building blocks of my thesis as well as my life and I could never repay what they have given to me. My special thanks to all my friends who supported me throughout my thesis work with their humour, laughs, suggestions, love and patience. I could never be a more complete of a person without them as they played a very vital role in completing my student life. I am indebted by the trust put by my parents and my sister on me, along with their unconditional love, care and invaluable suggestions, especially my parents who alway heard me patiently even during the stressed times of my Master's degree. Finally I am thankful to God for giving me this human form and destining me for accomplishing my righteous task in this world although till today I am still searching for the ultimate goal of my life and the reason for sending me here with a hope that I will surely be guided towards it.

Daksh Shelly

Abstract

Now days, glass fibre reinforced nanocomposites are replacing metals in many weight-critical components in military, aviation, automotive, and other industries due to properties shown by them are comparable or better than the traditional metallic materials because of their low density, high strength-weight ratios, and high modulus-weight ratios. The objective of this research work is to "**Effect of nanoclay addition on the mechanical properties of glass fibre reinforced epoxy nanocomposites processed through VARIM**." The epoxy resin and hardener used were CY 230-1 and HY 951 respectively. E glass fibre was used as reinforcement and nanoclays were used as nanofiller. Nanoclays used were Nanomer PGV and Nanomer I.28E. Nanoclay was mixed in epoxy resin by using mechanical stirrer followed by homogenization and probe sonication. Vacuum assisted resin infusion moulding (VARIM) was used to fabricate the glass fibre reinforced epoxy nanocomposites. The nanoclay content was varied form 0–4 phr. Tensile, flexural, fracture toughness and impact strength testing were evaluated according to ASTM D-3039, ASTM D 790–02, ASTM D 5045–99 and ASTM D 256–02 $^{\varepsilon 1}$ respectively. XRD and TEM analysis were used to study the morphology of the fabricated nanocomposites. SEM analysis was used to characterize fracture mechanisms involved during mechanical testing. XRD micrographs revealed that full or partial exfoliated morphology was observed for NV1 and NE1 formulations whereas, intercalated morphology was observed for NV2, NV4, NE2, and NE4 formulations. TEM results were also confirming the XRD results. The best tensile and flexural properties were observed in nanocomposite containing 1 phr Nanomer PGV (NV1 formulation). Whereas, best impact strength and fracture toughness were observed in nanocomposite containing 2 phr of Nanomer PGV (NV2 formulation). The nanocomposites fabricated using Nanomer PGV showed better properties as compared to Nanomer I.28E. SEM micrographs of fractured surface of glass fibre reinforced epoxy composite (reference sample) showed relatively smooth surface and indicated that the interfacial bonding between the glass fibre and the epoxy was weak. However, the fractured surfaces of nanocomposites containing 1 and 2 phr nanoclay looked rougher and were indicating a strong interface bonding between glass fibre and epoxy clay matrix. The SEM micrographs of nanocomposites with 4 phr nanoclay suggested that silicate platelets were not able disperse properly and resulted in formation of clay agglomerates or tactoids. These agglomerates of silicate platelets may act as crack initiating sites which may be the possible reason for deteriorated properties.

Table of Content

List of Figure

List of Tables

List of Acronyms

Acronym	Full name
AEP	Aminoethylpiperazine
ASTM	American society for testing and materials
CLD	Cross-link density
CLTE	Coefficient of linear thermal expansion
CPN	Cloisite epoxy nanocomposite
CTBN	Carboxyl-terminated poly (butadiene-*co*-acrylonitrile)
DDM	4,4’-diamino diphenylmethane
DGEBA	diglycidyl ether of bisphenol A
DSC	differential scanning Calorimetry
FESEM	Field emission scanning electron microscopy
IPDA	Isophoronediamine
IS	Impact strength
MMT	Montmorillonite
OMMT	Organo-montmorillonite
N0	Reference sample
NE	Nanomer I.28E clay
NE0.5	Nanocomposite with 0.5 phr Nanomer I.28E clay
NE1.0	Nanocomposite with 1.0 phr Nanomer I.28E clay
NE1.5	Nanocomposite with 1.5 phr Nanomer I.28E clay
NE2.0	Nanocomposite with 2.0 phr Nanomer I.28E clay
NE2.5	Nanocomposite with 2.5 phr Nanomer I.28E clay
NE3.0	Nanocomposite with 3.0 phr Nanomer I.28E clay
NE3.5	Nanocomposite with 3.5 phr Nanomer I.28E clay
NE4.0	Nanocomposite with 4.0 phr Nanomer I.28E clay
NV	Nanomer PGV clay
NV0.5	Nanocomposite with 0.5 phr Nanomer PGV clay
NV1.0	Nanocomposite with 1.0 phr Nanomer PGV clay
NV1.5	Nanocomposite with 1.5 phr Nanomer PGV clay
NV2.0	Nanocomposite with 2.0 phr Nanomer PGV clay
NV2.5	Nanocomposite with 2.5 phr Nanomer PGV clay
NV3.0	Nanocomposite with 3.0 phr Nanomer PGV clay

NV3.5	Nanocomposite with 3.5 phr Nanomer PGV clay
NV4.0	Nanocomposite with 4.0 phr Nanomer PGV clay
PMNC	Polymer Matrix Nanocomposites
SEM	Scanning electron microscopy
TEM	Transmission electron microscopy
TGA	Thermogravimetric analysis
UTM	Universal testing machine
WAXD	Wide angle X-ray diffraction
WAXS	Wide angle X-ray scattering
XRD	X-ray diffraction

List of Symbols

Symbol	Meaning
T_g	Glass transition temperature
K_{IC}	plain strain/ critical intensity factor
℃	degree Celsius
θ	Angle
λ	Wavelength
ρ	Density

Chapter 1

Introduction

1.1 Composites

'Composites' is not a human invention. Wood is a natural composite, a combination of polysaccharide lignin (resinous matrix) and cellulose fibres (good strength and stiffness). Humans were aware of the concept of combining two materials and take advantage of it e.g. combining mud and straw for construction of huts [Harris, 1999]. The science and technology of composite materials, from the last half a century, has developed tremendously and providing engineers a novel materials and tools to use them to full extent. Today's modern technology requires materials with unusual properties which are unachievable with conventional metal alloys, ceramics, and polymeric materials. These types of materials are needed in various industries like aircraft, automotive, military, infrastructure, marine, and sporting goods etc. [Harris, 1999; Callister, 2007].

Composites are considered to be combinations of materials differing in composition or form on a macroscale. The constituents retain their identities in the composite; that is, they do not dissolve or otherwise merge completely into each other although they act in concert. Normally, the components can be physically identified and exhibit an interface between one another [Composite Materials Handbook, 2002]. According to the matrix material, composites are divided into three categories [Thomas *et al*., 2012]:

- Polymer Matrix Composites (PMC)
- Metal Matrix Composites (MMC)
- Ceramic Matrix Composites (CMC)

1.2 Polymer Matrix Composites (PMC)

Polymer composites are defined as an interacting mixture of two phase's viz. a polymer matrix and a solid phase (fibres, particles etc.) [Kotsilkova, 2007]. There are various thermoplastic and thermoset materials used as matrix in the polymer matrix composites like epoxy, polyester, polyimide, polyamide vinyl ester, phenolic, polypropylene, polyether ether ketone (PEEK) etc. Polymer composites are preferred due to their low cost, ease of processability, good chemical resistance, low specific gravity, and simple fabrication

methods. There are various methods used for fabricating polymer composites to reduce the content of resin in the final product. Composites fabricated by hand layup result in a product containing about 60% resin and upto 40% fibre. On the other hand, composites fabricated using vacuum infusion moulding result in about 40% resin and 60% fibre content. Depending on the application of product, the matrix is selected on the basis of strength, modulus, melting point etc [Campbell, 2010; Thomas *et al*., 2012]. Depending on the reinforcement, polymer composites divided into various types as shown in Figure 2.1 [Callister, 2007]:

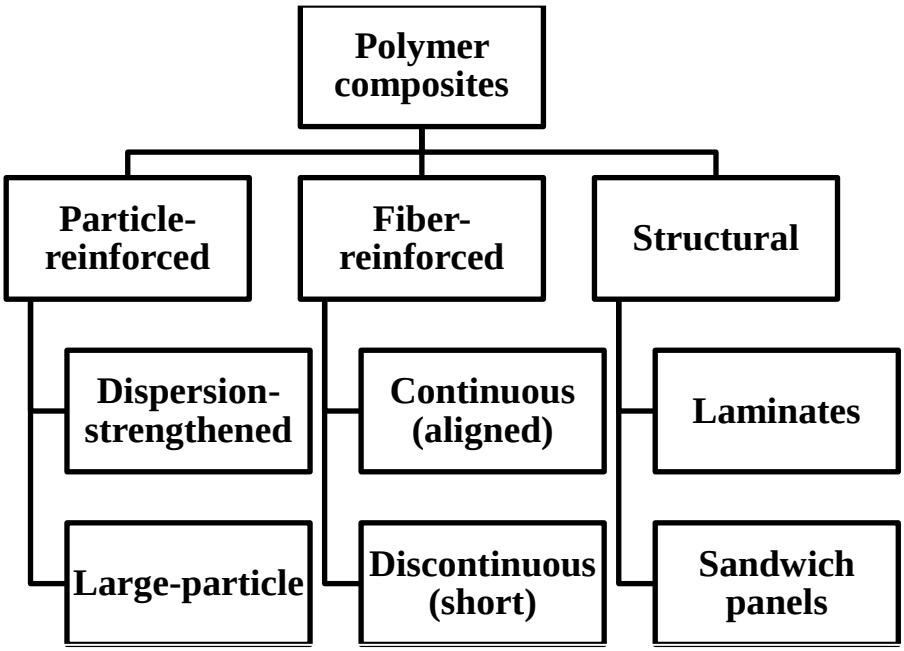

Figure 1.1: Types of polymer composites based on type of reinforcement [Callister, 2007]

1.3 Fibre Reinforced Polymer Composites

Fibre reinforced composites are a combination of fibres of high strength and modulus embedded in or bonded to a matrix with distinct interfaces (boundaries) between them. The matrix and the fibre, both retain their chemical and physical identities; even then they produce a combination of properties which are unachievable with either of the constituents acting alone. The properties shown by various fibre reinforced polymer composites are comparable or better than the traditional metallic materials due to their low density, high strength-weight ratios, and high modulus-weight ratios. Now days, fibre reinforced polymers are replacing metals in many weight-critical components in military, aviation, automotive, and other industries. Fibre reinforced composites are having high internal damping, consequently better vibrational energy absorption within the material and reduced transmission of vibrations and noise to neighbouring structures. Fibre reinforced polymer

composites are used for various applications like printed circuit boards, floor beams, chair springs, oil sucker rods used in lifting underground oil, offshore oil platforms, bone plates for fracture fixation, power transmission shafts etc. [Mallick, 2007; Kumar *et al*., 2014]. Fibres are the primary load bearing constituents of these composites. Different types of fibres used for fabrication of composites include glass fibre, carbon fibre, aramid fibre, boron fibre, kevlar fibre, and natural fibres. Glass fibres are the most common of all reinforcing fibres for polymeric matrix composites (PMC). The main features of glass fibres are low cost, high tensile strength, high chemical resistance, and excellent insulating properties [Mallick, 2007]. Glass fibres are manufactured by drawing molten glass into very fine threads and then immediately protecting them from contact with the atmosphere or with hard surfaces in order to preserve the defect free structure that is created by the drawing process [Harris, 1999]. Generally two types of glass fibres i.e. E-glass and S-glass are used for composites. S-glass has better mechanical properties as compared to E-glass but its higher cost limits its use [Harris, 1999; Mallick, 2007].

1.4 Nanocomposites

Nanocomposites are composites in which at least one of the phases shows dimensions in the nanometer range [Camargo *et al*., 2009]. In mechanical terms, nanocomposites are different from conventional composites due to their high aspect ratio and exceptionally high surface to volume ratio. The large surface area means small amount of reinforcement has observable effect on the properties of nanocomposites [Kotsilkova, 2007]. Nanocomposites are known for their outstanding mechanical properties (increased modulus and strength), barrier resistance (weight % gain, diffusivity), thermal properties (glass transition temperature etc.). Among the different nanofillers (clays, carbon nanotubes, nanofibers, silica nanoparticles etc.), special attention has been paid to clays in the field of nanocomposites. Layered silicates (clay) are found to be one of the ideal nano reinforcements for polymers because of their high aspect ratio, high intercalation chemistry, ease of availability and low cost [Azeez *et al*., 2013].

1.4.1 Constituents of Nanocomposites

Nanocomposites comprises of three main constituents:

- **Matrix (primary phase):** The polymer matrix is the primary phase of the polymer nanocomposites. The matrix binds the fibers together freezing in the fiber orientation.

Loads applied to the nanocomposites are transferred to the principal load-bearing component (fibers) through the matrix enabling the composite to withstand flexural, compression, and shear forces as well as tensile loads. The matrix must separate the fibers from each other so that they can act as separate entities. The matrix also protects the fibers from the environmental attack and mechanical damage [Harris, 1999]. The desirable properties of matrix include low shrinkage and moisture absorption, god strength, strength at elevated temperature, dimensional stability, and chemical resistance. The matrix must be elastic to transfer load to the fibre [Web Reference: http://nptel.ac.in].

- **Reinforcement (secondary phase):** The reinforcement (secondary / dispersed phase) is the load bearing constituent of a composite. These are of nano, micro, and macro levels. All loads applied to the matrix are transferred to the reinforcement through an interface. The reinforcement is generally harder or stiffer than the matrix. The improvement in properties depends upon the bonding between matrix and reinforcement [Smith and Hashemi, 2008].
- **Interface:** Interface is defined as the common boundary of the matrix and the reinforcement fiber that is in contact. It maintains bond between them for transferring loads. It has mechanical and physical properties that are different from those of the matrix or the fiber. The chemical, mechanical, and physical properties vary either continuously or in a stepwise manner between those of the matrix material and the bulk fiber (see Figure 1.2) [Kim and Mai, 1998]. Interface properties mainly depend upon the physical and chemical nature of the matrix and the fiber. There will be some modification of either physical or chemical characteristics or both resulting in a region which has properties quite different from those of either of the two major components. The stress transfer between the matrix and reinforcement mainly depends on the interface properties [Harris, 1999].

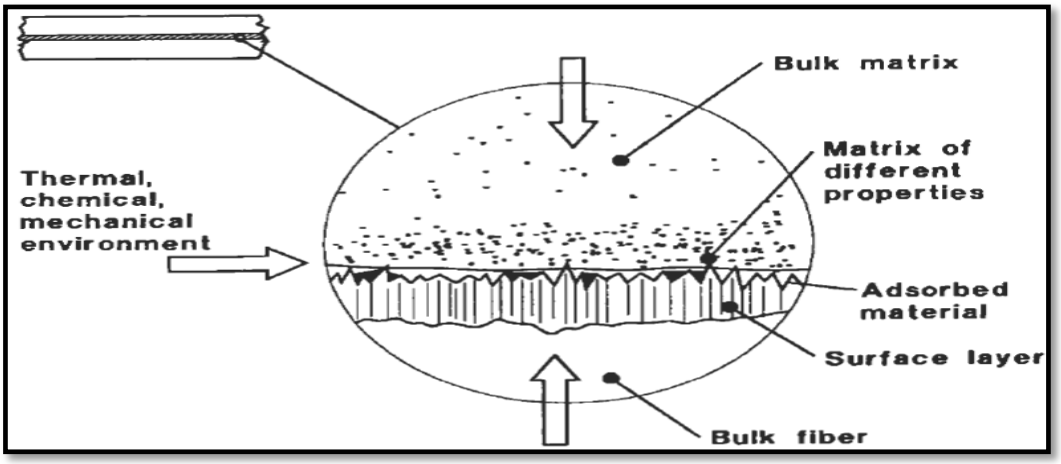

Figure 1.2: Schematic illustration of interface between fiber and matrix [Kim and Mai, 1998]

1.5 Epoxy Clay Nanocomposites

Among the different nanofillers (clay, carbon nanotube, nanofibers, silica nanoparticles etc.) special attention has been paid to clays in the field of nanocomposites. Layered silicates (clay) are found to be one of the ideal nano reinforcements for polymers because of their high aspect ratio, high intercalation chemistry, ease of availability, and low cost [Azeez *et al*., 2013].

1.5.1 Epoxy Resin

The term 'epoxy resin' refers to both the prepolymer and its cured resin/hardener system. Its characteristic group is a three membered ring known as epoxy, epoxide, oxirane, and glycidyl or ethoxyline group. The general representation of epoxy group is shown in Figure 1.3.

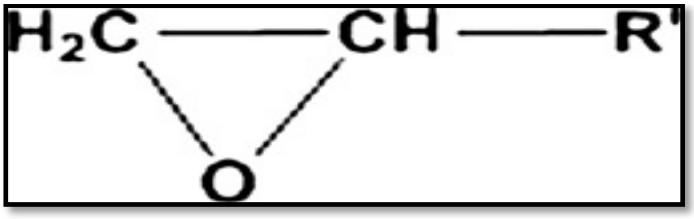

Figure 1.3: Epoxy or oxirane group [Azeez *et al.*, 2013]

The chemical structure of epoxy resin is much strained and highly reactive. Epoxy resins can be cross–linked through a polymerization reaction with a hardener at elevated temperatures (aromatic amines and acid anhydrides) or at room temperatures (aliphatic amines). Generally, the resin systems cured at high temperature have improved properties such as strength, stiffness, and higher glass transition temperature as compared to the resins cured at room temperatures. Epoxy resins have excellent heat resistance, high adhesive strength, chemical stability, good impact resistance, high strength, and hardness etc. The byproducts are also absent in epoxy resin during curing reactions [Azeez *et al.*, 2013].

1.5.2 Nanoclays

The layered silicates commonly used in nanocomposites belong to the structural family known as the 2:1 phyllosilicates. Their crystal lattice consists of two-dimensional layers where a central octahedral sheet of alumina or magnesia is fused into two external silica tetrahedron by the tip so that the oxygen ions of the octahedral sheet do also belong to the tetrahedral sheets (see Figure 1.4).

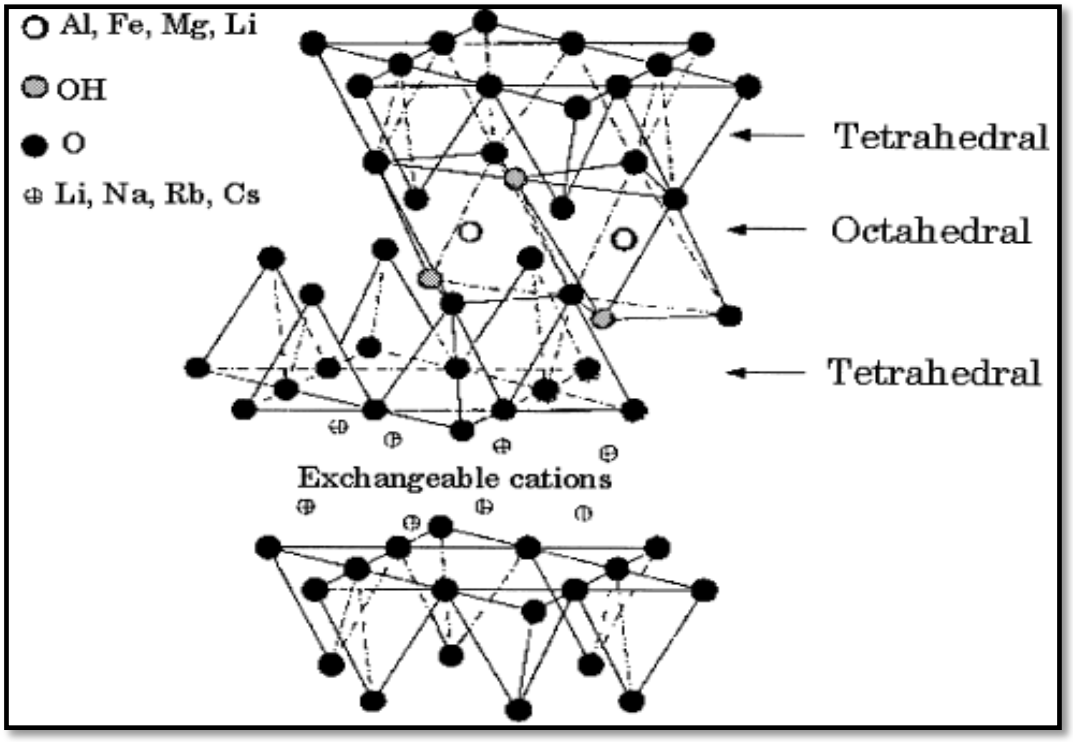

Figure 1.4: Structure of 2:1 phyllosilicates [Alexandre and Dubois, 2000]

The layer thickness is around 1 nm and the lateral dimensions of these layers may vary from 300 Å to several microns and even larger, depending on the particular silicate. These layers organize themselves to form stacks with a regular Vander Walls gap in between them called the interlayer or the gallery. Isomorphic substitution within the layers (for example, Al^{3+} replaced by Mg^{2+} or by $Fe2^{+}$, or Mg^{2+}, replaced by Li^{+}) generates negative charges that are counterbalanced by alkali or alkaline earth cations situated in the interlayer. As the forces that hold the stacks together are relatively weak, the intercalation of small molecules between the layers is easy. In order to render these hydrophilic phyllosilicates more organophilic, the hydrated cations of the interlayer can be exchanged with cationic surfactants such as alkylammonium or alkylphosphonium (onium) (see Figure 1.5). The modified clay (or organoclay) being organophilic, has lower surface energy and is more compatible with organic polymers. These polymers may be able to intercalate within the galleries, under well defined experimental conditions [Alexandre and Dubois, 2000]. Generally, the nature of clay is hydrophilic. The surface of the clay minerals must be modified to organophilic in order to make them compatible with organic polymers before its use. Organic cations such as phosphonium ion or an ammonium ion are the commonly used organic modifiers for clay minerals. Modification involves the exchange of interlayer inorganic cations with organic onium salts. The organic modification increases the d-spacing to a certain extent (normally

over 2 nm). Thus, the organic modification favors the diffusion of polymer into the interlayer space [Azeez *et al.*, 2013].

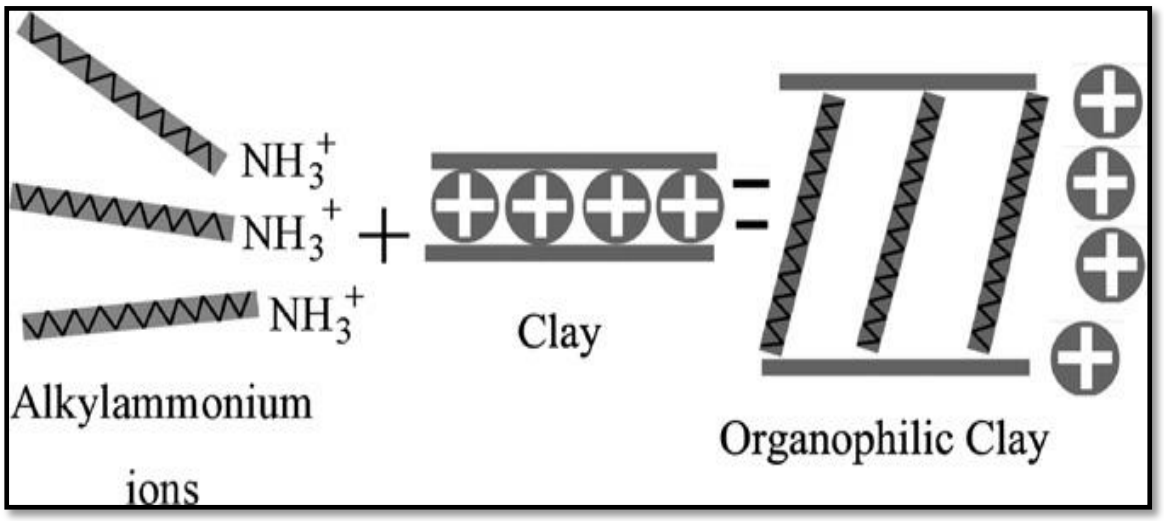

Figure 1.5: Organic modification of clay [Azeez *et al.*, 2013]

1.5.3 Structure of Polymer Clay Nanocomposites

The polymer clay nanocomposites can be divided into three categories depending upon the resulting morphology obtained.

- **Phase-separated microcomposites**: Phase-separated microstructure results when the polymer is unable to intercalate between the silicate sheets (see Figure 1.6 (a)) and properties of such type of nanocomposite stay in the same range as the traditional microcomposites [Alexandre and Dubois, 2000].
- **Intercalated nanocomposites:** Intercalated structure is obtained when a single (and sometimes more than one) polymer chain is intercalated between the silicate layers resulting in a well ordered multi-layer morphology built up with alternating polymeric and inorganic layers (see Figure 1.6 (b)) [Alexandre and Dubois, 2000]. The d–spacing in case of intercalated nanocomposites is in the range, 20–30 Å [Azeez *et al.*, 2013].
- **Exfoliated nanocomposites:** The exfoliated structure is obtained when the silicate layers are uniformly and completely dispersed in a continuous polymer matrix (see Figure 1.6 (c)) [Alexandre and Dubois, 2000]. The d–spacing is more than 50 Å [Azeez *et al.*, 2013].

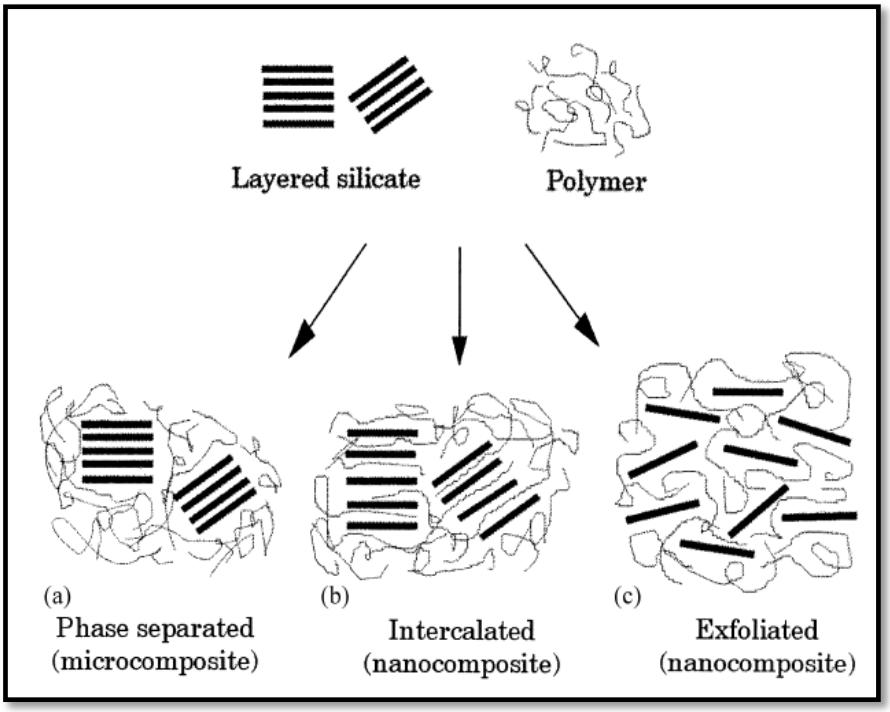

Figure 1.6: Different morphologies in clay reinforced nanocomposites arising from the interaction of layered silicates and polymers: (a) phase separated microcomposite, (b) intercalated nanocomposite, and (c) exfoliated nanocomposite. [Alexandre and Dubois, 2000]

1.6 Applications of Fibre Reinforced Polymer Composites

From the last half a century, there has been a tremendous growth in the field of fibre reinforced polymer composites. Due to such a huge growth in composites, the use of these in various industries starting from electronics to aviation has increased dramatically. Fibre reinforced composites show high strength-weight and modulus-weight ratios, even when compared with some metals [Kaushik *et al.,* 2006; Lin *et al.,* 2006; Bozkurt *et al.,* 2007; Chow, 2007]. The major applications of fibre reinforced composites are explained below:

- **Aircraft and Military Applications:** Fibre reinforced composites are extensively used in the aircraft and military applications. Airbus 310 was the first ever commercial aircraft to use composites extensively in 1987. The composite weight percentage in Airbus 310 was 10 % and it was increased to 25 % in Airbus 380 in 2006. The parts of Airbus 380 manufactured using composites are shown in Figure 1.7. The composites are used in many other military and commercial helicopters for making baggage doors, tail rotor spars, vertical fins, and many more. One major application of composites in helicopter is the rotor blades. Carbon or glass fibre-reinforced epoxy is used in this application. The main reason for using fibre reinforced composites in aviation and military industry is weight saving which consequently lead to increased speed and payloads. The other reasons for

giving preference to composites over titanium and aluminium alloys are low fabrication and assembly cost (less number of components and fasteners) and reduction in maintenance and repair costs (lesser corrosion and better fatigue resistance) [Mallick, 2007; Kumar *et al.*, 2014].

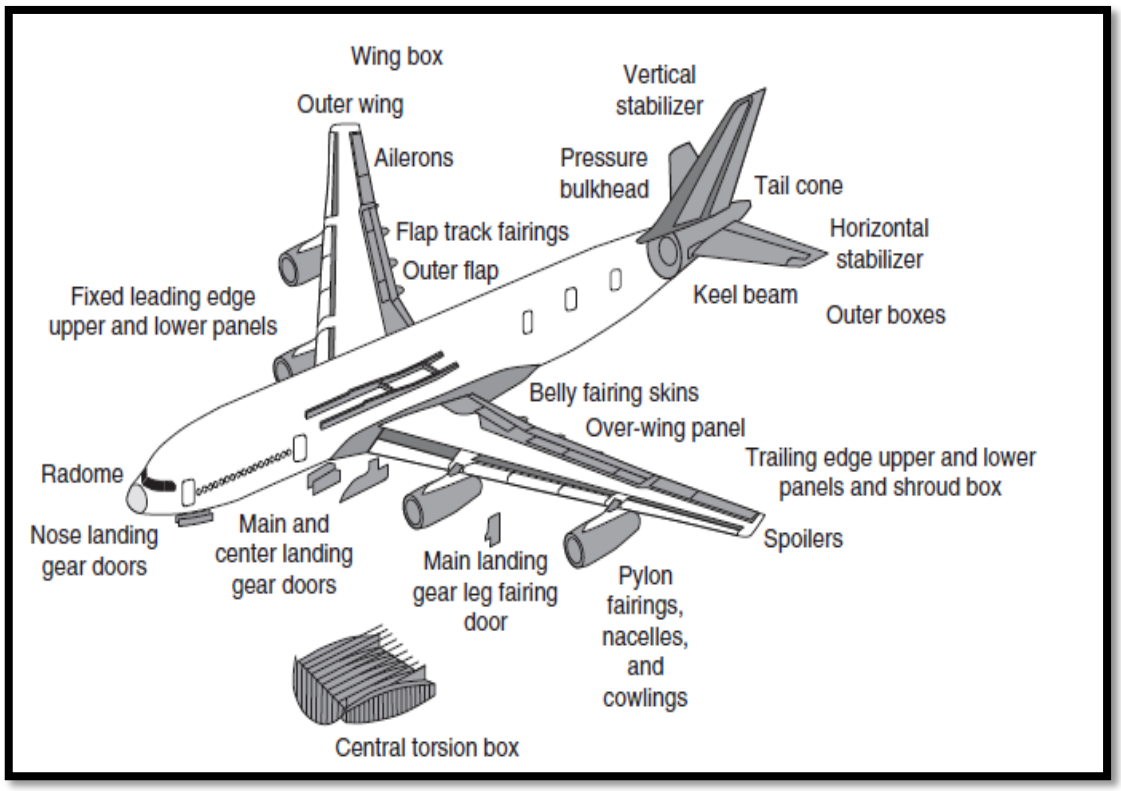

Figure 1.7 Applications of fibre reinforced polymer composites in Airbus 380 [Mallick, 2007]

- **Space Applications:** FRP composites are used for space applications due to their weight saving feature. They are find applications in the structure of space shuttles viz. the mid-fuselage truss structure (boron fiber-reinforced aluminium tubes), remote manipulator arm (ultrahigh-modulus carbon fiber-reinforced epoxy tube), payload bay door (sandwich laminate of carbon fiber-reinforced epoxy face sheets and aluminum honeycomb core), and pressure vessels (Kevlar 49 fiber-reinforced epoxy). They are also used in many other places for making support structures for optical platforms, solar arrays, antennas and many more [Mallick, 2007; Campbell, 2010].

- **Automotive Applications:** The use of FRP composites in automotive sector can be divided in to three categories i.e. engine components, chassis components, and body components. FRP composites are used for making hood or door panels, bumper beams, engine valve covers, timing chain covers etc. FRP are also used for making rear leaf

springs, drive shafts, and road wheels and so on. Unileaf E-glass fibre reinforced epoxy spring has replaced the multileaf steel spring because its weight is 80 % less than the steel spring. BMW M6 roof panel is manufactured by FRP using resin transfer molding (RTM). This panel is twice as thick as a compared to the steel panel, but is 5.5 kg lighter. Carbon reinforced epoxy composites are used in Formula 1 race car [Mallick, 2007; Kumar *et al.*, 2014].

- **Marine Applications:** FRP composites are used in many boats like sail boats, life boats, fishing boats, recreational boats, and so on. They are used in hulls, decks, bulkheads, masts, propulsion shafts, frames, rudders, and others of mine hunters, frigates, and aircraft carriers. The principal advantage of using FRP is weight saving which results in higher crushing speed, maneuverability, and fuel efficiency [Mallick, 2007; Campbell, 2010; Kumar *et al.*, 2014].

- **Sporting Goods Applications:** FRP composites are extensively used for manufacturing sporting goods due to their weight reduction, vibration damping, and design flexibility. Different sporting goods made of FRP are tennis rackets, hockey sticks, baseball bats, golf club shafts, arrows, archery bows, javelins, bicycle frames, exercise equipment, and helmets [Mallick, 2007; Campbell, 2010].

- **Infrastructure Applications:** FRP composites have potential to replace reinforced concrete and steel in bridges, buildings, and other civil infrastructures. They are used in infrastructure due to corrosion resistance (leads to longer life) and lower maintenance and repair costs. Another benefit of using FRP composites for large bridge structures is their light weight, which means lower dead weight for the bridge, easier transportation from the production factory to the bridge location, easier hauling and installation, and less injuries to people in case of an earthquake . Due to weight savings in construction, it is also possible to design bridges with longer span between the supports [Mallick, 2007; Campbell, 2010].

- **Miscellaneous Applications:** FRP composites used for making circuit boards (PCB's), TV, radios, cell phones, electrical motor covers and personal computers. They are also used in bathtub furniture, spa tubs, show racks, roof sheets and book racks etc. FRP composites are also used in medical applications (instrument enclosures to X-ray beds,

bone plates for fracture fixation, implants etc.). They are also used in oil industry (offshore oil platforms and oil sucker rods used in lifting underground oil) and in many industrial products, such as step ladders, oxygen tanks, and power transmission shafts [Mallick, 2007; Kumar *et al.*, 2014].

Chapter 2

Literature Review

This chapter represents literature review on polymer based nanocomposites. This review mainly focuses on epoxy based nanocomposites reinforced with silicate layers, glass fibre, or both. The literature review will be used to discuss the effect of different constituents, methods of preparation, use of impact modifiers etc. on the different properties (mechanical, barrier and thermal properties) of glass fibre reinforced epoxy layered silicate nanocomposites.

2.1 Review of Epoxy based Nanocomposites

Haque and Shamsuzzoha (2003) investigated the effect of the silicate platelets addition on the mechanical properties of the epoxy based nanocomposites reinforced with glass fibre. The epoxy matrix taken in two parts viz. Part A (bisphenol-A and bisphenol-F blend) and Part B (hardener cyclo aliphatic amine). The suggested mixing ratio is 100A: 30 B by weight. The nanoclay used was Nanomer 1.28E. The clay loading was varied as 0, 1, and 2 wt. %. The clay was mixed in part A at 25 ℃ with the help of mechanical stirrer for an hour. After that probe sonication was performed for homogenous mixing of clay. The hardener (part B) was added to mixture and mixed properly. Vacuum assisted resin infusion moulding (VARIM) was used for fabricating glass fibre reinforced epoxy nanocomposites. Curing was done for 24 h at room temperature followed by the post curing at 100 ℃ for 2 h. It was observed that intercalated morphology was achieved in all nanocomposite formulations (0, 1, and 2 wt. %). The interlaminar shear strength was increased upto 1 wt. % beyond it showed decreasing trend. It was increased from 23.05 MPa to 33.21 MPa (increased by 44 %). Interlaminar shear strength was a matrix dominant property and improvement in strength of nanocomposites was mostly due to addition of nanoclay into epoxy matrix. This property enhancement is achieved due to increased interfacial sites and improved bond characteristics of the epoxy based nanocomposites. The fracture toughness, flexural modulus and strength improved with addition of nanoclay upto 1 wt. % further addition of clay resulted in decreased flexural properties. The flexural strength of the nanocomposites were a fibre dominant property, whereas, the epoxy matrix had a dominating effect on the overall

properties of the nanocomposites. Consequently, glass fibre reinforced nanocomposites showed improvement in flexural properties due to addition of silicate platelets to the epoxy matrix and resulted in improved interfacial fibre matrix bond characteristics.

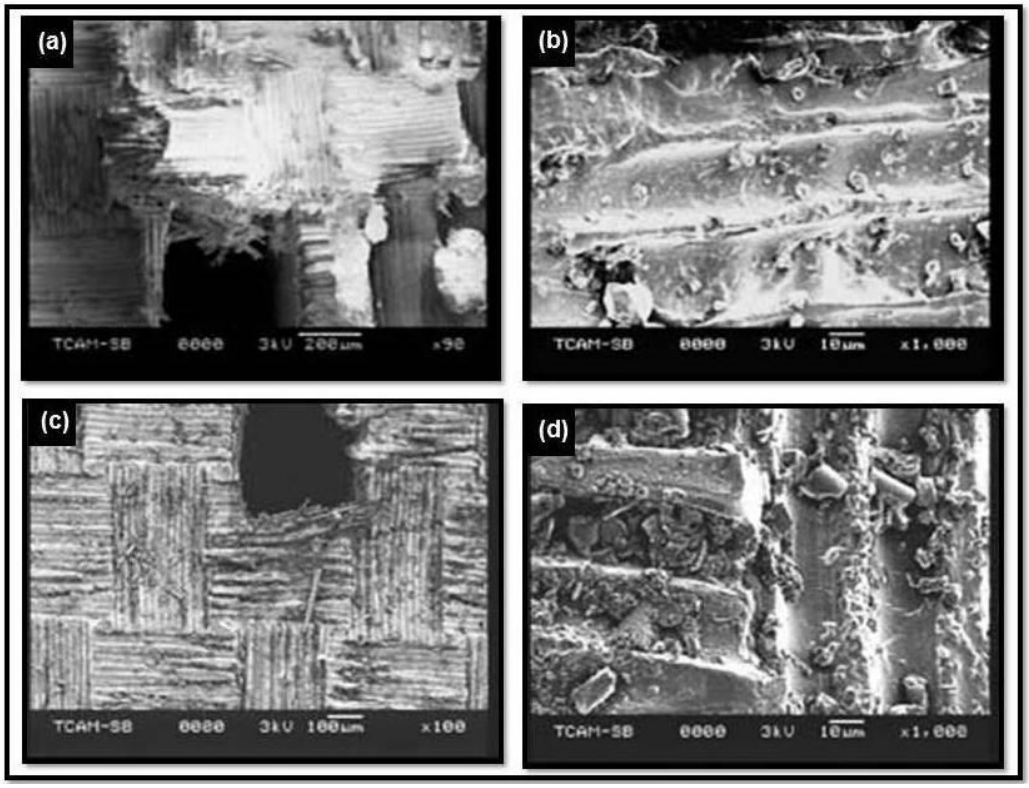

Figure 2.1: SEM micrographs of the fractured surface of fracture toughness specimens: (a–b) glass fibre reinforced epoxy composite, and (c–d) glass fibre reinforced epoxy clay nanocomposites [Haque and Shamsuzzoha 2003].

The increased fracture toughness in fibre reinforced nanocomposites due to Enhanced matrix agglomeration with significant matrix cracking and fragmentations were clearly seen at the interface region (as shown in Figure 2.1). An intercalated morphology indicated strong interfacial bonding and prolonged fracture process. However, conventional composites morphology was seen to be comparatively clean with comparatively less matrix agglomeration than that of nanocomposites.

Isik *et al.* (2003) studied the effect of addition of an impact modifier on the morphology, mechanical and thermal properties of epoxy based layered silicate nanocomposites. The epoxy resin, hardener, clay and impact modifier used were Araldite M, HY 956, Cloisite 30B and Voranol 3322 respectively. Nanocomposites containing 0, 1, 3, and 5 wt. % nanoclay and 0, 1, 3, 5 and 7 wt. % modifier were fabricated by mechanically stirring nanoclay and epoxy at 35 ℃ for

2 h and ultrasonication was done for 30 min. The impact modifier was added to the mixture and stirred for 1 h. It was followed by degassing and cooling mixture to room temperature. By weight epoxy and curing agent was mixed in ratio100:20. The curing and post curing were done at 75 ℃ for 16 h and at 130 ℃ for 3 h respectively. XRD analysis revealed that the d-spacing corresponding to the compositions viz (i) pristine Cloisite 30B, (ii) nanocomposite with 3 wt. % nanoclay and (iii) nanocomposite with 3 wt. % nanoclay and 7 wt. % polyether polyol were 1.83 nm, 3.82 nm and 4.01 nm respectively which showed that polyol domains do not enter into the clay galleries and interlayer spacing does not change (see Figure 2.2). SEM analysis showed that the average diameter of polyol domains increased with increase in clay loading at constant polyether polyol content (see Figure 2.3).

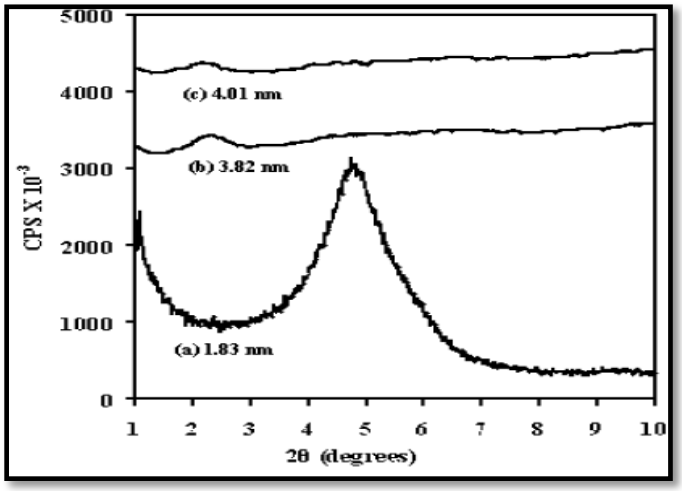

Figure 2.2: XRD patterns of (a) Cloisite 30B powder, (b) Nanocomposite with 3 wt. % Cloisite 30B, (c) Nanocomposite with 3wt. % Cloisite 30B and 7% polyether polyol [Isik et al., 2003]

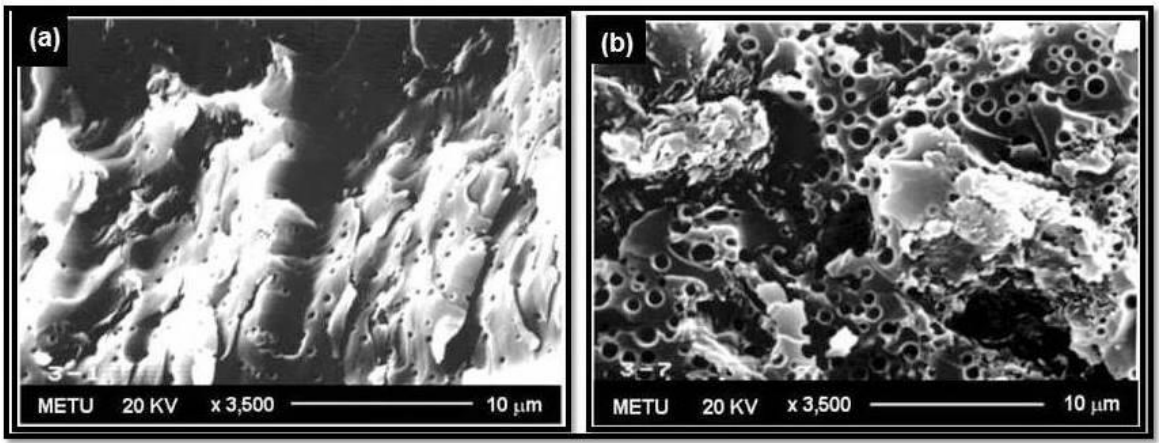

Figure 2.3: SEM micrograph of the nanocomposite containing (a) 3 wt% clay and 1 wt% polyether polyol (b) 3 wt% clay and7 wt% polyether polyol (× 3500) [Isik et al., 2003]

DSC analysis showed that at constant clay content, T_g increased with the increasing polyol concentrations. Compared to neat epoxy, impact strength increased by approximately 130 % with 1 wt. % montmorillonite and 1 wt. % polyether polyol content whereas it showed approximately 160 % increase when 7 wt. % polyol and no clay was present. Tensile strength showed the decreasing trend with increase in nanoclay loading at constant polyol content. Whereas, tensile modulus showed increasing trend with increase in nanoclay loading at constant polyol content but at high polyol contents, it gradually decreased. The strain at break increased for polyol modified epoxy (no nanoclay) increased upto 5 wt. % whereas, it decreased with increase in nanoclay loading in nanocomposites.

Kornmann *et al.* (2005) investigated the mechanical properties and water absorption of glass fibre/epoxy-layered silicate nanocomposites laminates. The epoxy, curing agent and clay used were Araldite CY 225, Araldite HY925 and Somasif ME-100 respectively. The fibre mat was having 0.3 mm thickness was used. For the preparation of epoxy layered silicate nanocomposite epoxy resin was heated to 80 ℃ and silicate platelets were added to it. For uniform dispersion mixture was stirred at 80 ℃ for 1 h, followed by addition of curing agent to it. The slurry was mixed at 80 ℃ for 10 min., followed by degasification. The preheated mould was used for fabricating nanocomposites. The curing and post curing were done at 140 ℃ for 2 h and at 140 ℃ for 10 h respectively. Nanocomposites were fabricated by applying epoxy or epoxy-clay mixture with the help of brush on a glass fibre and this procedure was repeated until required thickness was achieved. Nanocomposites were cured at 140 ℃ for 2 h. Wide angle X-ray diffraction (XRD) revealed that diffraction peak was not visible in all nanocomposite formulations. XRD results were also verified with Transmission electron microscopy (TEM) micrographs. The pristine epoxy/glass fibre nanocomposite images were shown in Figure 2.4 (a–b). These images showed that there was a weak bond between the glass fibre and the pristine epoxy. The glass fibres were debonded from the epoxy. The fracture surface appeared brittle in nature. On the other hand, glass fibre/ epoxy-layered silicate nanocomposite fracture surface showed much rougher surface (as shown in Figure 2.4 (c–d)). Figure 2.4 (d) showed the presence of silicate platelets at the surface of the glass fibres. The fracture surface of the laminate appeared more ductile. This indicated that nanocomposites were tougher that conventional composites. Young modulus increased by 54 % whereas, tensile strength and strain at break decreased in glass fibre reinforced epoxy based nanocomposites as compared to conventional composite. Young's

modulus increased because silicate layers uniformly distributed in the matrix as indicated by the XRD. Tensile strength and strain at break decreased because presence of silicate layers in matrix made it brittle. The flexural modulus and strength were increased by 6 % and 27 % respectively. The flexural strength improved because silicate platelets were present at the glass fibres surface which made it rough, resulted in strong interfacial bonding (as validated by SEM).

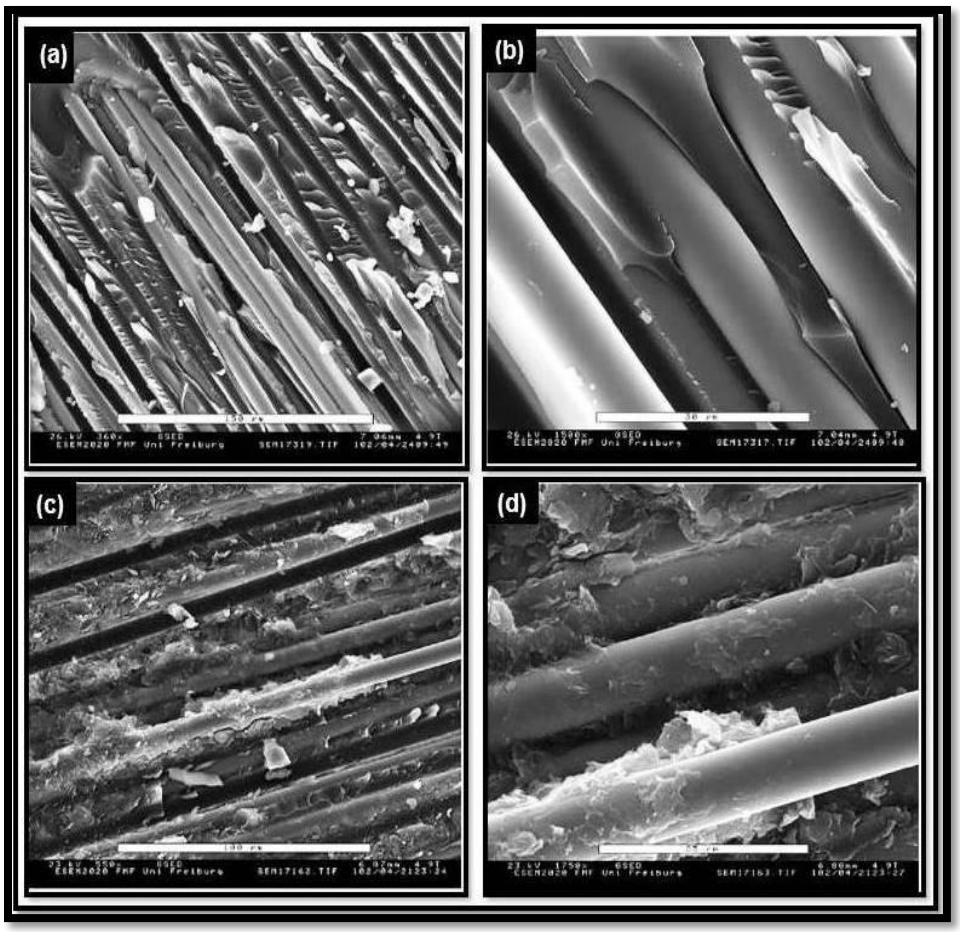

Figure 2.4: Scanning electron micrographs of the glass fibre reinforced laminates with (a–b) epoxy and (c–d) nanocomposite matrices at two different magnifications [Kornmann et al., 2005]

The water uptake was decreased in glass fibre reinforced epoxy based nanocomposites as compared to conventional composite at both temperatures (23 ℃ and 50 ℃). Nanocomposites mainly weight constitute of glass fibre which reduced the water uptake when exposed to water.

Lam *et al.* (2005) investigated the hardness and interlaminar shear properties of epoxy based layered silicate nanocomposites with different nanoclay loading, which resulted in formation of nanoclay/epoxy clusters of different sizes. Epoxy resin, hardener and nanoclay used were Araldite GY 251, HY 956 and Nanolin DK1 series SiO_2 respectively. Nanoclay was mixed in

epoxy resin by using mechanical stirrer. Probe sonication was done for 1 h at room temperature for proper mixing. The hardener was added to the mixture and mixed with the help of mechanical stirrer, followed by degassing for 24 h. Six composites containing 0, 2, 4, 6, 10 and 15 wt. % nanoclay loading were fabricated. Initially, hardness increased with increasing clay loading and reached its maximum value 12.57 Hv (4 wt % nanoclay) which got drastically reduced to 2.68 Hv (15 wt. % nanoclay) (see Figure 2.5 (a)). The high nanoclay loading resulted in incomplete curing of the nanocomposites. The size of the cluster increased with increase in nanoclay loading. The average diameter of the clusters for nanocomposite containing 4 wt. % clay was about 125 nm, which suggested that the viscosity of the epoxy resin at room temperature was high which did not allow epoxy monomers to diffuse into interfacial galleries of the nanoclay particles. The size of the clusters got increased to about 400 nm for composite containing 15 wt. % clay loading (see Figure 2.5 (b)).

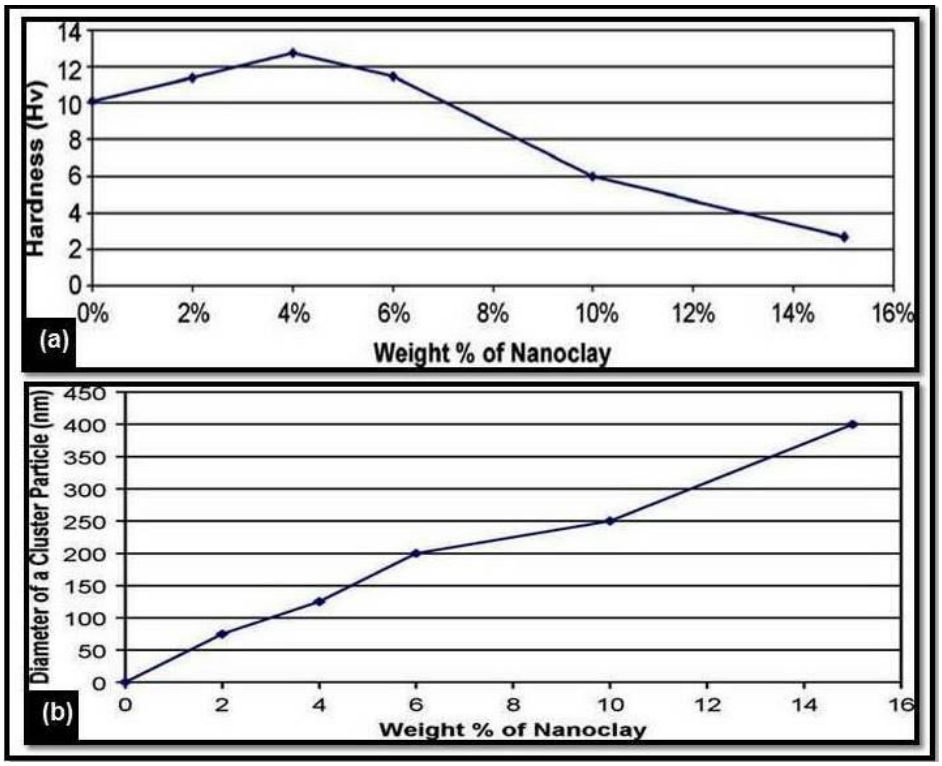

Figure 2.5: (a) Average value of the micro-hardness test at different wt. % of nanoclay. (b) Variation of the cluster size at different wt. % of nanoclay [Lam et al., 2005]

The load-extension curve of pristine epoxy sample, after interlaminar shear test, showed that it had a long plastic yielding zone leading to its high fracture energy consumption and toughness (see Figure 2.6 (a)). However, the ductility of epoxy based nanocomposites decreased with

addition of silicate platelets due to which their short beam shear strength decreased, compared to pure epoxy. The 4 wt. % nanoclay composite showed no plastic deformation (see Figure 2.6 (b)).

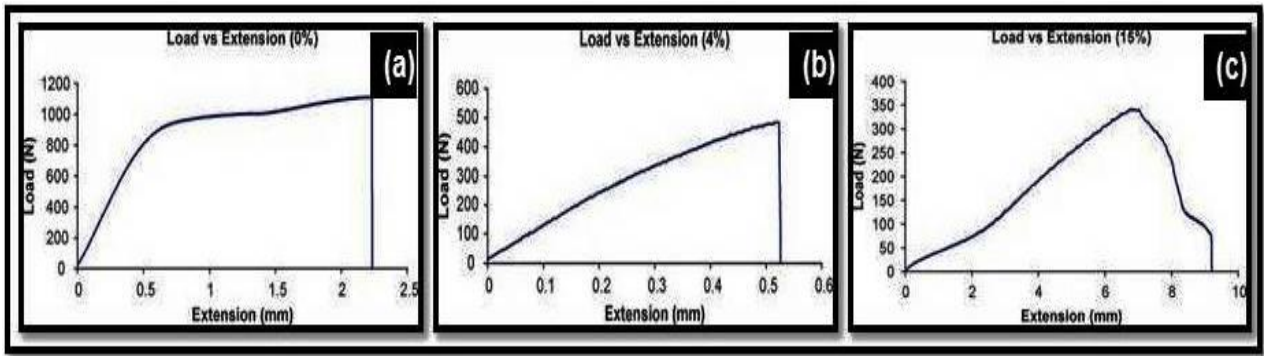

Figure 2.6: Load–deflection curve extracted from the interlaminar shear test (a) pure epoxy (b) nanocomposites with 4 wt. % of nanoclay particles and (c) nanocomposites with 15 wt. % of nanoclay particles [Lam et al., 2005]

The nanocomposite with 15 wt. % nanoclay loading showed strange load-deflection behavior because the amount of silicate platelets were very high and the mechanical behaviour was determined by the silicate platelets interaction rather than the epoxy-silicate platelet interface mechanisms (see Figure 2.6 (c)). The epoxy resin acted as glue between the silicate platelets. The breaking paths became rougher and in a 'zig-zag' manner with increase in size of cluster. Hence, the nanocomposite with 15 wt. % nanoclay showed higher fracture toughness as compared to pristine epoxy. Thus, the micro-hardness of the nanocomposite with 15 wt. % nanoclay was lower than the other nanocomposites due to its highest deformability.

Lin *et al.* (2006) revealed the effect of silicate platelets on the thermal and mechanical properties of the glass fibre reinforced epoxy hybrid nanocomposites. Epoxy, hardener and clay used were YD-128, Jeffamine D-230 and Cloisite 15A respectively. Unidirectional glass fibers (T800) were used for reinforcement of nanocomposites. The three different methods used for preparing epoxy-clay mixture. In direct mixing technique the nanoclay was mixed into the epoxy resin at 80 ℃ for 4 h, before adding curing agent added to the mixture the mixture was cooled to room temperature. In solution mixing, at room temperature, 8g nanoclay was mixed in the chloroform. The above mixture was added to the epoxy resin and cooled to room temperature. Finally, hardener was added to the epoxy-clay mixture. In ultrasonic mixing, sonication of nanoclay and hardener was done for 25 min for homogenous suspension. The homogenous suspension mixed in epoxy resin by using mechanical stirrer (for 15 min.). For preparing glass fibre reinforced epoxy layered silicate nanocomposite glass fibers were stacked layer by layer to get desired

thickness. The epoxy-clay mixture was injected into the mold at 50 ℃. The molded composites were cured and post cured at 80 ℃ for 4 h and at 125 ℃ for 3 h. X-ray diffraction (XRD) revealed that the basal spacing or d-spacing remained almost identical in all mixing methods indicated mixing method did not have significant effect on dispersion of nanoclay. The best morphology was obtained in ultrasonic mixing due to this clay/epoxy mixture prepared by ultrasonication was used for fabricating clay/glass fibre/epoxy hybrid composites. DSC and TGA showed that with increase in clay content glass transition temperature and thermal degradation improved because the clay present in the hybrid composite act as barrier and impeded the mobility of the epoxy monomers. The flexural modulus was slightly increased when glass fibre in transverse direction with increase in nanoclay loading.

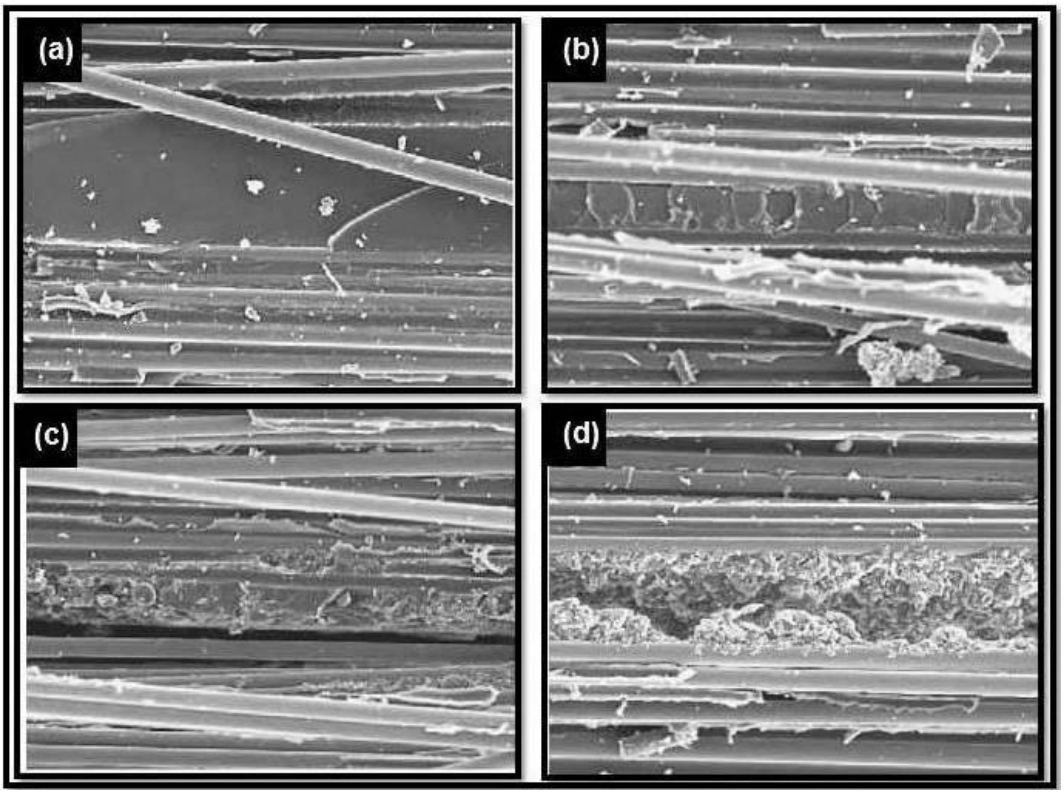

Figure 2.7: SEM images of the impact fracture surfaces of the composites with different clay loadings: (a) 0% clay, (b) 1% clay, (c) 3% clay and (d) 5% clay [Lin et al., 2006]

In longitudinal direction, flexural modulus was increased whereas flexural strength and strain at break decreased slightly. In longitudinal direction, nanocomposite showed exceptional mechanical properties due to better stress transfer to the glass fibre through matrix. The nanocomposites cohesive microstructures may also impeded the mobility of the epoxy matrix in the glass fiber and epoxy matrix interface or between the silicate platelets and epoxy matrix in

the nanocomposites and allowed better stress transfer to glass fibre. In case of impact testing, impact strength decreased with addition of nanoclay when the impact direction was perpendicular to the glass fiber. However, impact strength was increased with increase in clay loading when impact direction was along the fiber direction. Glass fibre surface became rough with addition of clay and it further increased with increase in clay content (as shown in Figure 2.7). Consequently, more energy required to break. The total energy required to break the nanocomposites when the direction along the fiber was dependent on the matrix properties and on interfacial interaction between the epoxy matrix and glass fibers.

Zunjarrao *et al.* (2006) studied the effect of various processing methods and different nanoclay loading on the mechanical properties of epoxy based nanocomposites. The epoxy resin, curing agent and nanoclay used were Epon 862, Epikure 3274 and Nanomer I.30E respectively. High speed shear disperser and ultrasonic agitator were used for proper dispersion of nanoclay in the epoxy matrix. Mechanical stirrer was used to disperse nanoclay into the preheated epoxy resin (at 60 ℃ for 1 h). The mixture was processed with either the high speed shear disperser or the ultrasonic agitator for 30 min., 65 ℃ temperature was maintained throughout processing. Degasification was done for 12 h. The hardener was mixed gently (to avoid entrapment of air bubble). Curing and post curing was done at room temperature for 24 and at 121 ℃ for 6 h. The density of epoxy-clay nanocomposites increased with increase in clay loading. The density value was increased by 2 % upon addition of 6 % volume fraction of nano clay (see Figure 2.8 (a)).

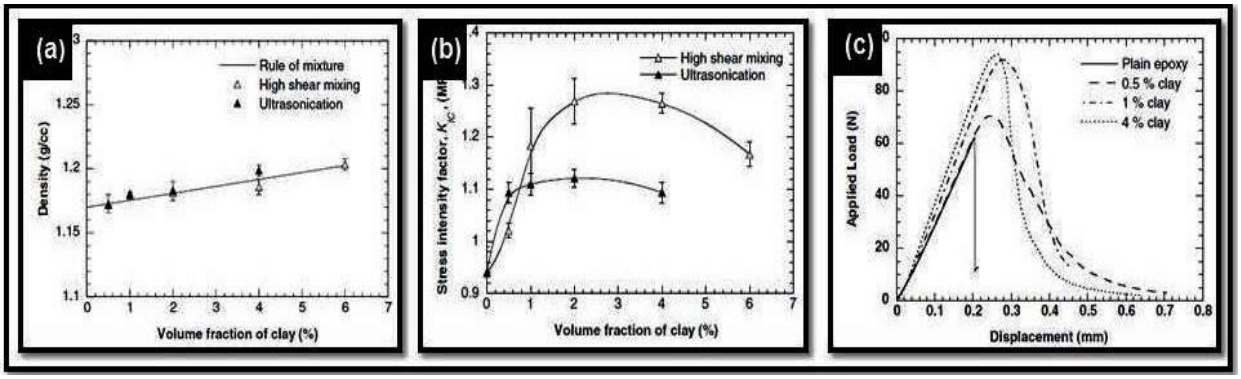

Fig 2.8: Variation of density as a function of volume fraction of clay for epoxy-clay nanocomposites (a) Variation of stress intensity factor as a function of volume fraction (b) Variation of load against cross-head displacement for plain epoxy specimen and nanocomposite specimens fabricated using high shear mixing [Zunjarrao et al., 2006]

The flexural modulus showed increasing trend with increase in nanoclay loading. The increase was more in nanocomposites with low clay loading as compared to higher clay loading. The

nanocomposites processed through HSM showed higher flexural modulus as compared to nanocomposites fabricated using ultrasonication. The nanocomposites processed through HSM showed increase in fracture toughness upto 2 % volume fraction of clay (increased by 35 % as compared to pristine epoxy).

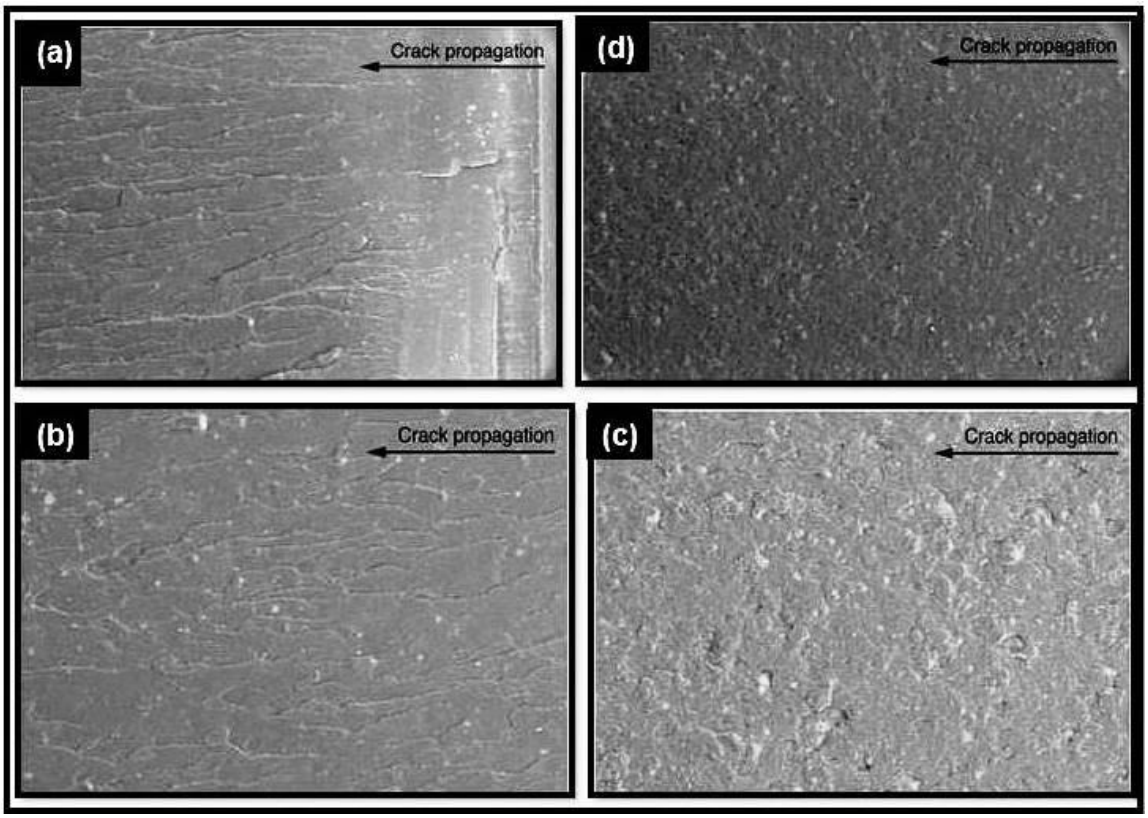

Figure 2.9: SEM micrographs of fracture surface of epoxy-clay nanocomposites (a) 1% clay volume fraction fabricated by high shear mixing, (b) 6 % clay volume fraction fabricated by high shear mixing, (c) 1% clay volume fraction fabricated by ultrasonication and (d) 6 % clay volume fraction fabricated by ultrasonication [Zunjarrao et al., 2006]

It remained constant for volume fraction between 2 % to 4 %. After that, fracture toughness started decreasing with addition of clay content. The nanocomposites processed through ultrasonication showed an increase upto 2 % volume fraction (increased by 20 %) after that start decreasing. The fracture toughness was higher for nanocomposites processed through ultrasonication below 1 % volume fraction beyond that higher for nanocomposites prepared by high shear method (see Figure 2.8 (b)). The pristine epoxy exhibited brittle fracture. The nanocomposites showed a decrease in the load after attainment of the peak load which suggested that there was sub-critical crack growth and that toughening was taking place in nanocomposites (see Figure 2.8 (c)). XRD showed no peaks for nanocomposites processed through high shear mixing. This indicated that complete exfoliation was achieved. The nanocomposites fabricated

by ultrasonication also did not show any peak except nanocomposite with 4 % clay content. The fractured surface of pristine epoxy exhibited a clean surface and indicated brittle fracture. The more river-line markings were observed in nanocomposites with lower clay loading viz. 0.5 % and 1 % nanoclay. Fewer river markings in fractured surface of nanocomposites with 6 % clay volume were indicated large clay agglomerates and reduced fracture toughness (see Figure 2.9).The clay agglomerates were not form in nanocomposites up to 2 % volume fraction processed through high shear mixing and ultrasonication techniques.

Bozkurt *et al.* (2007) studied the effect of MMT and OMMT on the mechanical and thermal properties of the glass fibre reinforced composite. The glass fibre used was woven E-glass. DGEBA epoxy and amine hardener was used as matrix. Epoxy/clay nanocomposite was used as matrix. To prepare epoxy/silicate layered suspension MMT and OMMT in different proportions (1, 3, 6, and 10 wt. %) mixed in epoxy resin. The suspension was mechanically stirred for 1 h for better dispersion of silicate platelets. After mixing, to exfoliate silicate platelets the suspension was hold in ultrasonic bath for 20 min. The hardener was added to the suspension, in last degassing was done. Hand lay-up method was used to prepare glass fibre reinforced composite. Epoxy/silicate layer suspension was applied to the glass fibre with the help of brush. Composites were cured at room temperature, followed by post curing at 150 ℃ (for 2h). X-ray diffraction (XRD) micrographs showed that d-spacing was more in OMMT (18.1 Å) as compared to MMT (14.3 Å). XRD diffractograms showed no peak in both types of nanocomposites (with MMT or OMMT nanoclay). SEM micrographs of fractured surface of pristine epoxy and nanocomposites (with MMT and OMMT nanoclay) were shown in Figure 2.10.

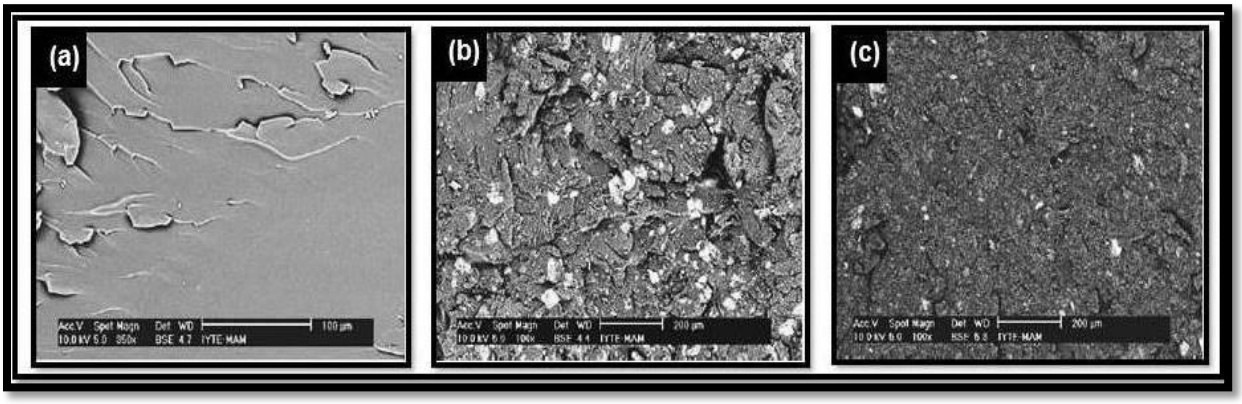

Figure 2.10: SEM micrographs of fracture surfaces of tensile testing (a) neat epoxy, (b) 10 wt. % MMT/Epoxy and (c) 10 wt. % OMMT/Epoxy [Bozkurt et al., 2007]

The SEM image of pristine epoxy (see Figure 2.10 (a)) showed smooth surface indicating brittle fracture. The clay agglomerates were visible in MMT and OMMT incorporated nanocomposites (see Figure 2.10 (b–c)). Clay agglomerates were small in size indicating better dispersion of the silicate platelets and resulted in better mechanical properties. The agglomerates in OMMT/epoxy composites were smaller than MMT/epoxy composites because OMMT dispersed better than MMT and indicating surface modification improved the tendency of clay to disperse uniformly. The tensile modulus remained almost constant up to 6 wt. % of nanoclay (for both MMT and OMMT) as compared to glass fibre reinforced composite. Tensile strength slightly improved for MMT/epoxy composite as compared to OMMT/epoxy composites. This indicated that silicate platelets had no significant effect on the tensile properties of the nanocomposites due to dominating effect of glass fibre reinforcement. SEM micrographs of fractured surfaces of nanocomposites after tensile testing were shown in Figure 2.11.

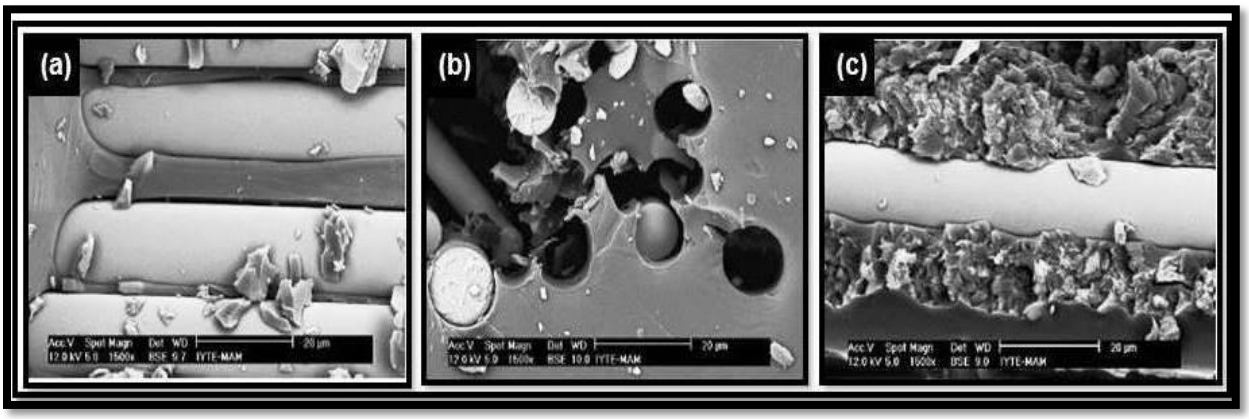

Figure 2.11: SEM fracture surface images of ((a) and (b)) glass fiber/epoxy composites without clay addition and (c) glass fiber/epoxy composites with 10 wt. % clay addition [Bozkurt et al., 2007]

In glass fibre reinforced epoxy composite fracture occurred along the interface and smooth fracture surfaces were seen due to weaker interfacial bonding (see Figure 2.11 (a–b)). In case of epoxy/clay matrix fracture mechanisms were changed due to the presence of silicate platelets (see Figure 2.11 (c)). The fracture modes indicated stronger interfacial bonding in nanocomposites. The flexural properties were increased with addition of clay in it and increase was more in case of OMMT as compared to MMT. The flexural properties increased because clay was present at the surface of the glass fibre made the surface rough, resulted in improved interfacial bonding. The addition of OMMT increased the fracture toughness (K_{IC}), whereas MMT decreased it. As a result of nanoclay loadings along the in-plane directions, fiber pull-out, fiber-matrix debonding, fiber and matrix fracture mechanisms were observed in nanocomposites.

The higher K_{IC} values were observed in nanocomposites with OMMT clay due to better dispersion of nanoclay. The K_{IC} values reduced in nanocomposites with MMT clay due to formation of large clay agglomerates. Glass transition temperature (T_g) increased with addition of OMMT upto 6 wt. % after that it decreased, whereas MMT has no effect on the T_g.

Chow (2007) studied the effect of 3 wt. % clay addition on the barrier properties and glass transition of glass fibre reinforced epoxy clay nanocomposite. The matrix, hardener and nanoclay used were DER 331, HY 2964 and Nanomer 1.30E respectively. Clay was added to the epoxy resin and mechanically stirred for 10 min. The curing agent was mixed for 5 min in the epoxy resin. Hand lay-up technique was used to fabricate glass fibre reinforced nanocomposites. It was cured for 60 min at 100 ℃. XRD results confirmed that silicate platelets were able to exfoliate themselves in the epoxy matrix. It was observed that very slight improvement was observed in the glass transition temperature. The increase was from 101 ℃ to 104 ℃ respectively. The slightly increment of T_g value of nanocomposites may be due to the interaction of OMMT and glass fibre in the epoxy network which could restrict the chain mobility. This can be attributed to confinement of polymer chain as a result of intercalation into the interlayer gallery of the clay. The water uptake property of the pristine epoxy, glass fibre reinforced epoxy composite (without clay), and glass fibre reinforced epoxy clay nanocomposite (3 wt. %) was observed. It was observed that water absorption of all epoxy samples was reached saturation after 35 days. The water uptake of pristine epoxy, glass fibre reinforced epoxy composite, and glass fibre reinforced epoxy clay nanocomposite after 40 days were 2.3 %, 1.1 %, and 1.25 % respectively. Fibre reinforcement in epoxy matrix reduced the penetration of water molecules in composites. However, the incorporation of OMMT in the glass fibre reinforced epoxy based nanocomposite slightly increased the water uptake because octadecylonium ion on OMMT surface reacted with water. The N–H+ groups of alkyl ammonium ions are hydrogen-bonded to water molecules by donating protons to the water-oxygen atoms. The ammonium group may form up to three hydrogen bonds with water molecules. Induction of ammonium group may increase the acid strength of the hydrating water molecules and latter may donate protons to additional water molecules.

Kumar *et al.* (2010) studied the effect of nanoclay addition on the mechanical properties of the epoxy and on the glass fibre reinforced epoxy composites. Epoxy resin, curing agent and clay used were LY-556, HY-951 and 1.28E respectively. Weave glass fiber reel was used having

density 350 g/m^2. Nanocomposites were fabricated with different clay contents (0, 2, 3, 5, 12 wt. %). Clay was mixed in the epoxy resin with the mechanical shear mixer at room temperature for 1 h. After that, curing agent was mixed for 20 min in the above mixture. For making glass fibre reinforced nanocomposites hand-layup technique was used. The closed mould was kept under pressure for 24 h at room temperature. Post curing was done for 1 h at 80 ℃. Tensile strength and modulus were improved by 133 and 58 % respectively in epoxy-clay nanocomposites (at 5 wt. % of clay) as compared to pristine epoxy. In epoxy/clay/glass fibre nanocomposites tensile properties increased upto 5 wt. % of clay after that showed a decreasing trend. At low clay content nanocomposites showed better tensile properties due to partially exfoliated structure. On the other hand, at high clay content the tendency of clay to agglomerate increased, reduced the strength of the nanocomposites by acting as stress concentration sites. The flexural properties of epoxy–clay nanocomposites increased upto 5 wt. % of clay with further addition of clay content it deteriorated the properties. In case of glass fibre reinforced nanocomposites (at 5 wt. % of clay) flexural strength improved by 56.8 % whereas, flexural modulus improved by 103.6 % as compared to glass fibre reinforced nanocomposite without clay. The increasing clay loading enhancing the viscosity of the mixture due to which degassing of mixture became difficult and some small air voids trapped in it. This entrapment of air bubbles made poor dispersion of clay and agglomerates start forming. The clay had much greater modulus than polymer. The stress concentration may exist at the interfaces of the clay and epoxy matrix. In case of, tensile loading cracks started at these weak stress concentration sites consequently, specimen failed at low strains. At high clay loading viscosity was not be low enough to allow monomer to diffuse into the clay layers or particles. Thus agglomeration formed during the curing process of nanocomposites. The Scanning electron microscopy (SEM) micrographs of pristine epoxy (see Figure 2.12 (a)) showed smooth fractured surface indicating a relatively brittle fracture. SEM images at 5 wt. % of clay nanocomposites (see Figure 2.12 (b–c)) showed that clay was well dispersed in the matrix, consequently better properties were achieved in both cases with or without glass fibre. At higher clay contents agglomeration formed which led to high deformability and another reason was higher fractions of clay resulting micro voids (see Figure 2.12 (d–e)) which act as stress concentration factors and facilitate shear yielding in the system and therefore, reduces tensile and flexural properties.

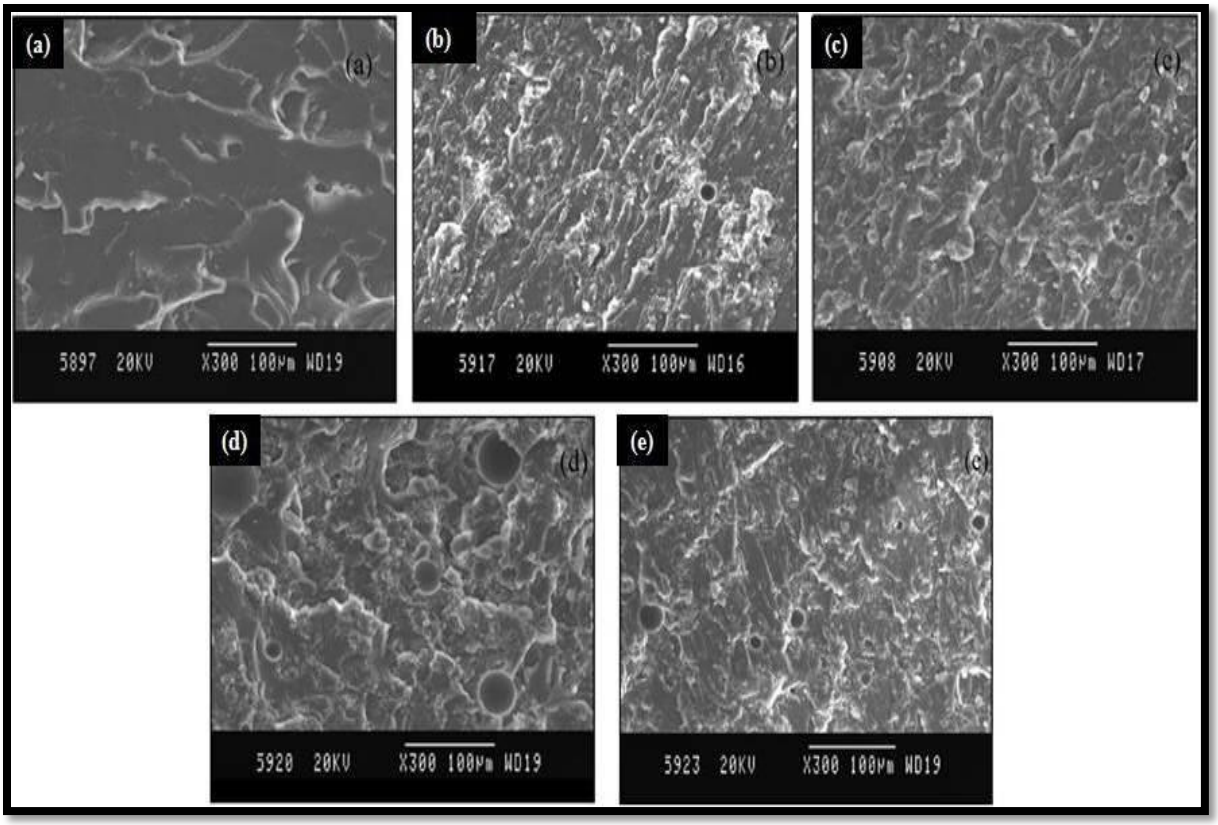

Figure 2.12: SEM micrographs as a function of nanoclay content of (a) neat epoxy, (b) epoxy + 5 wt. % nanoclay, (c) epoxy + 5 wt. % nanoclay + WGFR, (d) epoxy + 12 wt. % nanoclay and (e) epoxy + 12 wt. % nanoclay + WGFR nanocomposites [Kumar et al., 2013]

To conclude, best tensile and flexural properties were achieved at 5 wt. % of clay content in both types of nanocomposites with or without glass fibre.

Lim and Chow (2011) studied the effect of OMMT on the fracture toughness of epoxy based nanocomposites. The resin, hardener and nanoclay used were DGEBA, DER 331 and OMMT respectively. The OMMT clay was dried at 100 ℃ for 12 h. The OMMT (1–5 wt %) clay was mixed in hardener by using mechanical stirrer for 1 h (at 1000 rpm). After that, the mixture was added to the epoxy and mechanically mixed for 5 min (at 100 rpm). The above prepared mixture was kept in mold, followed by degasification at 35 ℃ for 25 min. The nanocomposites were cured at 100 ℃ for 1 h. The d-spacing of pristine OMMT was 2.14 nm. The nanocomposites containing 1, 2, 3, and 4 wt. % OMMT clay showed no diffraction peak. This indicated that exfoliated morphology was observed in all nanocomposites upto 4 wt. %. There was a small diffraction peak was observed for nanocomposite with 5 wt. % of clay loading at a $2\theta = 4.13^{o}$ and corresponding d-spacing was 2.14 nm. This indicated presence of clay agglomerates. These

d-spacing (2.14 nm) between silicate platelets were remained unchanged. The fracture toughness (K_{IC}) showed increasing trend with increase in OMMT loading in nanocomposites (see Figure 2.13). The fracture toughness of 5 wt % OMMT was increased by 80% as compared to pristine epoxy.

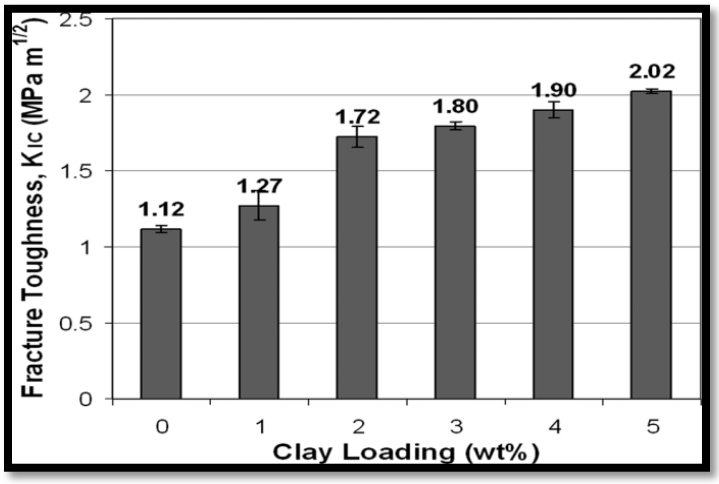

Figure 2.13: Fracture toughness of epoxy nanocomposites as a function of OMMT loading [Lim and Chow, 2011]

The OMMT showed remarkable toughening effect to the nanocomposites because clay size was in nanometer and having high aspect ratio. The fracture toughness was improved for various nanocomposites because stress transfer was uniform and better in exfoliated morphology as compared to other morphologies. The rigid silicate platelets act as stress concentration sites due to different elastic properties as compared to the pristine epoxy. Shear yielding or debonding of the silicate platelet and epoxy interface occured when the local stress exceeds the yield stress of the pristine epoxy or the interfacial strength between the silicate platelets and epoxy matrix. The nanocomposites absorbed large amount of energy before fracturing and resulted in higher fracture toughness values. The presence of clay agglomerates or tactoids at higher loading further increased the toughening effect of nanocomposites. The large clay agglomerates (in microns) enormously increased the effectiveness of clay to stop the crack growth or propagation. The fracture surface of the pristine epoxy which was smooth glassy surface with a few of sharp and straight path running through the material (with almost no deflection) along the direction of crack propagation (see Figure 2.14 (a)). Smaller numbers of shallow shear bands were seen in the epoxy matrix for the nanocomposite (1 wt. % clay) (see Figure 2.14(b)).

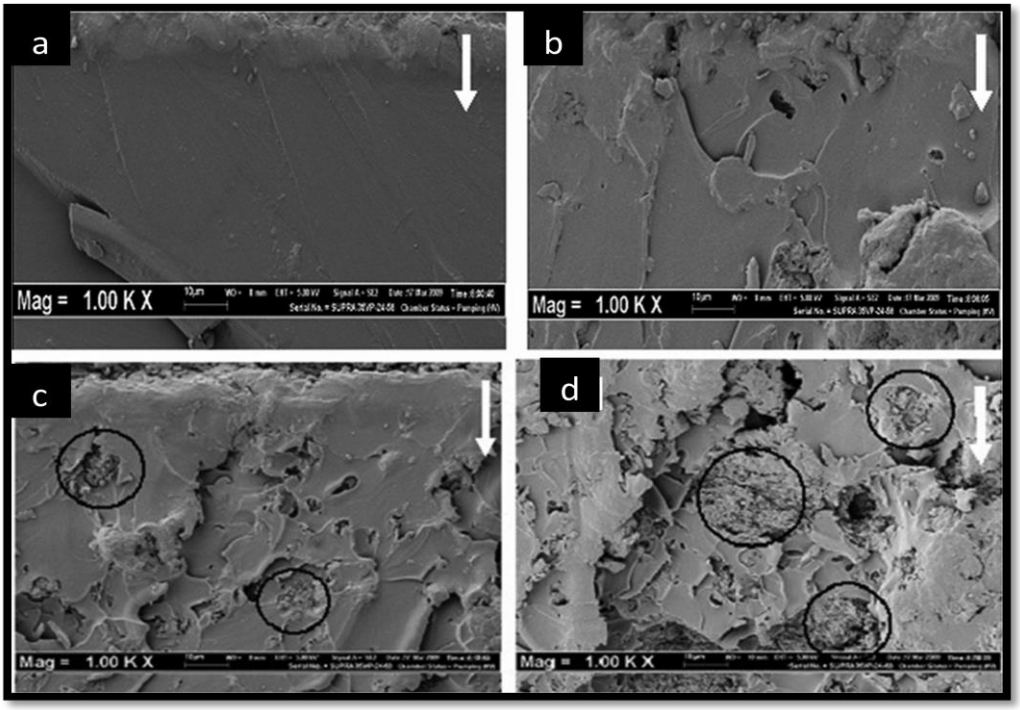

Figure 2.14: FESEM micrographs taken from the fractured surfaces of (a) pristine epoxy, (b) epoxy/1 wt. % OMMT, (c) epoxy/3 wt. % OMMT and (d) epoxy/5 wt. % OMMT nanocomposites [Lim and Chow, 2011]

The much rougher surfaces, deeper shear bands and clay agglomerates were seen in nanocomposites with 3 wt. % and 5 wt. % OMMT. A few voids were observed because only a few parts of the interfaces between the epoxy resin and the silicate platelets were debonded (see Figure 2.14(c) and (d)). This suggested that strong interfacial bonding exists due to exfoliated morphology between epoxy and silicate platelets. The strong interfacial interactions means better stress transfer between epoxy and clay takes place and resulted in more energy absorption before failure.

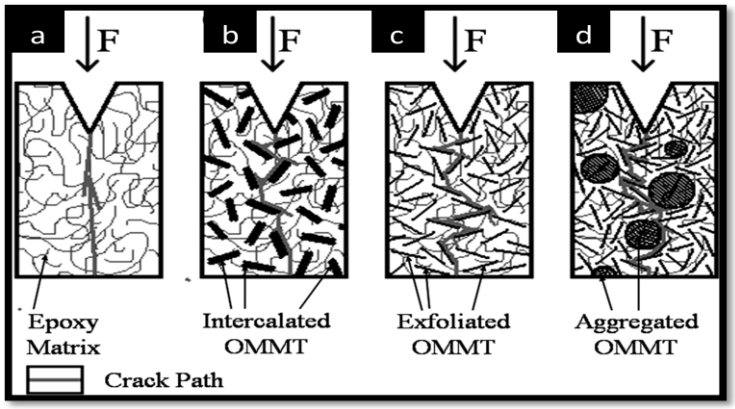

Figure 2.15: The possible mechanism for the crack propagation in (a) neat epoxy, (b) intercalated nanocomposites, (c) exfoliated nanocomposites and (d) epoxy nanocomposites containing clay aggregates [Lim and Chow, 2011]

In pristine epoxy the crack will propagate easily with the least deflection along the direction of crack propagation. The exfoliated or an intercalated morphologies or even clay agglomerates restrict the propagation of cracks and distorted the path of crack. The exfoliated morphology showed more efficient toughening of the nanocomposite as compared to other morphologies. The agglomerated structure further enhances frature toughness (see Figure 2.15).

Bakar *et al.* (2012) investigated epoxy nanocomposite systems to study the effect of modified epoxy [Poly (methyl methacrylate) (PMMA) and montmorillonite (MMT)] on the impact strength (IS), critical stress intensity factor (K_C), flexural strength and strain at break. The epoxy, curing agent, modifier and nanoclay used were Epidian 5, triethylene tetramine (trade name Z1), Poly (methyl methacrylate) (PMMA) and Cloisite 30B respectively. Nanocomposites of three different compositions were prepared (i) Compositions with Cloisite 30B, (ii) Compositions containing poly (methyl methacrylate) and (iii) Hybrid epoxy compositions. The MMT was mixed with acetone to form a 20 % solution. Then, epoxy-based compositions containing 1, 2, and 3 wt% MMT respectively were prepared by means of a homogenizer (15 min at 2400 rpm). These compositions were then kept under vacuum at 40 ℃ to remove air bubbles and residual acetone. The hardener was added, followed by 3 min mixing. The curing and post curing were carried out at room temperature for 24 h and at 80 ℃ for 3 h respectively. A 20 % PMMA solution was prepared in dichloromethane and compositions containing 2.5, 5, 7.5, 10, and 15 wt % PMMA were prepared with epoxy resin by mechanical mixing for 20 min. These were then degassed in vacuum oven at 40 ℃. Hardener was added followed by 5 min mixing prior to pouring into the moulds. Curing and post curing were carried out as previously. Two types of hybrid compositions were prepared having 1 % and 2 % MMT with different amounts of PMMA. Epoxy resin was mixed with MMT (solution in acetone) with the homogenizer at 2400 rpm for 15 min. The solvent was removed at 40 ℃ and then a specific amount of PMMA (as solution in dichloromethane) was added. Mixing of all ingredients was carried out for 15 min and after dichloromethane removal, the hardener was added. The curing and post curing were carried out as for the one-modifier compositions. For composites containing only MMT, Composition containing 1 % MMT exhibited the highest values of IS, $K_{C,}$ facture energy. The improvements in IS, K_c and facture energy were 75 %, 125 % and 100 % respectively in comparison with pristine epoxy resin. The addition of 2.5 % PMMA alone increased IS and K_c by 130 % and 85 % respectively. For hybrid systems, the epoxy nanocomposite containing 1 % MMT and

2.5 % PMMA exhibited maximum IS improvement (approximately 175 % w.r.t pristine epoxy and 55 % w.r.t. nanocomposite containing 1 % MMT only). The hybrid nanocomposite containing 1 % MMT and 5 % PMMA exhibited maximum resistance to crack propagation expressed by the highest value of the K_C parameter. The improvement attained was 125 % and 55 % as compared with K_C of pristine epoxy resin and nanocomposite containing only MMT. The maximum energy of nanocomposite containing 2.5 % PMMA and 1 % MMT was increased by 345 % and 120 % as compared to pristine epoxy samples and samples with only MMT respectively (see Table 2.1).

Table 2.1: The EP properties as function of MMT and PMMA content [Bakar et al., 2012]

MMT content (%)	Impact strength* (kJ/m²)	K_C [MPa(m)$^{1/2}$]*	Fracture energy (kJ/m²)	PMMA content (%)	Impact strength* (kJ/m²)	K_C [MPa(m)$^{1/2}$]*	Fracture energy (kJ/m²)
0	0.95	1.84	1.36	0	0.95	1.84	1.36
1	1.68	4.21	2.75	2.5	2.2	3.41	4.62
2	1.44	4.05	1.9	5	1.77	2.56	3.28
3	1.38	3.39	1.7	7.5	1.3	2.14	2.55
				10	1.1	1.49	1.72
				15	1.03	0.94	0.45

The increase of flexural strength and strain was not so significant with either PMMA or MMT. Indeed, the maximum strength improvement reached only about 15 % with either 1 % MMT or 5 % PMMA in comparison with pristine epoxy resin samples. The flexural strength of hybrid compositions containing 1 % MMT and 2.5 % PMMA was maximally improved by approximately only 13 % in comparison with pristine epoxy resin (see Table 2.2).

Table 2.2: Flexural properties of EP as function of MMT and PMMA content [Bakar et al., 2012]

Compositions with one modifier			Hybrid compositions		
Modifier content (%)	Flexural strength (MPa)	Strain at break (—)	Modifier content (%)	Flexural strength (MPa)	Strain at break (—)
EP	79.4	0.023	1% MMT + 2.5%PMMA	89.9	0.033
EP + 1% MMT	91.5	0.043	1% MMT + 5%PMMA	71.3	0.028
EP + 2% MMT	74.9	0.031	1% MMT + 7.5%PMMA	40.8	0.018
EP + 2.5% PMMA	87.3	0.032	1% MMT + 10%PMMA	27.0	0.011
EP + 5% PMMA	91.4	0.028	2% MMT+ 2.5%PMMA	41.5	0.017
EP + 7.5% PMMA	43.3	0.016	2% MMT + 5%PMMA	43.4	0.018
EP + 10% PMMA	28.1	0.012	2% MMT + 10% PMMA	36.9	0.017

A micrograph of the pristine epoxy fracture surface is flat and glassy indicating the occurrence of a regular crack propagation path and low fracture energies of the tested samples (see Figure 2.16 (a)). The micrograph of epoxy resin containing 1 % MMT and 2.5 % PMMA shows a rough surface along with large domains and well-dispersed MMT particles in the polymer matrix (see Figure 2.16 (b)). The hybrid composition based on 1 % MMT and 5 % PMMA exhibits a different morphology with more homogeneity but less roughness (see Figure 2.16 (c)). The structures for systems with the simultaneous incorporation of 2 % MMT and 2.5 % PMMA as well as 2 % MMT and 5 % PMMA they differ from the previous micrograph for pristine epoxy resin but are similar to hybrid epoxy compositions containing 1 % MMT and 5 % PMMA. The addition of MMT and PMMA resulted in an improvement of IS and critical stress intensity factor (K_C) values.

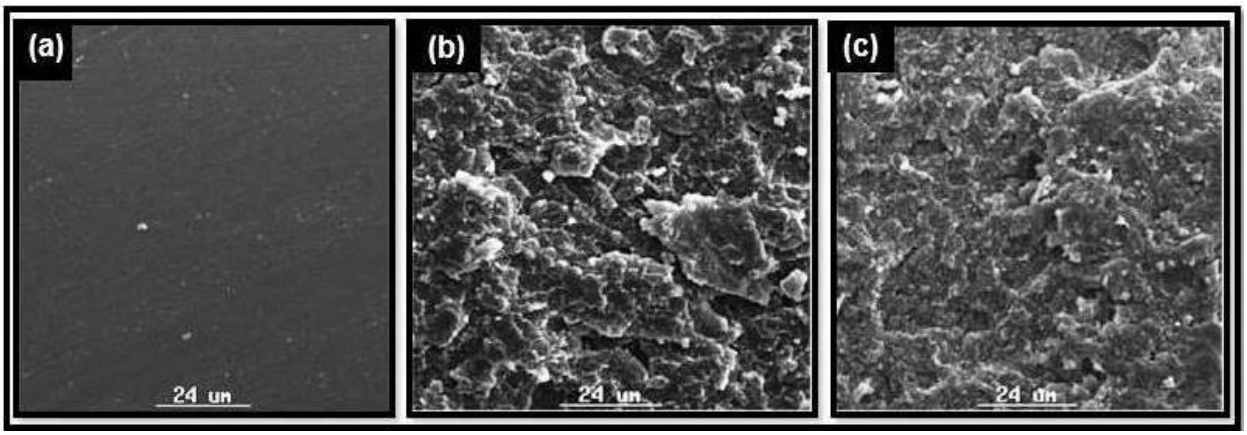

Figure2.16: Micrograph of the impact fracture surface of (a) pristine EP sample (b) hybrid compositions containing 1 % MMT and 2.5 % PMMA and (c) 1 % MMT and 5 % PMMA [Bakar et al., 2012]

To conclude, the addition of MMT and PMMA resulted in an improvement of IS and critical stress intensity factor (K_C) values of the epoxy resin. Hybrid compositions containing 1 % MMT and 2.5 % PMMA exhibited maximum IS. In addition, hybrid composition based on 1 % MMT and 5 % PMMA showed maximum value of K_C.

Al-Qadhi *et al.* (2013) investigated the effect of nanoclay addition on different properties of epoxy-based nanocomposites. The epoxy, curing agent and nanoclay used were DGEBA, IPDA and Nanomer I.30E respectively. The nanoclay (1–10 wt %) was manually mixed with epoxy for 5 min. The nanoclay dispersed into epoxy matrix by using high shear mixer (HSM) at 6000 rpm for 1 h, the temperature was maintained between 35 ℃ to 45 ℃ . After that, degasification was done. The curing agent was gently mixed for 5 min in the mixture. The curing and post curing

was done at 100 ℃ for 1 h and 170 ℃ for 1 h respectively. The XRD micrographs showed absence of diffraction peaks in the pristine epoxy and in nanocomposites. This exhibited either fully or partial exfoliated morphology was achieved. This was also supported by the TEM (see Figure 2.17).

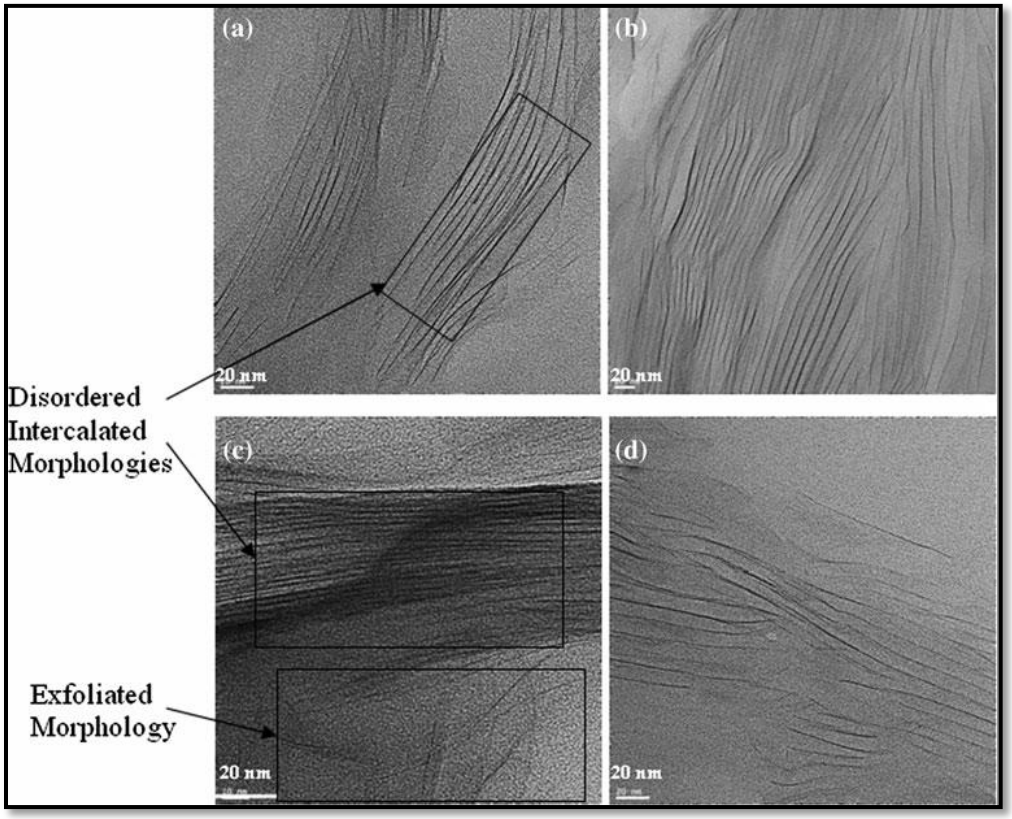

Fig. 2.17: TEM micrographs for nanocomposites containing different clay loadings (a) 1 %, (b) 2 %, (c) 3.5 % and (d) 5 % [Al-Qadhi et al., 2013]

The tensile strength increased upto 1 wt. % clay loading beyond that showed decreasing trend. The fracture strain decreased from 6.02 % to 5.18 % for nanocomposite containing 1 wt. % of clay loading as compared to pristine epoxy. The fracture strain decreased almost linearly with increasing clay loading up to 5 wt. %. The agglomerates increased with increase in clay loading. These tactoids acted as stress sites consequently, reduce the tensile strength and fracture strain. The surface of neat epoxy was smoother. The surface roughness increased with increase in clay loading. The roughness of fracture surfaces changes the direction of crack. Hence, silicate platelets present in nanocomposites impede the crack. The glass transition temperature (T_g) decrease with increase in clay loading, T_g decreased from 152 ℃ to 135 ℃ for nanocomposite (10 wt. % of clay) as compared to pristine epoxy (see Figure 2.18 (a)). The percentage weight

gains increased linearly with square root of exposure time for neat epoxy and nanocomposites containing different clay loadings (upto 40 days). The diffusivity was decreased by 51 % for the nanocomposite (1 wt. % of clay) as compared to pristine epoxy. The negligible improvement was observed in diffusivity for nanocomposites (more than 1 wt. % clay). The large clay agglomerates reduced the efficiency of nanoclay to act as barrier.

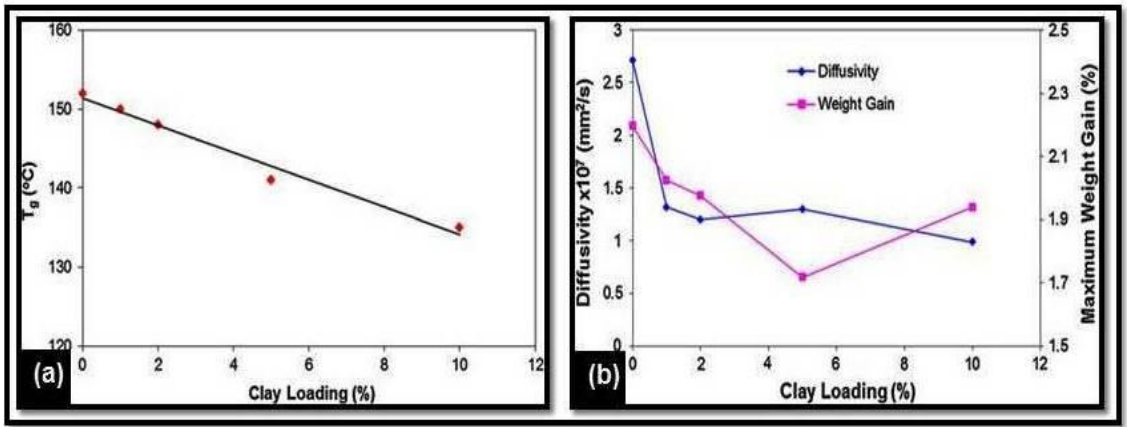

Fig. 2.18: (a) Variation of glass transition temperature with clay loadings (b) Variation of diffusivity and maximum weight gain with nanoclay loading [Al-Qadhi et al., 2013]

The maximum water uptake reduced with addition of nanoclay addition. The water uptake increased above 5 wt. % of clay content (see Figure 2.18 (b)). The mixing technique and degassing process played significant role in the diffusion process.

Kusmono *et al.* (2013) studied the effect of nanoclay addition on various properties of epoxy-clay nanocomposites. The matrix, hardener and nanoclay used were DER 331, polyaminoamide and Nanomer 1.28E respectively. The clay loading was varied as 0, 2, 3, 4, 5 and 6 wt. %. Clay was dried at 80 ℃ for 8 h, and then mixed with resin while mechanical stirring at 75 ℃ for 2 h, followed by degassing for 15 min. The hardener was added to the mixture and mixed at 75 ℃ for 5 min. At last, degasification was done for 10 min. The curing and post curing carried out at 80 ℃ for 2 h and at 150 ℃ for 2 h respectively. The ASTM standards for tensile, flexural, impact and fracture toughness testing were ASTM D638M, D790, D 256-02 and D5045-96 respectively. No sharp peak was observed in the XRD diffractogram of nanocomposite containing 3 wt. % clay content suggesting the complete exfoliation was obtained whereas for nanocomposite containing 6 wt. % clay content, a sharp peak corresponding to $2\theta = 3.54^{o}$ (d-spacing = 2.49 nm) was obtained which suggested an intercalated structure or clay agglomeration. Water absorption

analysis showed that the water uptake increased rapidly during the initial stage followed by reaching a saturation point after 131 days for all nanocomposites.

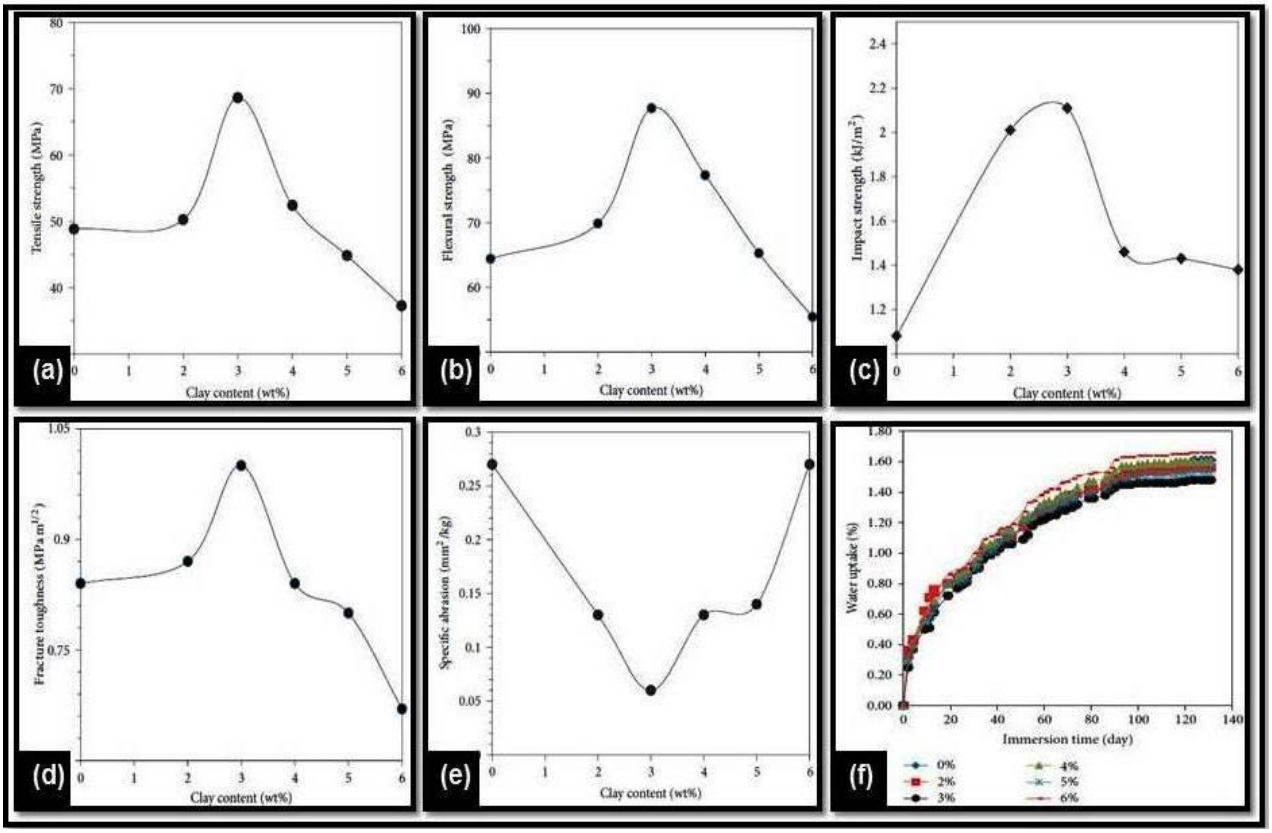

Figure 2.19: Effect of clay content on (a) tensile strength (b) flexural strength (c) impact strength (d) fracture strength (e) specific abrasion (f) weight uptake % of epoxy/clay nanocomposites [Kusmono et al., 2013]

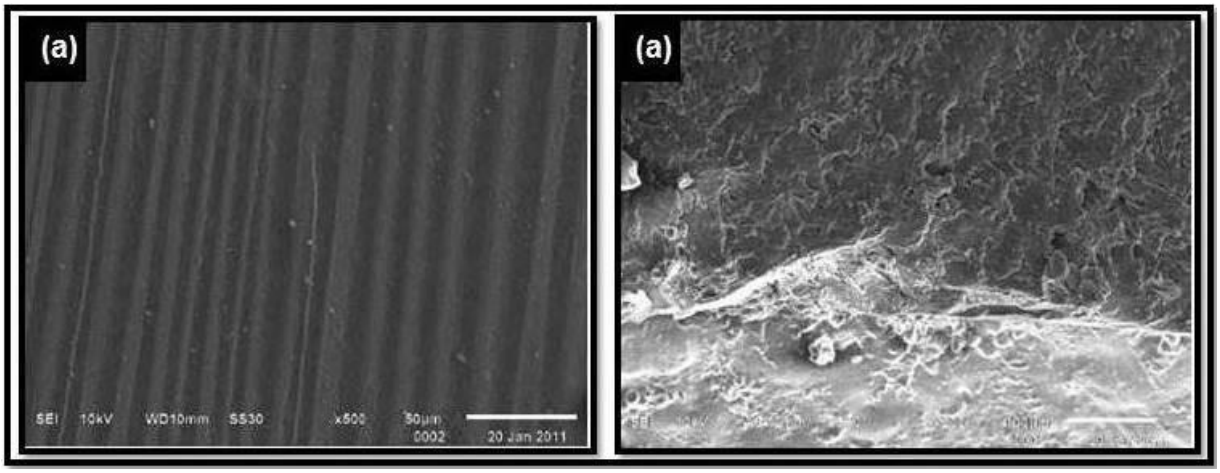

Figure 2.20: SEM micrographs of SEN-3PB fracture surface of: (a) neat epoxy. (b) Epoxy/clay nanocomposite with 3 wt. % of clay content [Kusmono et al., 2013]

Nanocomposite containing 3 wt. % clay exhibited the lowest value of saturation point (1.48 %), indicating best barrier properties attributed to exfoliated clay structure (see Figure 2.19 (f)).

Mechanical strengths (tensile, flexural, impact and fracture toughness) showed maximum improvement corresponding to 3 wt. % clay loading due to the exfoliated structure as confirmed by the XRD. This improvement was 41, 20, 95 and 19 % for tensile, flexural, impact and fracture toughness respectively (see Figure 2.19 (a–d)). Beyond this optimum clay content mechanical properties deteriorated due to agglomeration of clay particles. Specific abrasion showed its minimum value corresponding to the 3 wt. % clay content, attributed to the exfoliated structure (see Figure 2.19 (e)). SEM micrographs showed that the epoxy nanocomposites with 3 wt. % clay content showed increased roughness of the fracture surfaces depicting crack deflection mechanism whereas the micrograph of pristine epoxy sample indicated a brittle fracture (see Figure 2.20).

Al-Qadhi *et al.* (2014) investigated the effect of water and crude oil uptake on different properties of nanocomposites. Fick's and Langmire's models were used for modeling water diffusion into pristine epoxy and its nanocomposites. DGEBA epoxy, isophoronediamine (IPDA) and Nanomer I.30E were used as matrix, curing agent and nanoclay respectively. High shear mixing (HSM) technique was used for processing nanocomposites. The curing and post curing was done at 100 ℃ for 1 h and at 170 ℃ for 1 h respectively. The XRD micrograph showed absence of diffraction peak for nanocomposites with 1, 2, 3.5, 5 and 10 wt. % clay loadings. This indicated that fully or partially exfoliated morphologies were observed. The diffusion constant for water uptake decreased by 51 % for nanocomposite containing 1 wt. % clay as compared to pristine epoxy.

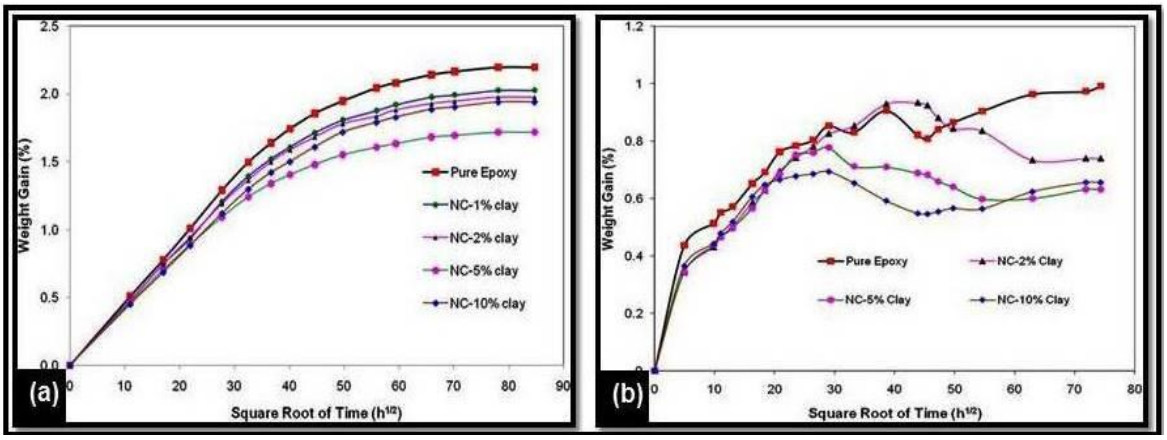

Figure 2.21: (a) Variation of percentage weight gains for neat epoxy and nanocomposites with square root of exposure time in water. (b) Change of percentage weight gains for neat epoxy and nanocomposites with square root of exposure time in crude oil [Al-Qadhi et al., 2014]

The maximum water uptake showed decreasing trend with increase clay loading. It was reduced by 22 % for nanocomposite with 5 wt. % clay as compared to pristine epoxy. The increased clay loading decreased the oil ingress rate and maximum intake. The maximum water uptakes for pristine epoxy and the nanocomposite containing 2wt. % clay were 2.2 % and 1.98 % respectively, which was nearly double than the 1 % and 0.9 % uptake respectively for maximum crude oil uptake (see Figure 2.21).

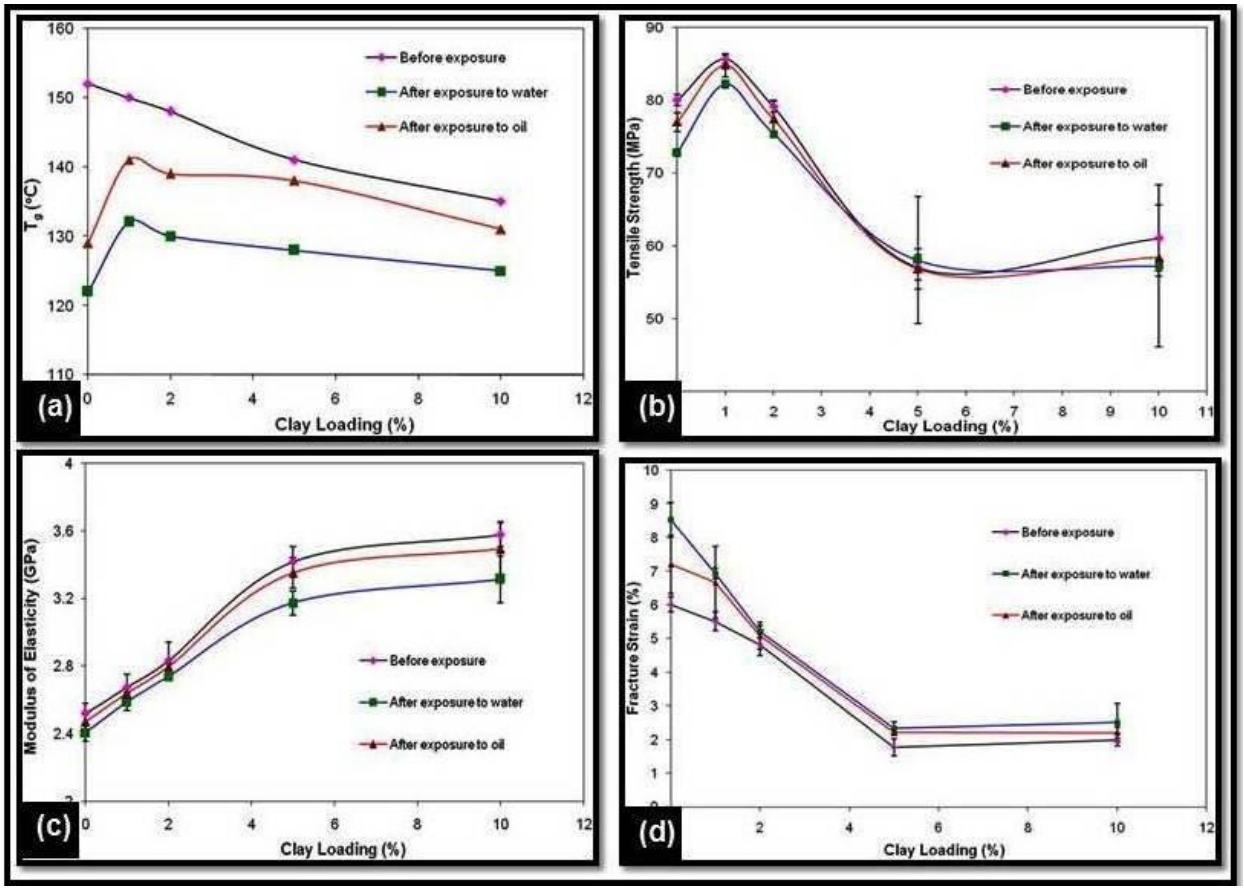

Figure 2.22: (a) Variation of Tg with clay loading for epoxy and nanocomposites before and after water and oil exposure. (b) Variation of tensile strength with clay loading for neat epoxy and nanocomposites before and after exposure to water and crude oil. (c) Variation of elastic modulus with clay loading for pristine epoxy and nanocomposites before and after exposure to water and crude oil. (d) Variation of fracture strain with clay loading for neat epoxy and nanocomposites before and after exposure to water and crude oil [Al-Qadhi et al., 2014]

The Fickian model was followed by diffusion and water absorption of pristine epoxy whereas nanocomposites did not fit into it. However, the results predicted by LMD and experimental data were in good agreement. The degradation in T_g for the neat epoxy was about 30 ℃ and 23 ℃ for saturated water and crude oil uptake respectively, which got reduced to 18 ℃ and 9 ℃ for water and crude oil at 2 wt. % clay loading nanocomposite respectively (see Figure 2.22 (a)). It was

observed that while small reductions in stiffness resulted from crude oil ingress, an obvious decline was observed due to water uptake. Moreover, noticeable increase in fracture strain for pristine epoxy and nanocomposites was observed due to both water and crude oil uptake, with more marked effect of water. After exposing, water and oil molecules acted as plasticizers in epoxy and resulted in reduced strength and modulus, and increased strain. The fracture strain was increased by 42 % and 34 % for pristine epoxy and for nanocomposite with 1 wt. % clay due to water uptake as compared to unexposed specimens respectively (sees Figure 2.22 (d)). The tensile strength of all the formulations decreased when exposed to different medium as compared to unexposed samples at all clay loadings except 5 wt. % nanocomposite (see Figure 2.22 (b)).

Bashar *et al.* (2014) studied the effect of different nanoclays and different processing methods on the properties and morphology of nanocomposites. EPON 826 and EPIKURE 9551 were the used epoxy and hardener respectively whereas the nanoclays used were Nanomer I.30E, Nanomer I.28E and PGW respectively. Two different dispersion methods were used to fabricate the nanocomposites viz (i) mechanical dispersion (ii) ultrasonic dispersion. In mechanical dispersion, the Nanomer I.30E was dried at 120 ℃ for 24 h. Nanoclay was added to preheated epoxy resin at 60 ℃ and mechanically mixed at 900 rpm for 30 min. The hardener was mechanically mixed at 60 ℃ for 5 min in the epoxy-clay mixture. The degassing of the mixture was done with the help of a vacuum pump at 80 kPa for 20 min. Curing was done in an oven at 120 ℃ for 2 h. Nanocomposites were made with this method with I.30E clay loading of 1 wt. %, 2 wt. %, and 3 wt. %. In second method of ultrasonic dispersion, dried clay was added to acetone and the mixture was held for 6 h. After that, the solution was added to the preheated epoxy at 60 ℃ and subsequently sonicated at 80 ℃ for 8 h. After that the solution was mechanically blended for 2 h. Acetone was removed from the solution by vacuum extraction. Finally, hardener was added to the solution, as done in mechanical dispersion. Nanocomposites were prepared with this method for the same clay loading of I.30E. Also for this method, nanocomposites were prepared similarly for I.28E and PGW clays respectively. X-Ray Diffraction (XRD) showed no sharp characterstics diffraction peak for nanocomposites produced by ultrasonic mixing containing 1 wt. % and 2 wt. % I.30E clay but the composite with 3 wt. % clay showed a distinct peak revealing an interlayer spacing of (d_{001}) = 2.73 nm. All nanocomposites fabricated by mechanical dispersion method showed sharp peaks giving an evidence of intercalated and phase-separated structures. The intergallery spacing of the inorganic PGW clay remained unaltered indicating

that this composite has phase-separated clay structures. TEM images also supported the results of XRD. TEM also showed randomly distributed intercalated clay tactoids in the epoxy that was modified with the I.28E clay and larger clay microaggregates for the composite made with the unmodified PGW clay (see Figure 2.23).

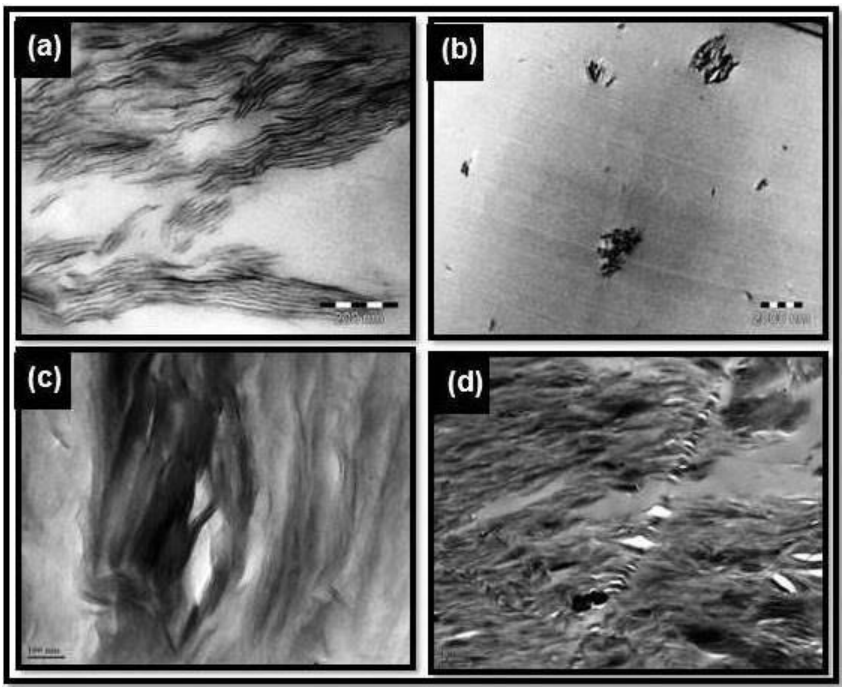

Figure 2.23: TEM micrographs of nanocomposites containing (a) 1 wt. % I.30E made by ultrasonic dispersion (b) 1 wt. % I.30E made by mechanical mixing (c) 1wt. % I.28E (d) 1 wt. % PGW [Bashar et al., 2014]

The tensile modulus and strength of the pristine epoxy were measured to be 2.8GPa and 82MPa respectively. Amongst the three nanoclays, I.30E was used for preparing nanocomposites for further investigations because this nano filler with ultrasonic dispersion method showed maximum improvement in d-spacing of the composite system (see Table 2.3).

Table 2.3: Clay, organic modifier, *d*-spacing and corresponding nanocomposite morphology [Bashar et al., 2014]

Clay	Organic modifier	*d*-spacing of the organoclay, d_{001} [a]	Morphology and *d*-spacing of the organoclay (1 wt%) in cured epoxy[a,b]
I.30E	$CH_3(CH_2)_{17}NH_3^+$	2.23 nm	10~15 nm, exfoliated/intercalated (U) (measured by TEM) 2.68 nm, phase-separated (M)
I.28E	$CH_3(CH_2)_{17}N(CH_3)_3^+$	2.39 nm	2.85 nm, intercalated (U)
PGW	None	1.24 nm	1.24 nm, phase-separated (U)

[a] Interlayer spacing was measured using the prominent diffraction peak from XRD traces.
[b] U: ultrasonic mixing; M: mechanical mixing.

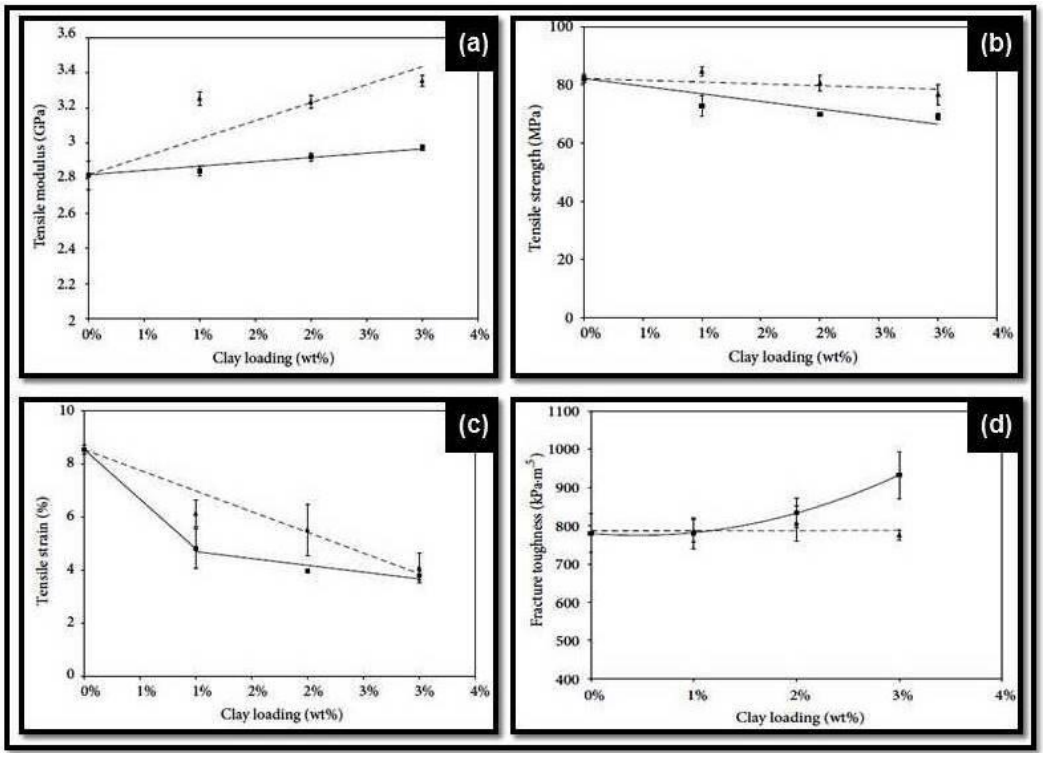

▲ ultrasonication mixing, ■ mechanical mixing.

Figure 2.24: Influence of I.30E clay concentration on (a) tensile modulus (b) tensile strength (c) tensile strain (d) fracture toughness of nanocomposites [Bashar et al., 2014]

The tensile modulus of the nanocomposites prepared by ultrasonic blending increased by 20 % in nanocomposite containing 3 wt. % I.30E nanoclay. Stiffness improved slightly in the nanocomposites processed by a mechanical agitator for the same clay loadings (see Figure 2.24 (a)). Tensile strength values remained almost unchanged for samples formulated by ultrasonic mixing. Nanocomposites made by mechanical mixing method exhibited a considerable loss in tensile strength (see Figure 2.24 (b)). Strain values at break reduced significantly with the addition of clay nanoparticles in the epoxy matrix for all clay nanocomposites. The reduction in tensile elongation is believed to stem from an embrittlement effect caused by the stiffer clay nanofillers in the epoxy network (see Figure 2.24 (c)). Fracture toughness remained almost same for pristine epoxy and nanocomposites prepared by ultrasonic dispersion. The fracture toughness increased substantially for nanocomposites prepared by mechanical dispersion method (see Figure 2.24 (d)). Similar behavior was also observed for the critical stain energy release rate. The fracture surfaces of the nanocomposites made by blending I.30E clay using the ultrasonic dispersion method exhibited epoxy network penetration in between the silicate layers which

correlated well with the intercalated morphology. The fracture surface of mechanically mixed nanocomposites showed phase-separated clay structure and agglomerated clay of various sizes.
To conclude, TEM and XRD analysis of the nanocomposites revealed the creation of partly exfoliated and laminated silicate layers by ultrasonic dispersion and a mixture of intercalated and phase-separated clay agglomerates by mechanical blending. Full exfoliation was not achieved in any of the nanocomposite systems. Fracture toughness was found to be independent of silicate layer separation. The nanocomposites fabricated by mechanical dispersion method showed more resistance to fracture.

Rafiq *et al.* (2014) investigated the effect of nanoclay addition on the mechanical properties of glass fibre reinforced nanocomposites. The matrix, curing agent and nanoclay used were GY 6010 RS, Isophoronediamine (IPDA) and Nanomer 1.30E respectively. The clay loading was varied as 0, 1.5, and 3 wt. %. High shear mixer was used for homogenous mixing of silicate layers in the epoxy resin. The mixture was dried in the oven for 12 h and after that hardener was added to mixture and mixed with the help of stirrer. Glass fibre reinforced nanocomposites fabricated by using hand lay-up. XRD micrographs confirmed that fully or partially exfoliated morphology was achieved. The flexural modulus and strength both showed the similar trend. Both of these properties showed increasing trend upto 1.5 wt. % beyond it showed the decreasing trend. The flexural modulus and strength increased by 23 % and 15 % respectively at 1.5 wt. % of clay addition. The higher stiffness of silicate platelets improved the reinforcing ability of the matrix. The silicate platelets were present at the glass fibre surface and resulted in strong interfacial bonding between glass fibres and epoxy matrix consequently, flexural properties improved. Fully or partially exfoliated morphologies resulted in better reinforcement as compared to other morphologies. The addition of nanoclay improved fracture toughness by 77 % at 1.5 wt. % loading. The fracture toughness improved due to strong interfacial interaction. The presence of silicate platelets in matrix also deflects the crack. The improved interfacial bonding resulted in better stress transfer between the glass fibre and epoxy matrix. However, the major contributor towards toughening is thought to be crack deflection and the presence of silicate platelets act as an obstacle for crack propagation. The homogenous dispersion of nanoclay in epoxy matrix became very difficult at higher clay loading due to increase in viscosity and resulted in clay agglomeration. These tactoids or agglomerates acted as stress concentrators for

crack initiation. These clay agglomerates deteriorate the interfacial bonding between glass fibre and epoxy matrix.

Sharmila *et al.* (2014) studied the effect of nanoclay in improving various properties of Cloisite epoxy nanocomposite (CPN). The epoxy, curing agent and clay used were Araldite GY 250, triethylenetetramine and Cloisite 93A respectively. CPN (0–5 phr of nanoclay) were processed by using mechanical stirring (45 min) and sonication (30 min). After that, degasification was done for 30 min. Curing agent was mixed into the epoxy resin (for 5 min.), followed by degassing. Nanocomposites were cured and post cured for 24 h at room temperature and for 4 h at 80 ℃ respectively. The basal spacing of pristine nanoclay was 2.372 nm ($2\theta = 3.722^{o}$). No peak was observed for 0.5 phr and 1 phr clay loading which suggested that exfoliated morphology may be obtained. At a higher loading (5 phr Cloisite) peak was observed that indicated increase in inter layer spacing (intercalated structure). Transmission electron microscopy (TEM) confirmed the XRD results (see Figure 2.25). The tensile and flexural strength of epoxy composite (without clay) was 54 MPa and 64 MPa respectively. The tensile strength, flexural strength and elastic modulus of nanocomposite with 1 phr Cloisite increased by 15 %, 23 % and 19 % respectively as compared to pristine epoxy. The hardness of CPN at 1 phr clay loading was increased by 37 % as compared to pristine epoxy. Nanocomposites with lower clay loading showed improvement in tensile strength, elastic modulus, and hardness because nanoclay was uniformly distributed at low clay loading and resulted in strong interfacial bonding between the silicate platelets and the epoxy matrix.

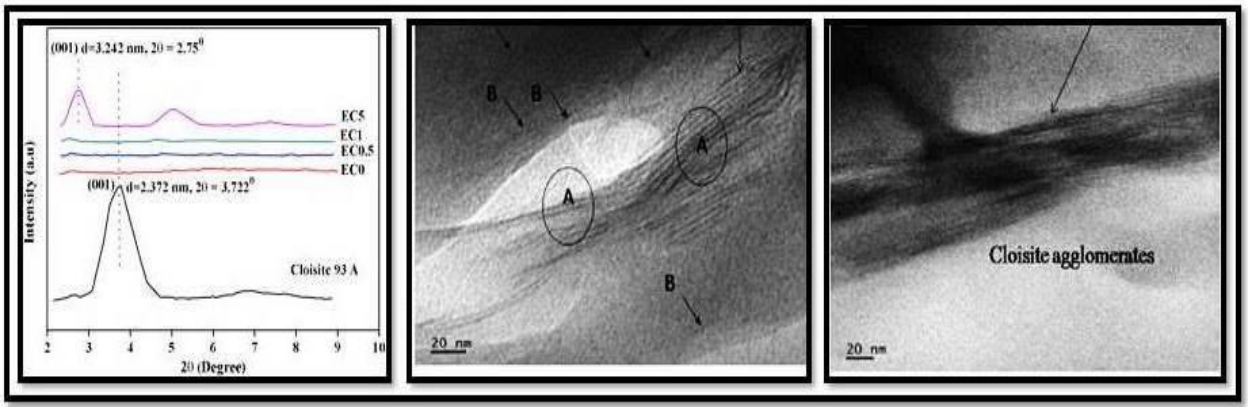

Figure 2.25: (a) XRD pattern of Cloisite 93 A and Cloisite epoxy nanocomposites (ECX), where X indicates the amount of Cloisite content in phr. (b) TEM micrograph of Cloisite epoxy nanocomposite system containing 1 phr Cloisite. Intercalated structure and exfoliated structure present in the microstructure of CPN is marked by A and B respectively (c) TEM micrograph of cloisite epoxy nanocomposite system containing 5 phr Cloisite [Sharmila et al., 2014]

SEM images showed that pristine epoxy resin showed a relatively smooth surface, no resistance to crack propagation and indicated brittle fracture. The fractured surfaces of nanocomposites with nanoclay looked rougher and restricting crack propagation. The barrier properties of nanocomposite with 5 phr nanoclay in acidic, aqueous, and basic medium were improved by 50, 61 and 45 % respectively. The tensile and flexural strength of nanocomposites at lower clay loading increased due to cross-linking in the matrix due to nanoclay infusion. Glass transition temperature (T_g) was higher for the nanocomposite with 1 phr loading and higher loading of nanoclay reduced T_g as compared to that of pristine epoxy. The strong interfacial bonding between the epoxy and silicate platelets resulted in higher T_g because silicate platelets in the matrix reduced the flexibility of the matrix. Polymer chains in this region were restrained and segmental motion near the organic and inorganic interfaces decreased. Nanoclay present in the epoxy matrix also hinder the mobility of epoxy monomers and resulted in increased T_g values. However, at higher nanoclay loading the glass transition temperature decreased because more intercalated sites were seen as well as due to the plasticizing effect of the organic content in nanoclay.

Vijayan *et al.* (2015) investigated and compared the solvent uptake of liquid rubber toughened layered silicate reinforced epoxy nanocomposites. The epoxy, curing agent, accelerator and nanoclay used were GY250 grade, HY906, DY062 and Nanomer I.28E respectively. Three types of nanocomposites were prepared viz. epoxy-clay nanocomposite, epoxy-CTBN nanocomposites, and epoxy-clay-CTBN nanocomposites. Epoxy resin mixed with CTBN (10–20 phr) for 10 min. and resulted in epoxy-CTBN blends. Hardener and catalyst were then added and mixed well for 10 min. The epoxy, curing agent and accelerator were mixed in the ratio 100:80:1 respectively. The mixture was then poured into a preheated mold and cured. The epoxy/clay nanocomposite was prepared with 3 phr. The nanoclay was mixed with epoxy using mechanical stirrer for 30 min followed by homogenization for 10 min. Degasification of the mixture was done for 2 h. Similar steps were followed for epoxy-clay-CTBN nanocomposites. Degasification was followed by CTBN mixing into the mixture for 10 min. Nanocomposites were cured at 120 ℃ for 1 h, followed by post curing at 150 ℃ for 1 h and 180 ℃ for 2 h respectively. The fractured surface of the pristine epoxy was smooth and crack propagation was easy in the matrix. Whereas, fractured surface of nanocomposite with 3 phr nanoclay looked rough and indicated that the dispersed silicate platelets imped the fracture propagation (see Figure 2.26 (a–b)).

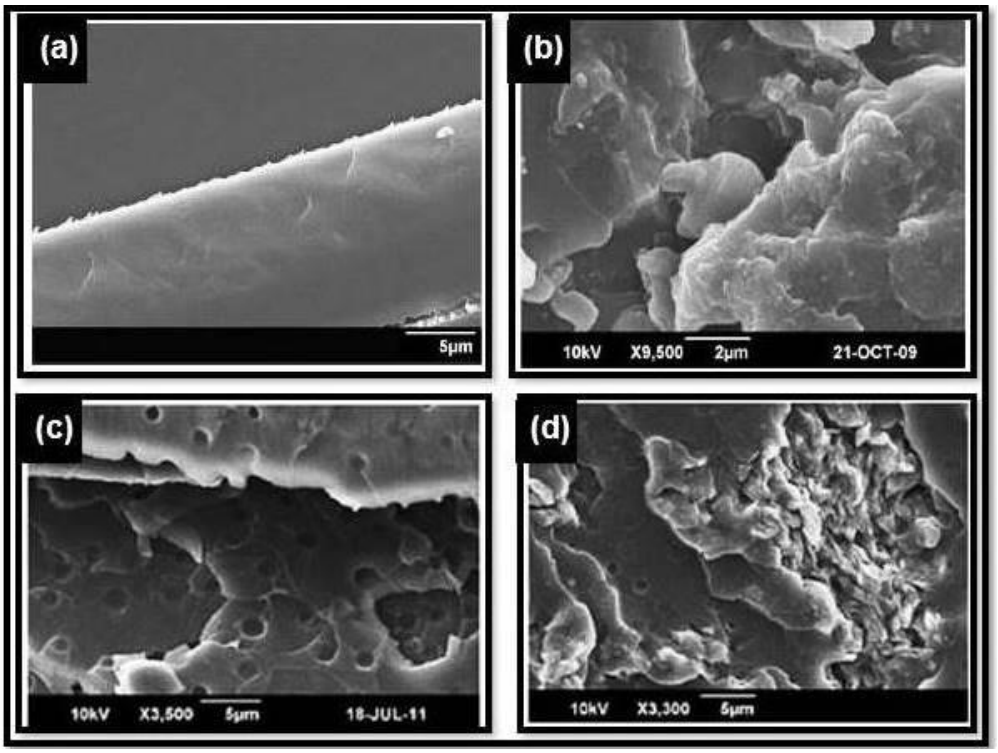

Figure 2.26: SEM images of (a) epoxy, (b) epoxy/3 phr clay nanocomposite, (c) epoxy/CTBN blend with 15 phr CTBN and (d) epoxy/3 phr clay/CTBN nanocomposites with 15 phr CTBN [Vijayan et al., 2015]

The fractured surfaces of the epoxy-clay-CTBN nanocomposites showed much rough surface indicated fine dispersion of silicate platelets along with the phase-separated CTBN particles. The size of the CTBN in epoxy-clay-CTBN nanocomposites was smaller as compared to epoxy-CTBN blend (see Figure 2.26 (c–d)). It was found that glass transition temperature (T_g) of the nanocomposites decreased with increase in CTBN content. The lowering of T_g was due to the dissolution of rubber in the epoxy phase and was increased with an increase in rubber content. The lowest T_g value was observed in nanocomposite containing 15 phr CTBN. After this, the miscibility of the system decreased and T_g for the nanocomposite containing 20 phr CTBN blend started to increase. The T_g of nanocomposite containing 3 phr nanoclay was 12 ℃ higher than pristine epoxy because intercalated morphology of the nanocomposites restricted the mobility of the epoxy network. The diffusion rate of acetone was increased with increase in rubber content from 10 to 20 phr for all formulations. The presence of silicate platelets decreased the acetone uptake. The weight gain of epoxy-clay nanocomposite was less than that for pristine epoxy. But the CTBN in epoxy-clay-CTBN nanocomposites increased the diffusion rate. The diffusion coefficient increased with an increase in CTBN content upto 15 phr loading beyond that it decreased. With a further increase in CTBN, the diffusion coefficient was found to decrease. The

variation of the diffusion coefficient with CTBN content was related to the amount of dissolved rubber. With increase in rubber content the flexibility of the matrix increased and resulted in more solvent diffusion. The phase-separated domains became denser at 20 phr CTBN loading (see Figure 2.26 (c)).

Table 2.4: T_g of the Samples Obtained From DSC Heat Flow versus Temperature Curves [Vijayan et al., 2015]

Sample	T_g (°C)
Neat epoxy	131.85
Epoxy/10Phr CTBN	128.96
Epoxy/15Phr CTBN	124.95
Epoxy/20 phr CTBN	127.03
Epoxy/3 phr clay	143.89
Epoxy/3 phr clay/10 phr CTBN	138.32
Epoxy/3 phr clay/15 phr CTBN	135.24
Epoxy/3 phr clay/20 phr CTBN	139.03

The blend having more than 15 phr CTBN loading formed more zig-zag path for the diffusion as compared to blends having 15 phr CTBN. The epoxy-clay-CTBN nanocomposites showed more zig-zag path, due to the presence of silicate platelets in the epoxy matrix.

Withers *et al.* (2015) investigated the effect of OMMT nanoclay on the epoxy based glass fibre reinforced composites. The matrix, clay and glass fibre used were epoxy, Cloisite 30B and E-glass fibre respectively. For fabricating epoxy–glass fiber (EP–GLF) nanocomposites, Cloisite 30B nanoclay (NC) at a prescribed 2 and 4 wt.% in respect to the epoxy was dispersed using a hot plate/magnetic stirrer at 75 ^{0}C for 30 min in Part B (a blend of Tetraethlyenepentamine and Nonylphenol). Part A (Bispenol-A Type Epoxy Resin) and Part B are mixed manually and applied evenly to both sides of each 6 plies of 305 mm square glass fabric pieces. The balanced and symmetric 6-ply laminate is compressed uniformly between two 305 mm square flat stiff smooth-surface plates under 550 N total force for 24 h at room temperature in laboratory. The pristine epoxy–glass fiber laminate is fabricated and cured similarly without any added nanoclays. The highest values of tensile strength and modulus were achieved in nanocomposite having 2 wt. % nanoclay in it. Nanocomposite without nanoclay showed a more brittle-like matrix behavior that would be more susceptible to failure. The surfaces of the fibers are devoid of a significant amount of epoxy matrix residue and these appeared to be weak fiber-matrix adhesion (as shown in the Figure 2.27 (a)). The fractured surface of nanocomposite containing 2

wt. % clay showed toughened and more ductile epoxy matrix which supported the improved mechanical properties observed for the nanocomposite. The micrograph image (see Figure 2.27 (b)) showed that nanoclay-reinforced matrix to have strong interfacial bonding to the fibers. Consequently, nanocomposite showed improved mechanical properties as compared to the pristine composite material.

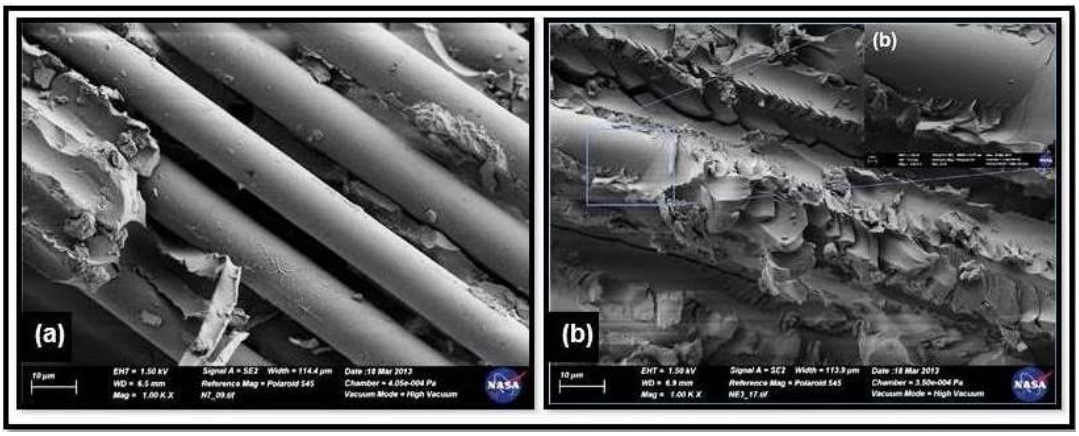

Figure 2.27: Fractured surfaces of (a) glass fibre reinforced composite and (b) glass fibre reinforced epoxy nanocomposite (2 wt.% clay) [Withers et al., 2015]

The addition of 2 wt% nanoclay decreases the average Tg of the EP–GLP composite from 91.5 ^{0}C to 74.5 ^{0}C.

Sharma *et al.* (2016) investigated the effect of addition of silane treated nanoclay on the glass fibre reinforced epoxy layered silicate nanocomposite properties. The matrix, curing agent and nanoclay used were Airstone 780E, Airstone 786H, and Cloisite® 15A respectively. The two different silane agents were used viz. 3-Aminopropyltriethoxy silane (APS) and 3-glycidyloxypropyltrimethoxy silane (GPS). Different amount of silane agents 10, 50, 200, and 400 wt % of nanoclay was to treat the nanoclay. FTIR spectroscopy results verified the grafting of silane agents on silicate platelets. Nanoclay was added to the epoxy resin mixed with help stirrer followed by homogenization and probe sonication for 5 min each. After adding curing agent it was degassed for 1 h. Glass fibre reinforced nanocomposites fabricated using VARIM technique. Curing was done at 70 ℃ for 7 h. XRD micrographs showed no peak for all nanocomposites confirming that clay was exfoliated. The tensile modulus and strength decreased for all nanocomposites containing silane treated nanoclays except AC15(2) and GC15A(2) which increased the tensile modulus marginally. Whereas, tensile strength in both cases were increased by 11 % and 8.5 % respectively. The exfoliated morphology was obtained in both

AC15(2)GFRC and GC15(2)GFRC and resulted in better stress transfer between silicate platelets and epoxy matrix. The functional groups present in silane agents chemically react with both nanoclay and epoxy resin and resulted in formation of a network. This network enhanced the interfacial bonding between them. Nanocomposite containing 200 wt. % silane treated nanoclay showed better flexural properties. AC15(0.1)GFRC, GC15(0.1)GFRC, AC15(0.5)GFRC, GC15(0.5)GFRC formulations showed decreased properties because quantity of silane agent was not enough to cover the large surface area of the nanoclay. In case of AC15(4)GFRC, GC15(4)GFRC visually poor dispersion of silane treated nanoclays in epoxy resin was seen, because of sedimentation of clay during processing and led to reduced strength of composites.

2.2 Summary of the reviewed literature

- Several authors have investigated the effect of nanoclay addition on the tensile and flexural properties of glass fibres reinforced epoxy nanocomposites. They have reported that tensile modulus, flexural modulus, and flexural strength increase with increasing content of the silicate layers. However, different authors report different effects of clay addition on the tensile strength [Kornmann *et al.,* 2005; Lin *et al.,* 2006; Bozkurt *et al.,* 2007; Kumar *et al.,* 2010; Agubra *et al.,* 2013; Rafiq *et al.,* 2014; Withers *et al.,* 2015].

- A few authors have investigated the effect of nanoclay addition on the thermal properties of glass fibre reinforced epoxy nanocomposites and have revealed that glass transition temperature (T_g) increases with addition of OMMT [Lin *et al.,* 2006; Bozkurt *et al.,* 2007; Chow., 2007].

- A few authors have reported that the water uptake of glass fibre reinforced nanocomposites decreased with the addition of the OMMT [Kornmann *et al.,* 2005; Chow, 2007].

2.3 Gaps in the reviewed literature

- A large number of studies have been conducted to investigate the tensile and flexural properties of glass fibre reinforced epoxy based nanocomposites. The authors have reported on the effect of varying clay content on these properties but the reasons for improvements

achieved have not been dealt in detail the structure-property correlation or the mechanisms behind the change/improvement have not been clearly established.

- Very few authors have investigated the effect of silicate platelets addition on the impact strength and fracture toughness of glass fibre reinforced epoxy layered silicate nanocomposites.

- Various researchers have used different curing and post curing temperatures and time period during the processing of nanocomposite systems. The reasons for selecting those particular temperature-time combinations have not been discussed.

Chapter 3

Design of the Study

3.1 Introduction

This chapter covers the overall objective of the present work, the research methodology, basic information regarding nanocomposites and details of equipment used in the experimental work.

3.2 Scope of the Study

The present work developed glass fibre reinforced epoxy based nanocomposites for superior mechanical properties. Glass fibre reinforced nanocomposites have a wide range of applications ranging from electronics goods to aviation industry. Due to the large amount of applications this study has a huge scope and need. Some of the important applications are stated below [Mallick, 2007; kumar *et al.*, 2014]:

- **Electronics:** Circuit board manufacturing (PCB's), electrical motor covers etc.
- **Home Appliances:** Tea tables, sun shades, book racks, show racks, roof sheets, bathtub furniture, and spa tubs.
- **Sporting Goods:** Tennis rackets, bicycle frames, hockey sticks, baseball bats, fishing rods, helmets, javelins, arrows, and many more.
- **Medical industries:** Bone plates for fracture fixation, implants, prosthetics and from instrument enclosures to X-ray beds (where X-ray transparency is important).
- **Automotive industry:** Auto-body components, chassis components, and engine components like body panels, seat cover plates, bumpers, and engine cover etc.
- **Military and Aircraft industry:** Engine cowlings, luggage racks, skins on vertical fin box, fin leading edge, instrument enclosures, bulkheads, ducting, storage bins, and antenna enclosures. It is also widely used in ground-handling equipment.
- **Marine Applications:** Boat hulls, decks, bulkheads, frames, masts, spars, propulsion shafts, rudders.

3.3 Establishing the Objective Function

The present study focuses on the processing and resulting mechanical behavior of glass fibre reinforced epoxy layered silicate nanocomposites. In this study, glass fibre is used as the reinforcement; clay is used as the nano-filler and epoxy as the matrix. Two types of the nanoclays viz organically modified montmorillonite (OMMT) and unmodified montmorillonite (MMT) have been used. The overall objective of the present research is to **evaluate the effect of addition of different nanoclays on the mechanical performance of glass fibre reinforced epoxy based nanocomposites**. In the present work, mechanical properties viz. tensile strengths and modulus, flexural strengths and modulus, impact strength, and fracture toughness of the nanocomposites were evaluated. The key issues that have been taken up during this study are explained below:

- Synthesis of the glass fibre reinforced epoxy based nanocomposites with different concentration levels of nano-filler. Synthesis of nanocomposites was done using the vacuum assisted resin infusion moulding technique (VARIM).
- Evaluation of mechanical properties of various nanocomposite formulations. Also analyzing the effect of nanoclay loading and type on the mechanical properties.
- Characterizing the nanocomposites using XRD, SEM and TEM to determine the morphology (phase separated, intercalated or exfoliated) to draw the structure-property correlation.

3.4 Methodology

The detailed procedure followed during fabrication, testing, and characterization of the glass fibre reinforced epoxy nanocomposites is explained as follow:

- The detailed literature review was conducted to gain basic knowledge in the area and to determine the range of concentrations of nano-fillers used for processing the nanocomposites.
- For fabrication of nanocomposites, first the nanoclay was added to epoxy. Initially, the constituents were hand mixed followed by homogenization and probe sonication.
- The curing agent (hardener) was then added to the epoxy/clay mixture and was mixed with the help of mechanical stirrer.
- The nanoclay-epoxy-hardener mixture was infused into the VARIM set-up. Here, the glass fibre reinforced epoxy based nanocomposites were prepared.
- Mechanical testing of samples of various nanocomposites formulations are done on the UTM and impact tester.

- Characterization of various samples to determine the extent of dispersion of nanoclay.

3.5 Material Selection

This section describes the various constituents are selected for fabricating the nanocomposite systems.

3.5.1 Epoxy Resin

In the present study epoxy-hardener system is used. The epoxy and the curing agent (hardener) belonged to the Araldite family. The epoxy used was **Araldite CY 230-1** having viscosity of 1350–2000 mPa-s and density of 1.1–1.2 g/cm^3 at 25 ℃ and the curing agent used was **Aradur HY 951** having viscosity of 10–20 mPa-s (25 ℃) and density of 0.98 g/cm^3 (20 ℃) supplied by Huntsman Advanced Materials, India. The epoxy and hardener were mixed in the weight ratio of 10:1 (as recommended by the supplier).

3.5.2 Montmorillonite

The clays used were **Nanomer® PGV** (without any organic modification) and **Nanomer® I.28E** (modified with 25-30 wt. % trimethyl stearyl ammonium). Both clays were supplied by the Sigma-Aldrich, India. Nanomer clays are white in color, with aspect ratio of 150–200, active surface area of 750 m^2/g, and minimum mineral purity of 98.5% [http://www.sigmaaldrich.com/].

3.5.3 Glass Fibre

Advantex® E-glass woven roving fiber mat (GF), WR310 was used as reinforcement for fabricating the nanocomposites. The glass fibre was supplied by Owens Corning, India. The properties of glass fibre include density of 2.62 g/cm^3, tensile strength of 3100–3800MPa, and elastic modulus of 80–81GPa.

3.5.4 Concentration of Various Constituents

The concentration of nanomer clays were selected in the range of 0–4 phr (parts per hundred resin) through a detailed literature review [Haque and Shamsuzzoha., 2003; Lin et al., 2006; Bozkurt et al., 2007; Chow., 2007; Kumar et al., 2010; Augbra et al., 2013; Rafiq et al., 2014; Withers et al., 2015]. The maximum limit was selected as 4 phr because it is reported that beyond this clay loading deterioration in mechanical properties takes place mechanical owing

to the possible agglomeration of clay particles due to high clay content. The weight percentage of the glass fibre in the nanocomposite formulations varied between 65–70% (as fraction of the nanocomposite weight). Two plies of glass fibre were used to prepare samples for tensile and flexural testing, whereas twelve plies of glass fibre were used for sample for impact and fracture toughness testing. Table 3.1 shows the clay loading values selected for investigating the performance of nanocomposites.

Table 3.1: Concentration of nanoclay in different nanocomposite formulations

S No.	Clay Type	Clay Loading in phr	Sample Designation
1	–	0.0	N0
2	Nanomer® PGV (without any organic modification)	0.5	NV0.5
3		1.0	NV1.0
4		1.5	NV1.5
5		2.0	NV2.0
6		2.5	NV2.5
7		3.0	NV3.0
8		3.5	NV3.5
9		4.0	NV4.0
10	Nanomer® I.28E (modified with 25-30 wt. % trimethyl stearyl ammonium)	0.5	NE0.5
11		1.0	NE1.0
12		1.5	NE1.5
13		2.0	NE2.0
14		2.5	NE2.5
15		3.0	NE3.0
16		3.5	NE3.5
17		4.0	NE4.0

3.6 Experimental Equipment and Facilities

This section describes the various experimental facilities utilized in the present work.

3.6.1 Homogenizer

Homogenizer system (Make: *IKA T25 ULTRA-TURRAX*, Cole-Parmer, Chicago, US) as shown in Figure 3.1. This was used to ensure uniform dispersion of nanoclay in the epoxy matrix. Its speed ranges from 3000–25000 rpm that enables users to work at high circumferential speeds even with small rotor diameters.

Figure: 3.1 Homogenizer
[Photo courtesy: Chemical Engineering Department, Thapar University, Patiala]

This is used when volume ranges from 1–2000 ml. The dispersion is based on the rotor-stator principle. The rotor is moved with a high circumferential speed. The rotation produces suction, which pulls the medium into the rotor and then pushes it to the outside with help from the stator's teeth. This process results in uniform dispersion of the nano-filler in the epoxy [Web Reference: http://www.ika.com/Dispersing_appl-5.html].

3.6.2 Probe Sonicator

Probe Sonicator (Make: *Q Sonica Sonicators*, Newtown, US) as shown in the Figure 3.2 was used in the present work. Probe sonication is highly recommended for effective processing of nano-materials (nanoclays, carbon nanotubes etc.). The rapid vibration of the tip in the epoxy resin and clay mixture causes cavitation. This results in the formation and collapse of microscopic bubbles. These thousands of bubble collapse at same time and release tremendous energy in the cavitation field. This tremendous energy does not allow the nanoparticles to settle down in the mixture [Web Reference: http://www.sonicator.com/literature/how-it-works.shtml].

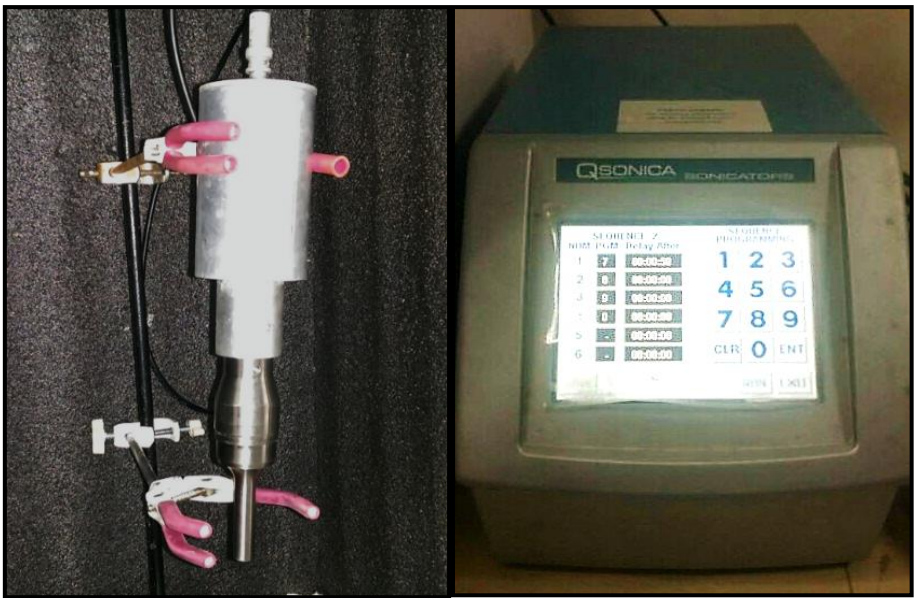

Figure: 3.2 Probe Sonicator
[Photo courtesy: Chemical Engineering Department, Thapar University, Patiala]

3.6.3 Mechanical Stirrer

Mechanical stirrer as shown in Figure 3.3 (Make: REMI Laboratory Instruments, Mumbai, India) was used. Its speed varies between 50–2000 rpm.

Figure: 3.3 Mechanical Stirrer
[Photo courtesy: Chemical Engineering Department, Thapar University, Patiala]

It is used to thoroughly mix curing agent (hardener) to the epoxy/layered silicate suspension after homogenization and probe sonication [Web Reference: http://www.remilabworld.com/Direct_Drive_Stirrers.asp].

3.6.4 Vacuum Oven

The vacuum oven (Make: *MSW-218, Macro Scientific Works Pvt. Ltd*., New Delhi, India) as shown in Figure 3.4 was used in the present work. It is used for out-gassing solids and liquids, vacuum drying, and for post curing.

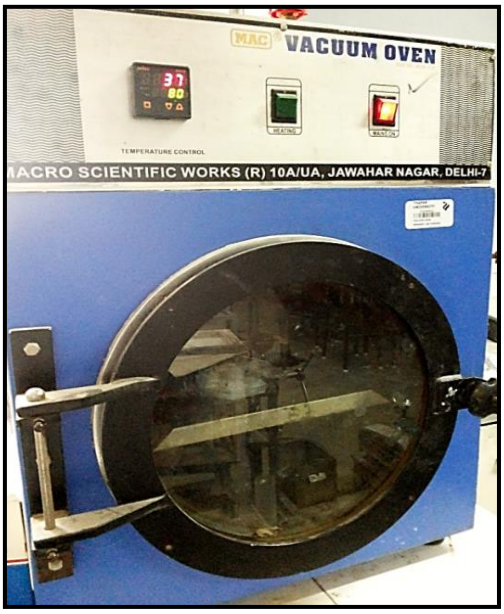

Figure 3.4: Vacuum Oven
[Photo courtesy: Chemical Engineering Department, Thapar University, Patiala]

In the present research, it was used to dry the nanoclay before the fabrication to remove the moisture content from it. There is also facility to create vacuum at high temperature which can be used to remove air bubbles from the epoxy-hardener-clay mixture to make it free from air bubbles [Web Reference: http://www.macroscientificworks.com/ovens-incubators8.html#ove8].

3.6.5 Vacuum Assisted Resin Infusion Moulding (VARIM)

Vacuum assisted resin infusion moulding (Make: *Indutch, Composites Technology pvt. ltd*, India) as shown in the Figure 3.5 was used for fabricating the nanocomposites. VARIM set-up to overcome the problem of leveling and entrapment of air bubbles as are commonly encountered in the hand lay-up method.

Figure 3.5: Vacuum assisted resin infusion moulding (VARIM)
[Photo courtesy: Chemical Engineering Department, Thapar University, Patiala]

The mould table has 1250×1250 mm outer dimensions and 1000×1000 mm working area with a height of 800 mm. This setup is provided with a vacuum pump (capacity of 40 m^3/h). The vacuum pump can continuously work for 6 hours. The maximum temperature of VARIM is 120 °C (for curing purposes) [Web Refrence: http://www.indutch.in/products.html].

3.6.6 Weighing Balance

The digital weighing balance (Make: *CAS*, Korea; Model: CAUW220D) as shown in Figure 3.6 was used. Its weighing capacity is upto 220 g and has a resolution of 0.0001g. Its case material is made of plastic whereas the platform material is stainless steel [Web reference: http://ipelican.com/en/131570].

Figure 3.6: Weighing Balance
[Photo courtesy: Chemical Engineering Department, Thapar University, Patiala]

3.6.7 Universal Testing Machine

The universal testing machine (Make: *Zwick/Roell*, Ulm, Germany, Model: Z010TN, ProLine) as shown in Figure 3.7 is used for conducting different types of tests viz tensile, flexural, and fracture toughness.

Figure 3.7: Universal Testing Machine

[Photo courtesy: Chemical Engineering Department, Thapar University, Patiala]

These tests were performed according to the ASTM standards. The standards used for tensile, flexural, and fracture toughness tests are ASTM D-3039, ASTM D 790–02 and ASTM D 5045–99 respectively. UTM used in the present work has a capacity of 10 kN. This set up also has the provision to alter the speed of the test according to the different standards [Web Reference: http://senselektro.hu/wp-content/uploads/zwick/ProLine.pdf].

3.6.8 Low Capacity Izod Impact Tester

The Izod impact tester (*Make: ATS Faar*) as shown in the Figure 3.8 was used in the present research work. This set-up is available at Central Institute of Plastics Engineering & Technology, this impact tester has a range of 2–25 J.

Figure 3.8: Low capacity Izod Impact Tester
[Photo Courtesy: CIPET, Amritsar]

The least breaking energy given by the tester is 0.001 J. Impact test specimens fabricated according to the ASTM D 256–02 $^{\varepsilon 1}$. V-notch is made in the specimens with the help of notch cutter available at CIPET, Amritsar [Web Reference: http://www.atsfaar.it/].

3.6.9 X-Ray Diffractometer (XRD)

The X-ray Diffractometer (Make: *PANalytical*, Almelo, Netherlands, Model: X'Pert^3 Powder) as shown in Figure 3.9 was used. This set-up is available at Indian Institute of Technology, Ropar. The dispersion of silicate layers in the matrix is ensured with the help of X-ray diffraction micrographs of nanocomposites. It is based on the Bragg's diffraction law as follow:

$$n\lambda = 2d\sin\theta \qquad \text{(i)}$$

whereas, n is an integer, d is the distance between atomic layers in a crystal, λ is the wavelength of the incident X-ray beam and θ is the angle of incidence [Web Reference: http://www.panalytical.com/XPert3-Powder/Specifications.htm].

Figure 3.9: X-Ray Diffractometer
[Photo courtesy: Indian Institute of Technology, Ropar]

Nanocomposites were crushed into powder with the help of grinder and this powder was used for preparing samples for XRD. These micrographs were used to study the dispersion of clay particles in the epoxy matrix. The peak in the XRD micrographs shows that the morphology is either intercalated, or phase separated. However, if there is no peak, it means that exfoliated morphology is obtained.

3.6.10 Transmission Electron Microscopy (TEM)

The transmission electron microscopy was shown in the Figure 3.10 (Make: Hitachi H-7500) and is available at SAIF Labs, Punjab University, Chandigarh. It was operate at 110kV to take the TEM images of various nanocomposites [Web Reference: http://www.hitachi.com/]. Nanocomposites were converted into powder with the help of grinder. The suspensions of powdered nanocomposites were prepared in the ethanol. This suspension was ultrasonicated for 3 hours before preparing sample for TEM. The TEM micrographs are used to study the degree of dispersion of clay particles in the nanocomposites.

Figure 3.10: Transmission Electron Microscopy

[Photo courtesy: SAIF Labs, Punjab University, Chandigarh]

3.6.11 Scanning Electron Microscopy (SEM)

The scanning electron microscopy (SEM) as shown in the Figure 3.11 (Make: *JEOL Ltd, JSM-6510LV*, Tokyo, Japan) is available at SAI Labs, Thapar Technology Campus, Patiala.

Figure 3.11: Scanning Electron Microscope

[Photo courtesy: SAI Labs, Thapar Technology Campus, Patiala]

SEM is used to generate micrographs of the fractured surfaces to determine various mechanisms responsible for change /improvement in the mechanical properties of the nanocomposites. It has magnification in the range of × 5–300000 [Web Reference: www.jeol.com].

3.7 Experimental Procedure

This section focuses on the procedure followed for fabricating the glass fibre reinforced epoxy layered silicate nanocomposites.

3.7.1 Procedure for Fabrication of Fibre Reinforced Nanocomposites

- In the present work, mechanical properties viz. tensile, flexural, impact and fracture toughness were mainly evaluated. For each property, five samples were prepared according to the ASTM standards. For requisite samples for each property, the size of nanocomposite sheet to be fabricated for each composition/formulation was decided.
- Nanocomposite sheets prepared for tensile and flexural test specimens were of dimensions, 30×40×0.7 mm^3 (with two plies of glass fibre mat). Sheet for impact strength and fracture toughness were of dimensions, 30×10×3.2 mm^3(with twelve plies of fibre mat). Each experimental run was for a particular composition (with a specific clay type and loading). In each run for fabrication of nanocomposite, both sheets (30×40×0.7 and 30×10×3.2 mm^3) were fabricated as single big sheet. The weight of the processed nanocomposite (i.e. weight of big sheet) was 290 g. Out this total weight of 290 g, the weight of glass fibre mat used was 200 g.
- The amount of resin (i.e. epoxy and curing agent) was decided on the basis of the weight of the glass fibre being used for fabricating a nanocomposite sheet. The weight of glass fibre used for fabricating the nanocomposite sheet was 200 g. The initial amount of resin infused into the VARIM set-up for fabrication of nanocomposite was twice the weight of the glass fibre (400 g).
- As recommended by the supplier, epoxy and curing agent were mixed in the weight ratio of 100:10. So for infusing 400 g of resin into the VARIM set-up, the amount of epoxy and hardener were calculated as follow:

  Amount of epoxy: (100*400)/110 = 363.64 g (2)

  Amount of curing agent: (10*400)/110 = 36.36 g (3)

The amount of epoxy used was 363.64 g and curing agent used was 36.36 g respectively.

- To this 400 g of resin, the required amount of nanoclay in parts per hundred parts of resin is shown in the Table 2.

Table 3.2: Amount of clay in different nanocomposite formulations

S No.		1	2	3	4	5	6	7	8	9
Clay loading in the resin	in phr	0.0	0.5	1.0	1.5	2.0	2.5	3.0	3.5	4.0
	in g	0.0	2.0	4.0	6.0	8.0	10.0	12.0	14.0	16.0

- Before fabricating each nanocomposite sheet nanoclay was heated in a vacuum oven at 120 ℃ for 18 h to remove the moisture contents from the clay.
- The required amount of epoxy was taken in a beaker; the required amount of clay was added into the beaker and mixed with hand using a stirrer. After hand mixing, homogenization was carried out at 20,000 rpm for 10 minutes. Homogenization was followed by ultrasonication at amplitude of 80 % for 10 minutes. The pulse was on for 40 s and off for 20 s. During ultrasonication, the beaker was placed in the ice bath so that temperature of the mixture does not become very high.
- After mixing the clay, curing agent was added to the mixture at 40 ℃ and mixed with the help of mechanical stirrer for 10 minutes at 500 rpm. Finally, mixture was degassed for 10 minutes to remove the entrapped bubbles from the mixture.
- The resin prepared in the last step was now ready to be infused into the VARIM set-up. For this, VARIM was cleaned with a cleaning agent. Then the releasing agent was applied on it for easy removal of the nanocomposite sheet. Finally, breather was applied on all four sides of the work table for removing air bubbles entrapped in the resin (as shown in Figure 3.12 (a)).
- Glass fibre mats were now placed on the VARIM work table within the breather. A separator sheet was placed on the Glass fibre mats (see Figure 3.12 (b)) followed by placement of a perforated sheet and wire mesh on it (see Figure 3.12 (c)).
- In the last, a plastic pipe was placed on the wire mesh for infusion. Vacuum was created by sealing the VARIM with the help of a plastic laminated sheet. When pressure (vacuum) reached 0 bar, the resin was infused through the pipe. Care was taken that before and after infusion, pipes were made leak proof using tape so that 0 bar pressure is maintained throughout the fabrication process (as shown in Figure 3.12 (d)).

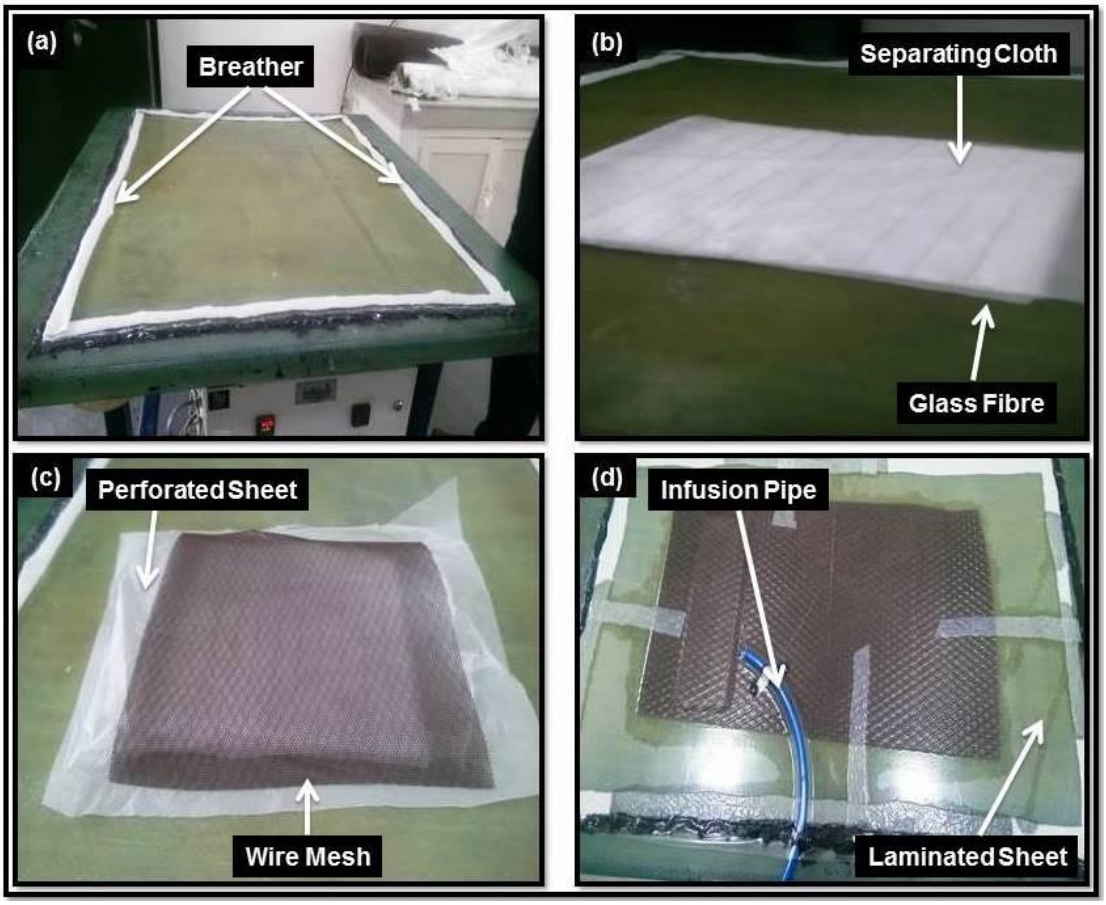

Figure 3.12: Various steps involved in fabricating glass fibre reinforced epoxy layered silicate nanocomposites using VARIM (a) breather for removing entrapped air, (b) glass fibre mat covered with separating cloth, (c) perforated sheet and wire mesh placed on separator and (d) infusing pipe below the laminating sheet

- The curing schedule used for fabricating the nanocomposites were 6 h at room temperature followed by 6 h at 60 ℃ as recommended by the supplier.

3.7.2 Sample Preparation

The samples of evaluating various properties i.e. tensile, flexural, impact strength, and fracture toughness were prepared in the Central Workshop, Thapar University, Patiala. The various steps involved in preparing the samples were as follow:

- The tensile test specimens were prepared according to the ASTM D-3039 (as shown in Figure 3.13 (a)). The length, width and thickness of the specimens were 250 mm, 25 mm, and 0.7 mm respectively.
- The samples for flexural test were prepared according to the ASTM D 790–02 (as shown Figure 3.13 (b)). The dimensions of length, width, and thickness were 60 mm, 12.7 mm, and 0.7 mm respectively.

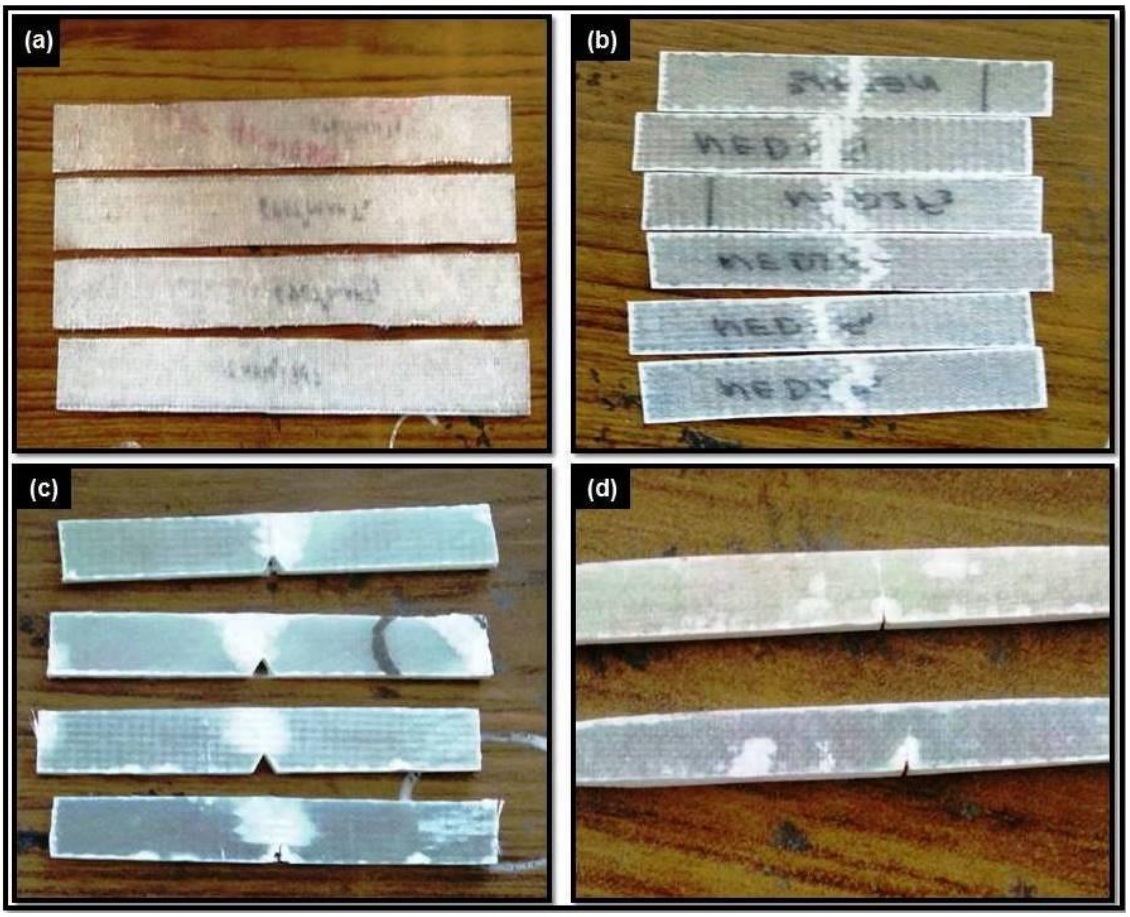

Figure 3.13: Specimens prepared for evaluating various properties (a) tensile specimens, (b) flexural, specimens, (c) impact strength specimens and (d) fracture toughness specimens

- The samples for impact testing were prepared according to the ASTM D 256–02 $^{\varepsilon 1}$ (as shown in Figure 3.13 (c)). The length, width, and thickness of samples were 63.5 mm, 12.7 mm, and 3.2 mm respectively. The notch was cut in the samples with the help of notch cutter available at CIPET Amritsar.
- The fracture toughness samples were prepared according to the ASTM D 5045–99 (as shown in Figure 3.13 (d)). The sample length, width, and thickness were 60 mm, 6.4 mm, and 3.2 mm respectively. The samples were prepared with the help of hand hacksaw. The notch was cut in the specimens with the help of razor blade as mentioned in the standard.

3.8 Summary of the Chapter

This chapter focuses on the design of the current study. This chapter begins with the scope followed by the overall objective and research methodology. The next section of this chapter coveres the detailed information about the constituents (raw materials) used for fabricating the glass fibre reinforced epoxy layered silicate nanocomposites. After that, general

information regarding machines and equipments used in fabrication was mentioned. In the last, detailed procedure of nanocomposite fabrication and sample preparation was discussed.

Chapter 4
Results and Discussion

4.1 Introduction

This chapter presents a detailed discussion of the results obtained after characterization and testing of various formulations of the glass fibre reinforced epoxy layered silicate nanocomposites. For characterizing the nanocomposites, the main techniques used were XRD, SEM and TEM. TEM micrographs were used to study the dispersion of silicate layers in the epoxy matrix. SEM micrographs were used to investigate the fractured surface of specimens after mechanical testing. Finally, the trends observed and reasons thereof in the mechanical properties (tensile, flexural, impact, and fracture toughness properties) with different nanoclays and varying clay loadings have been reported.

4.2 X-Ray Diffraction (XRD) Analysis

XRD micrographs of various nanocomposite formulations were analysed to evaluate the morphologies obtained during processing. Two types of nanoclays, an unmodified (i.e. Nanomer PGV, referred to as NV) and an organically modified (i.e. Nanomer I.28E, referred to as NE)) were used in the present research. XRD micrographs for the two pristine clays and some selected formulations are presented in this section. These include NV (clay powder), NE (clay powder), N0 (the reference sample), NV1, NV2, NV4, NE1, NE2, and NE4 formulations. XRD patterns obtained are shown in Figure 4.1. The NV clay powder showed a peak at a diffraction angle of 3.72° ($2\theta = 3.72°$) resulting in a d-spacing of 23.74 Å. The NE clay powder showed the peak at a diffraction angle of 3.35° resulting in a d-spacing of 26.36 Å. The basal spacing (d-spacing) was more for NE nanoclay as compared to NV because of its organic modification. Organically modified nanoclays show more basal spacing as compared to unmodified [Bozkurt et al., 2007; Das et al., 2011]. Further, for nanocomposite formulations, it was observed that the diffraction peak of nanoclay in various glass fibre reinforced epoxy layered silicate nanocomposites either shifted towards a lower angle or was absent. The diffraction peak was absent in the reference sample (i.e. the glass fibre reinforced epoxy composite without any clay addition) due to the amorphous structure of epoxy resin [Al-Qadhi *et al.*, 2013]. For the nanocomposites, the diffraction peak was absent for nanocomposites containing 1 phr nanoclay (for both NV1 and NE1). This suggested presence

of a fully or a partially exfoliated morphology [Al-Qadhi *et al.*, 2013; Kusmono *et al.*, 2013; Al-Qadhi *et al.*, 2014; Rafiq *et al.*, 2014; Sharmila *et al.*, 2014].

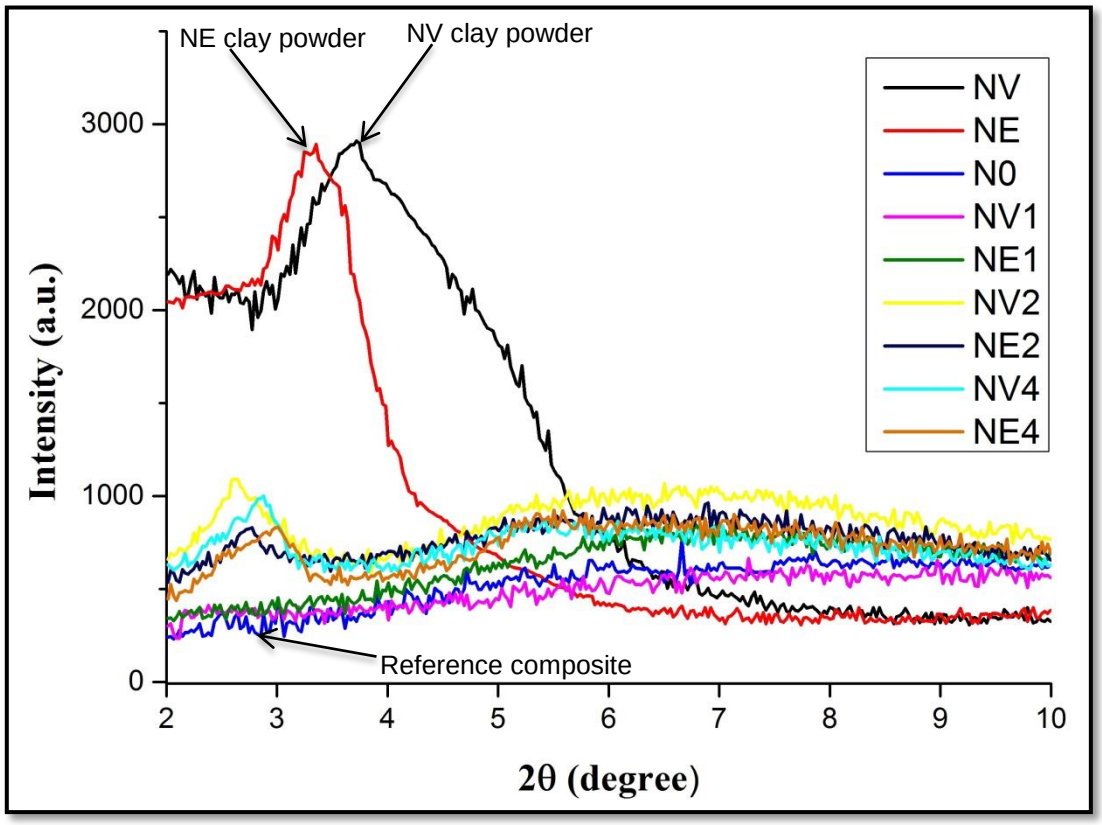

Figure 4.1: XRD patterns of the neat polymer, nanoclays, and nanocomposites

This indicated that epoxy monomers were able to enter into the basal spacing between the clay platelets and resulted in a fully or a partially exfoliated morphology. These results were also supported by TEM micrographs (see Section 4.3 for detailed discussion). For the remaining nanocomposite formulations (NV2, NE2, NV4, and NE4), diffraction peaks were observed. This indicated an exfoliated morphology could not be obtained for these formulations. However, for all such formulations, peaks observed were at an angle lower than what was obtained in case of respective pristine nanoclay powders. This indicated that in all such nanocomposites, an intercalated morphology was obtained [Alexandre and Dubois, 2000; Azeez *et al.*, 2013]. The d-spacing for NV2, NE2, NV4 and NE4 formulations were 33.54 Å (2θ=2.64°), 31.89 Å (2θ=2.77°), 30.66 Å (2θ=2.88°), and 29.34 Å (2θ=3.01°) respectively. The presence of diffraction peak in the micrographs suggested that an intercalated morphology was obtained. Similar type of results were also reported by Kusmono et al. (2013), Bashar et al. (2014), Sharmila et al. (2014). The exfoliation of silicate platelets was impeded beyond 1 phr clay content due to the higher clay content and resulted in an intercalated morphology only. The d-spacing of various nanocomposite formulations

showed a decreasing trend with increase in nanoclay content. At higher clay concentrations, viscosity of the epoxy resin increases and does not allow monomers to diffuse into the basal spacing of silicate platelets and results in intercalated morphology or clay agglomerates [Kumar et al., 2010]. It was observed that unmodified clay (NV) showed more d-spacing as compared to modified clay (NE) in various nanocomposite formulations, which was an interesting observation. The large increase in d-spacing in nanocomposites with NV nanoclay (unmodified clay) was observed in XRD strongly suggest that there is a chemical bonding between the cations exists in the clay galleries of NV clay and the epoxy resin.

4.3 Transmission Electron Microscopy (TEM) Analysis

TEM micrographs of various nanocomposite formulations were analysed to evaluate the degree of dispersion of silicate platelets in the epoxy matrix. Two types of nanoclays viz. the unmodified (i.e. Nanomer PGV, designated as NV) and the organically modified (i.e. Nanomer I.28E, designated as NE) were used in the present work. TEM micrographs were obtained for N0, NV1, NV2, NV4, NE1, NE2, and NE4 formulations (see Table 3.1 for designation details). Figure 4.2 (a–b) show the TEM micrographs of the neat epoxy.

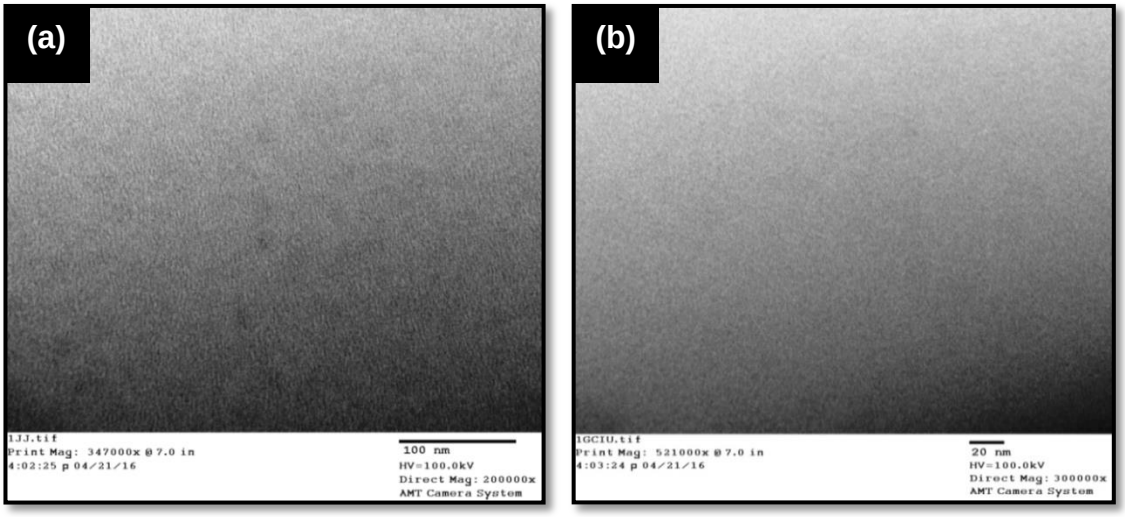

Figure 4.2: TEM micrographs of the neat epoxy at two different magnifications of (a) 200000 X, and (b) 300000 X

The micrographs were absolutely clear conforming the absence of the silicate platelets in the reference sample i.e. N0 composition.

Figure 4.3 and Figure 4.4 show the TEM micrographs of glass fibre reinforced epoxy based nanocomposites containing 1 phr nanoclay. Figure 4.3 (a–b) is for unmodified clay (NV1) whereas Figure 4.4 (a–b) is for organically modified clay. It can be observed from the micrographs that for nanocomposites with 1 phr clay, the silicate platelets were

homogenously dispersed in the matrix. The dark black lines (Figure 4.3 and Figure 4.4) are representing the clay platelets (encircled in red colour) and the grey background is representing the epoxy matrix [Chung *et al.*, 2009; Ha *et al.*, 2010]. Clay was observed to be present in the form of layers and these layers were stacked one over the other [Chung *et al.*, 2009; Mouloud *et al.*, 2012]. For the NV1formulation, Figure 4.3 (a–b) reveals that the silicate platelets were not parallel to each other (were randomly distributed) and the distance between the platelets was also not uniform. This indicated an exfoliated morphology for the NV1 composition [Al-Qadhi *et al.*, 2013].

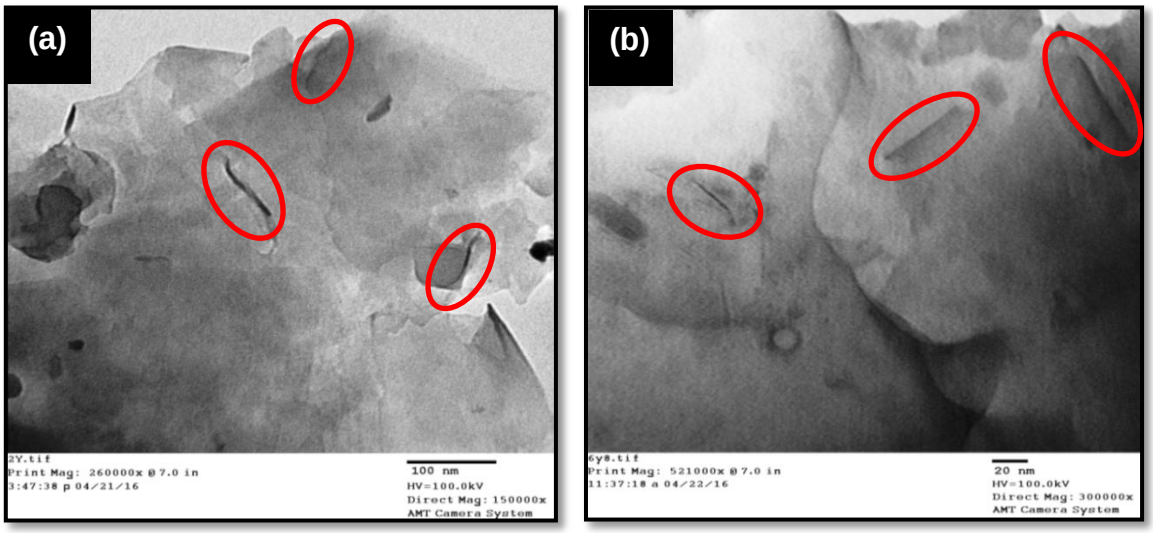

Figure 4.3: TEM micrographs of the glass fibre reinforced epoxy layered silicate nanocomposite with 1phr clay showing NV1 at (a) 150000X, and (b) 300000X

For NE1composition, the TEM micrographs (Figure 4.4) showed a partially exfoliated morphology.

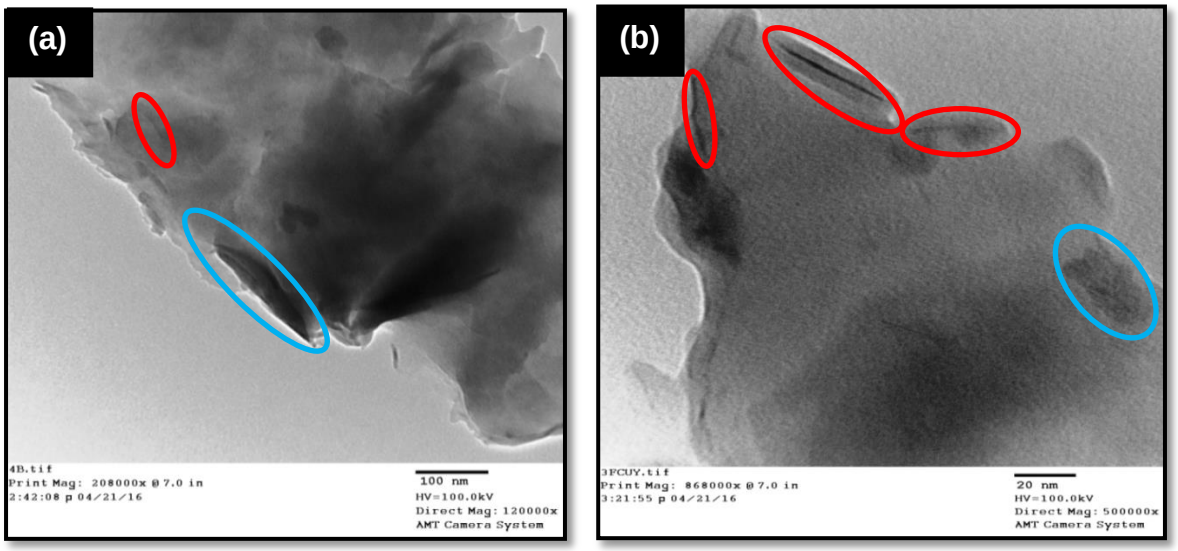

Figure 4.4: TEM micrographs of the glass fibre reinforced epoxy layered silicate nanocomposite with 1phr clay showing NE1 at (a) 120000X, and (b) 500000X

In some regions, the clay layers were still parallel to each other (regions encircled in blue colour in Figure 4.4) whereas in other regions, the clay layers were randomly distributed (regions encircled in red colour in Figure 4.4). This indicated a partially exfoliated morphology for NE1 composition. Thus, NE1 composition showed partial rather than complete exfoliation [Camino *et al.*, 2005; Al-Qadhi *et al.*, 2013; Sharmila *et al.*, 2014].

Figure 4.5 (a–b) shows the TEM micrographs of nanocomposite formulations containing 2 phr nanoclay (NV2 and NE2 respectively). The micrographs indicated intercalated morphologies where clay platelets were still parallel (see sky blue circles in Figure 4.5) but with increased interlamellar spacing. It showed that the epoxy matrix was not able to exfoliate the silicate platelets. The silicate platelets retained their stacked layer structure, but with increased basal spacing between any two platelets (as indicated by X-ray diffraction results). The increased loading of the silicate platelets (i.e. increase in nanoclay loading from 1 phr to 2 phr) favours face to face alignment of the platelets and gradually degrades the exfoliation potential of the polymer [Chakradhar *et al.*, 2011; Mouloud *et al.*, 2012; Sharmila *et al.*, 2014]. It was observed that despite the increased loading to 2 phr, no agglomerates were observed in the micrographs.

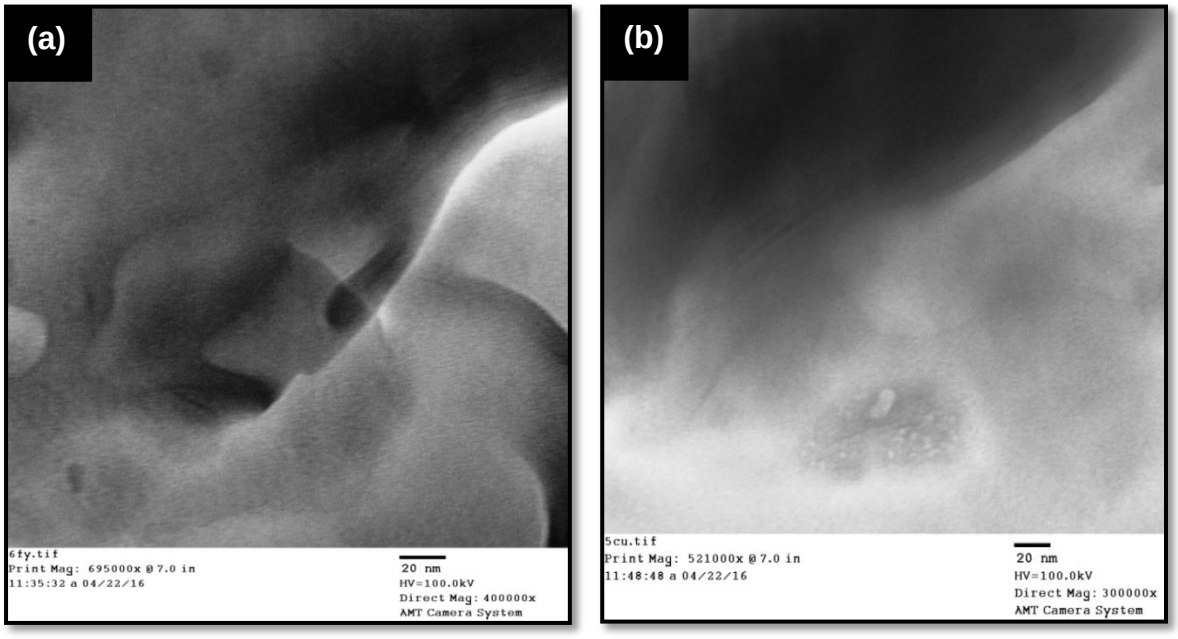

Figure 4.5: TEM micrographs of the glass fibre reinforced epoxy layered silicate nanocomposite with 2 phr clay for (a) NV2, and (b) NE2 formulations

Figure 4.6 (a–b) shows the TEM micrographs of nanocomposite formulations containing 4 phr nanoclay (NV4 and NE4 respectively).

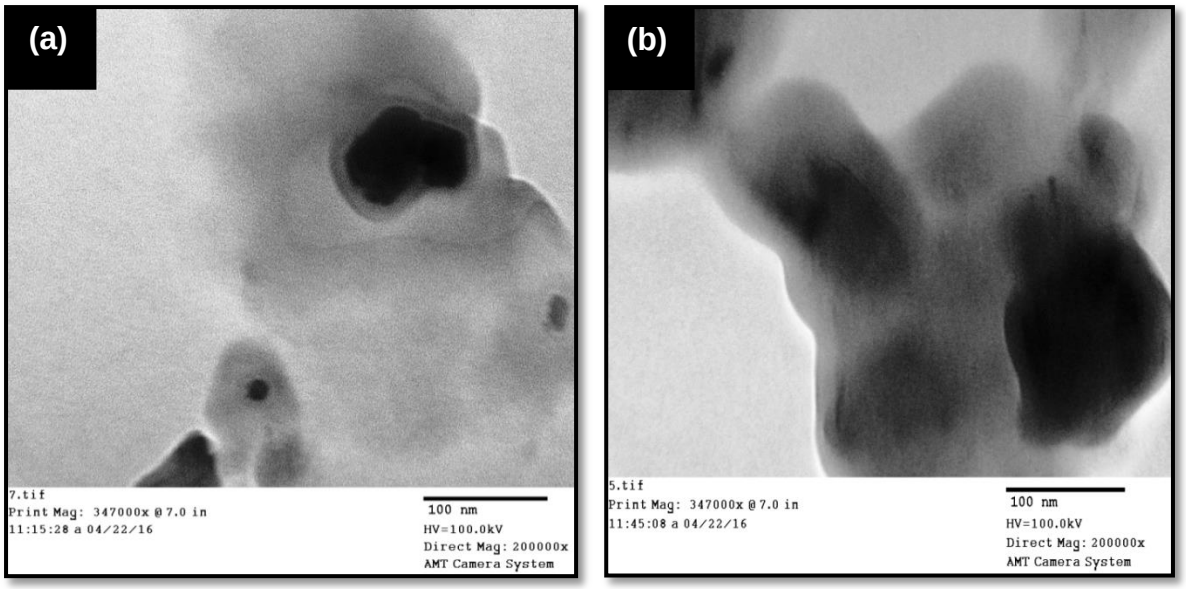

Figure 4.6: TEM micrographs of the glass fibre reinforced epoxy layered silicate nanocomposite with 4 phr clay for (a) NV4, and (b) NE4 formulations

The micrographs indicated a heterogeneous morphology and showed the presence of large clay agglomerates. These clay agglomerates indicated poor dispersion of nanoclay in the epoxy matrix. At such high clay loadings, the silicate platelets retain their face to face alignment as tactoids (intercalated and phase separated clay agglomerates were visible) as reported by Bashar et al. (2014) also.

4.4 Evaluation of Mechanical Properties

This section discusses the results of various tests conducted in the present work for different nanocomposite formulations to evaluate the tensile, flexural, impact, and fracture toughness properties.

4.4.1 Effect of Clay Addition on Tensile Properties

This section describes the effect of nanoclay addition on the tensile modulus and tensile strength of the fabricated nanocomposites. The effect of addition of each of the two clays in varying amounts was investigated separately. The results for tensile modulus and tensile strength are shown in Figure 4.7 and Figure 4.8 respectively. For nanocomposites containing NV clay, the tensile modulus and strength showed an increasing trend with the addition of NV clay upto 1 phr. Tensile modulus increased from 7790 MPa (for the reference sample) to 8283 MPa (for the nanocomposite with 1 phr nanoclay), an improvement of 6 %.

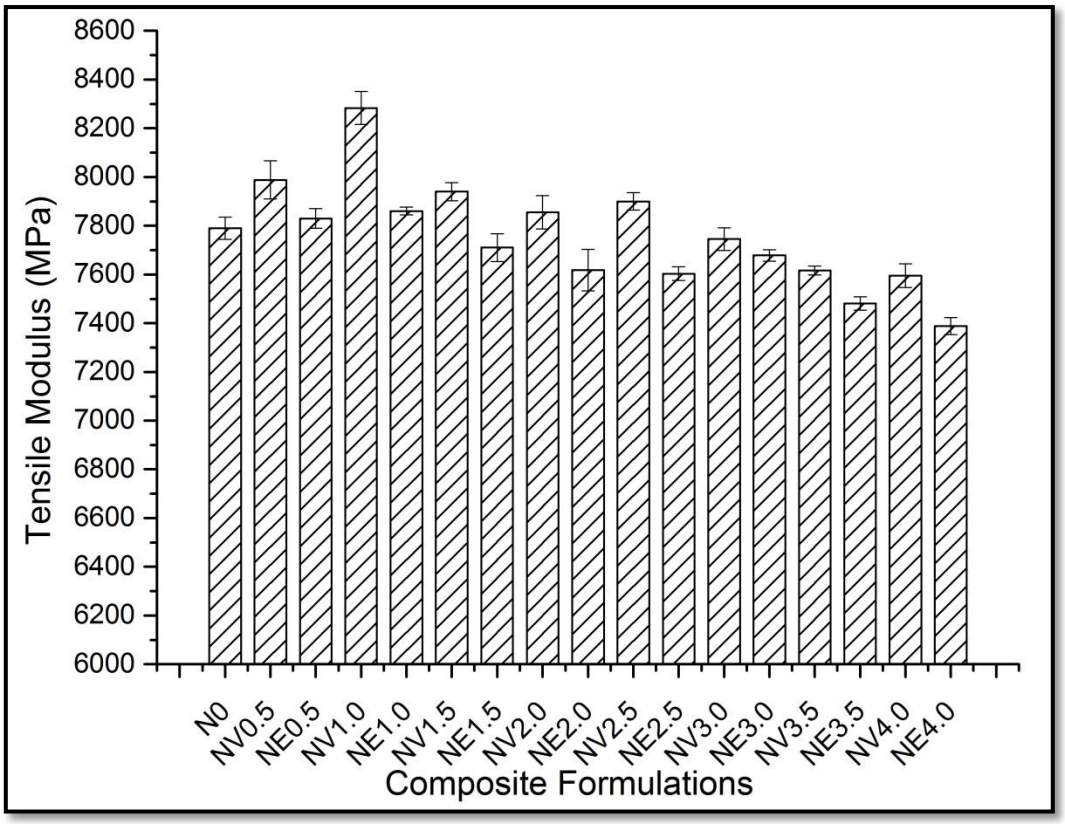

Figure 4.7: Effect of addition of Nanomer PGV (NV), and Nanomer I.28E (NE) on Tensile Modulus

The tensile strength increased from 347 MPa (for the reference sample) to 382 MPa (for the nanocomposite with 1 phr nanoclay), an improvement of 10 %. However, for nanocomposites containing NE clay, the tensile modulus and strength remained almost unchanged with addition of clay upto 1 phr and any clay addition beyond 1 phr resulted in a decreasing trend as compared to the glass fibre reinforced epoxy composite (with no clay addition). Similar results have been reported by other researchers like Kornmann et al. (2005), Bozkurt et al. (2007), Kumar et al. (2010), and Withers et al. (2015). The above results show that modifying the pristine epoxy matrix with nanoclay (NV or NE) does not have a significant effect on the tensile properties of glass fibre reinforced epoxy composites due to dominating effect of the fibre reinforcement as reported by Bozkurt et al. (2007) also. Tensile properties deteriorated with higher clay loading due to the formation of large clay agglomerates. These agglomerated clay particles impede the exfoliation of clay and act as stress concentration sites [Kumar *et al.*, 2010; Withers *et al.*, 2015].

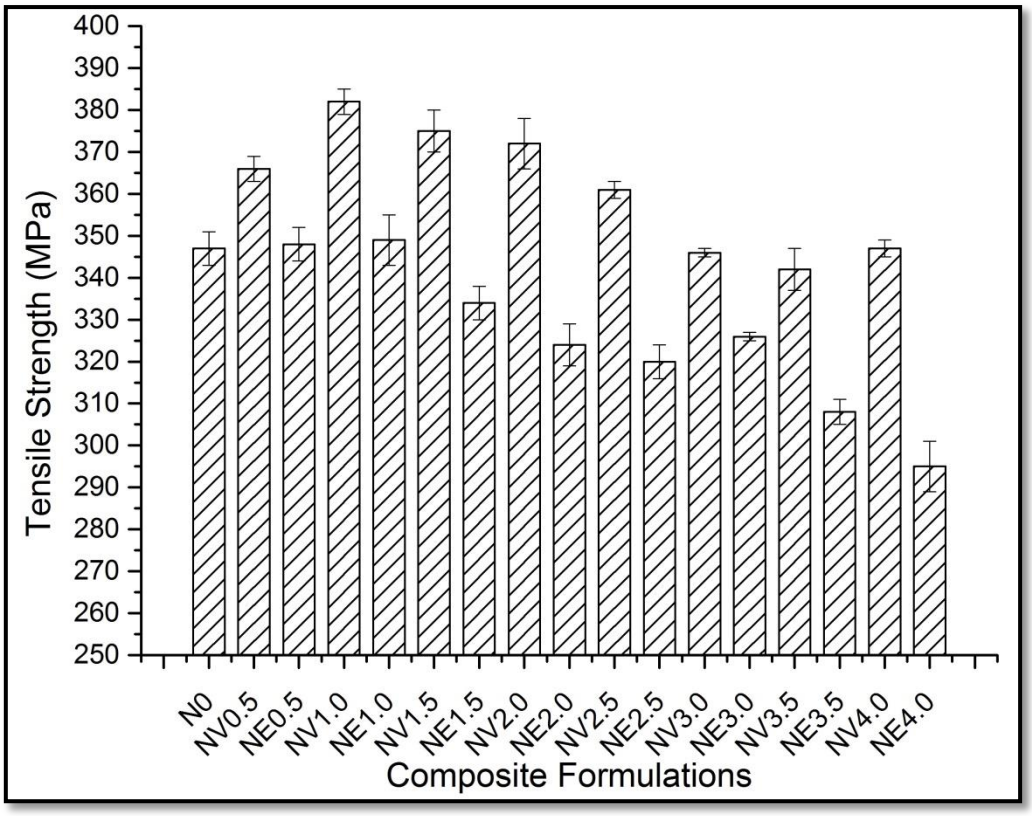

Figure 4.8: Effect of addition of Nanomer PGV (NV), and Nanomer I.28E (NE) on Tensile Strength

Kumar et al. (2010) reported that for fabricating nanocomposites, optimal silicate layer content is the key parameter. The reduction in interfacial interactions reduces the efficiency of the silicate platelets in strengthening the epoxy matrix.

4.4.2 Effect of Clay Addition on Flexural Properties

This section describes the effect of nanoclay addition on the flexural modulus and flexural strength of the fabricated nanocomposites. The effect of addition of each clay in varying amounts was investigated separately. The results for flexural modulus and flexural strength are shown in Figure 4.9 and Figure 4.10 respectively. For nanocomposites containing NV clay, the flexural modulus and strength showed an increasing trend with the addition of NV clay upto 1 phr. Flexural modulus increased from 12125 MPa (for the reference sample) to 15850 MPa (for the nanocomposite with 1 phr nanoclay), an improvement of 31 %. Similarly, the flexural strength increased from 367 MPa (for the reference sample) to 464 MPa (for nanocomposite with 1 phr clay), an improvement of 26 %. Further, for nanocomposites containing NE clay, the flexural modulus and strength also showed an increasing trend with addition of NE nanoclay upto 1 phr. Flexural modulus increased from 12125 MPa (for the reference sample) to 15800 MPa (for the nanocomposite with 1 phr

nanoclay), an improvement of 30 %. The flexural strength increased from 367 MPa to 428 MPa, an improvement of 17 % w.r.t the reference composite.

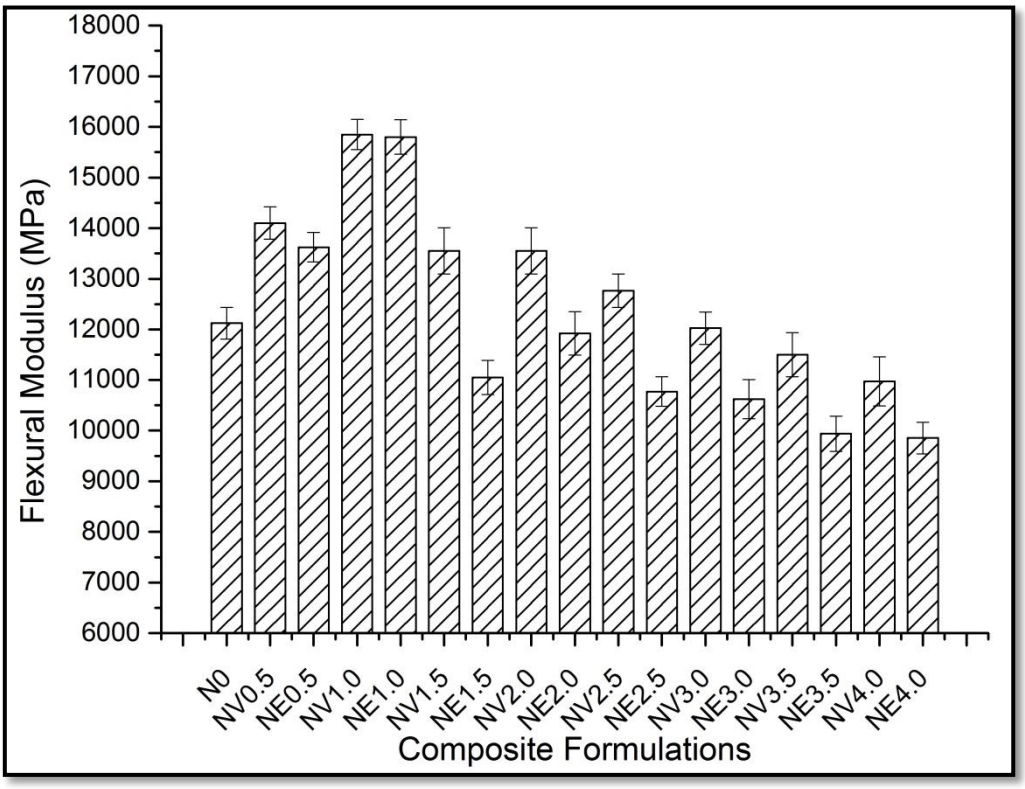

Figure 4.9: Effect of addition of Nanomer PGV (NV), and Nanomer I.28E (NE) on Flexural Modulus

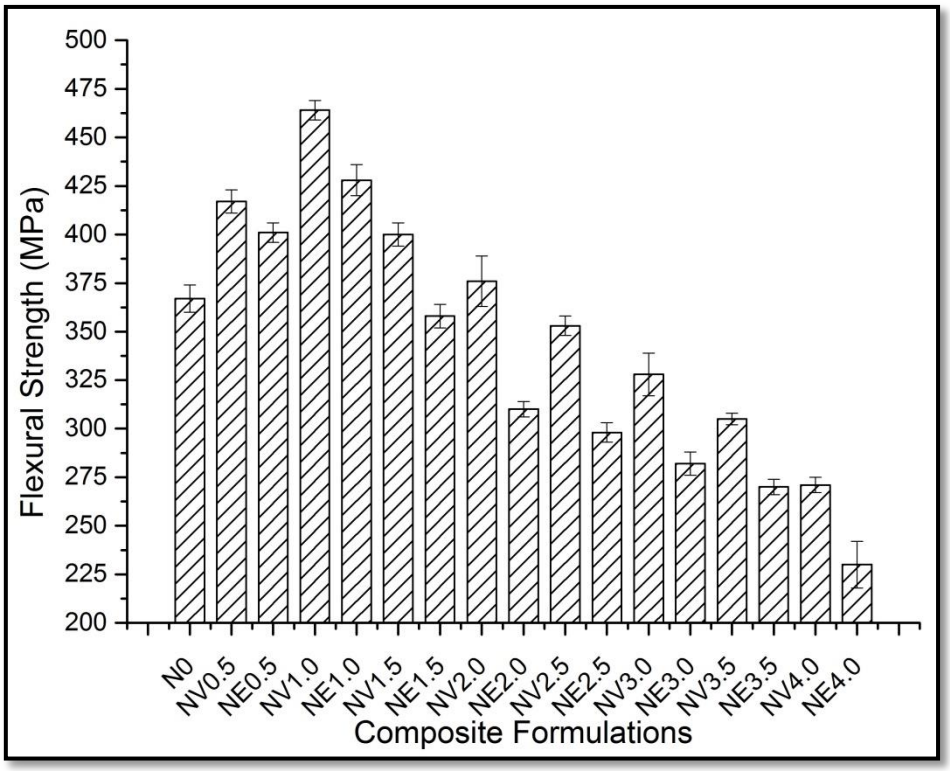

Figure 4.10: Effect of addition of Nanomer PGV (NV), and Nanomer I.28E (NE) on Flexural Strength

Similar trends have been reported by other researchers including Haque and Shamsuzzoha, (2003), Kornmann et al. (2005) Lin et al. (2006), Bozkurt et al. (2007), Kumar et al. (2010), and Rafiq et al. (2014). This remarkable improvement in flexural properties confirmed the formation of nanocomposite structures during the fabrication process (separation of the silicate platelets on a nanoscale has taken place) [Kornmann *et al.,* 2005]. Flexural properties increased with addition of silicate plates due to the higher stiffness of silicate platelets. Higher stiffness improved the ability to reinforce the epoxy matrix. These silicate platelets may improve the interfacial interaction upto optimal clay loading (here 1phr) as also reported by Kornmann et al. (2005), Bozkurt et al. (2007), and Rafiq et al. (2014). Another possible reason was that addition of silicate platelets increased the compressive strength and consequently bending strength of glass fibre reinforced epoxy nanocomposites also improved [Kornmann *et al.,* 2005; Rafiq *et al.,* 2014]. Exfoliated and partly exfoliated epoxy clay morphologies act as better reinforcement as compared to other morphologies (intercalated or phase separated) [Rafiq *et al.,* 2014]. However, at higher clay concentrations (beyond 1 phr), increase in viscosity of the resin may have made degassing very difficult. In such cases small air bubbles remain entrapped in resin and cause poor dispersion of silicate platelets and can result in clay aggregates which act as stress concentration sites for crack initiation. These agglomerates also degrade the epoxy glass fibre interactions [Kumar *et al.,* 2010; Rafiq *et al.,* 2014]. Another possible reason was that the viscosity of the epoxy resin at room temperature was not low enough to allow monomers to diffuse into the planar structure of silicate platelets beyond an optimum amount (here, 1 phr), and resulted in clay agglomerates [Kumar *et al.,* 2010].

4.4.3 Effect of Clay Addition on Impact Strength

This section describes the effect of nanoclay addition on the impact strength of the fabricated nanocomposites. The results for impact strength are shown in Figure 4.11. For nanocomposites containing NV clay, the impact strength showed an increasing trend with the addition of NV clay upto 2 phr. Impact strength increased from 145 kJ/m^2 (for the reference sample) to 177 kJ/m^2 (for the nanocomposite with 2 phr nanoclay), an improvement of 22 %. Similarly, for nanocomposites with NE clay, the impact strength also showed an increasing trend with the addition of NE clay upto 2 phr. Impact strength increased from 145 kJ/m^2 (for the reference sample) to 167 kJ/m^2 (for the nanocomposite with 2 phr nanoclay), an improvement of 15 %.

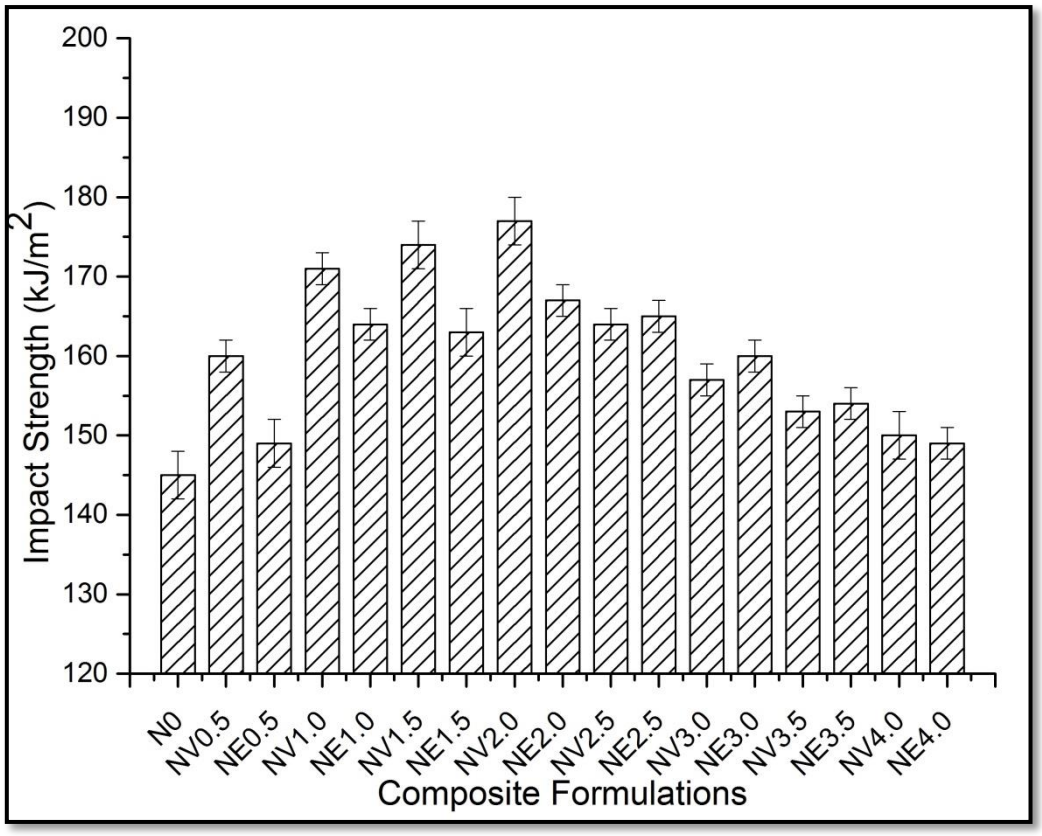

Figure 4.11: Effect of addition of Nanomer PGV (NV), and Nanomer I.28E (NE) on Impact Strength

The possible reason for this improved strength was an intercalated morphology observed at 2 phr (see Figure 4.5). The intercalated silicate platelets act as crack stoppers and form a torturous crack propagation path, because of which the impact strength increased. However, at even higher clay contents, intercalated morphology with agglomerated silicate platelets was observed (see Figure 4.6). These agglomerated silicate platelets act as stress concentration sites which result in reduced impact strength [Isik *et al.,* 2003; Mouloud *et al.,* 2012; Kusmono *et al.,* 2013].

4.4.4 Effect of Clay Addition on Fracture Toughness

This section describes the effect of nanoclay addition on the fracture toughness of the fabricated nanocomposites. The results for fracture toughness are shown in Figure 4.12. For nanocomposites containing NV clay, the fracture toughness showed an increasing trend with addition of NV clay upto 2 phr. Fracture toughness increased from 20.49 MPa.m$^{1/2}$ (for the reference sample) to 35.57 MPa.m$^{1/2}$ (for the nanocomposite with 2 phr nanoclay), an improvement of 73 %. For NE based nanocomposites also, the fracture toughness showed an increasing trend with addition of NE clay upto 2 phr. Fracture toughness increased from

20.49 MPa.m$^{1/2}$ (for the reference sample) to 32.24 MPa.m$^{1/2}$ (for the nanocomposite with 2 phr nanoclay), an improvement of 57 %.

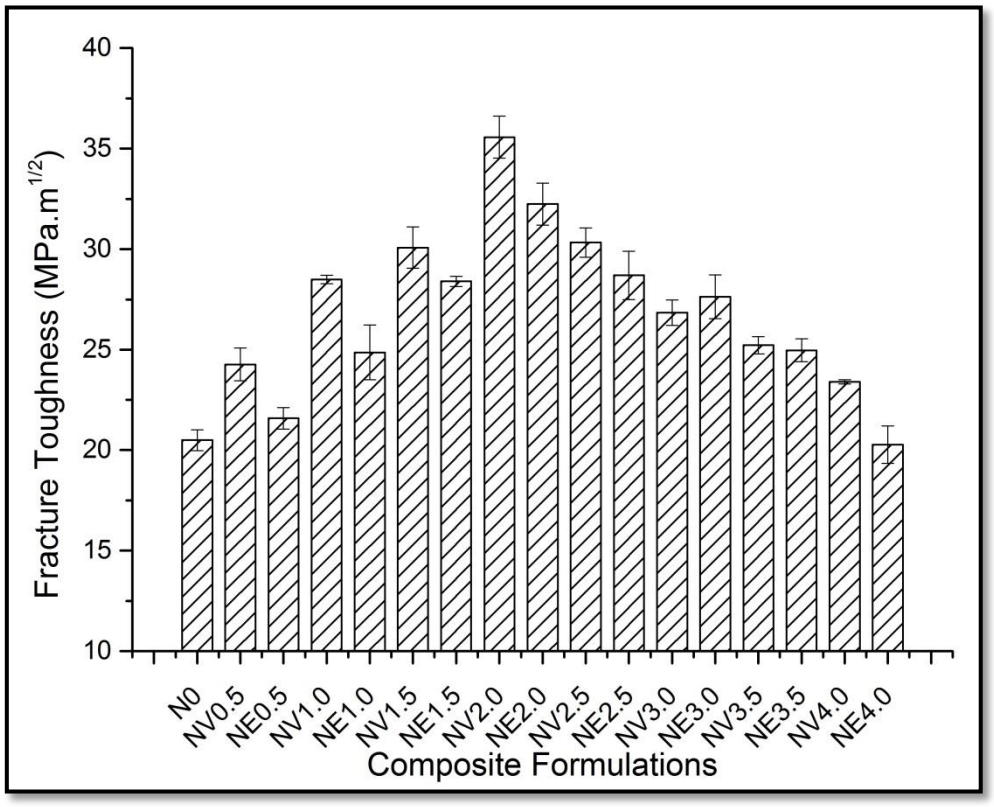

Figure 4.12: Effect of addition of Nanomer PGV (NV), and Nanomer I.28E (NE) on Fracture Toughness

Similar results have been reported by other researchers including Haque and Shamsuzzoha, (2003), Bozkurt et al. (2007), and Rafiq et al. (2014). The addition of silicate platelets to the epoxy matrix improved the interfacial bonding (epoxy and glass fibre bonding), and consequently better stress transfer occurred between the matrix and glass fibres (discussed in Section4.5; Figure 4.16). The presence of silicate platelets in the matrix deflect or impede the crack propagation. Rafiq et al (2014) also reported that a major contributor towards toughening is crack deflection due to presence of silicate platelets in the epoxy matrix. However, beyond 2 phr nanoclay addition, the fracture toughness values deteriorated. This is because at higher clay loadings viscosity of the resin increased which resisted the homogenous dispersion of clay, resulting in formation of clay agglomerates. These agglomerated clay particles act as stress concentration sites for crack propagation and also reduced the interfacial bonding between the epoxy matrix and the glass fibre [Bozkurt *et al.*, 2007; Rafiq *et al.*, 2014].

4.5 SEM Analysis of Fractured Surfaces

In the present work, four mechanical properties were mainly evaluated. It was observed that addition of nanoclay to glass fibre reinforced epoxy based nanocomposites improves all the four types of properties investigated in the present work. The improvements obtained were justified through characterization means of XRD and TEM analysis. The major improvements were observed in two mechanical properties viz. flexural properties and fracture toughness. For these two properties, additional characterization was done to validate the improvements in the properties. For the said purpose, SEM analysis of the fractured surfaces of flexural and fracture toughness specimens was conducted. Figure 4.13 shows the SEM micrograph of the fractured surface of the glass fibre reinforced epoxy nanocomposite (with no clay addition; reference sample) under flexural testing. The fractured surface appeared to be very smooth. It was observed that the glass fibres were devoid (debonded) from the epoxy matrix. This indicates that the interfacial bonding between the glass fibre and the epoxy is weak [Kornmann *et al.,* 2005; Bozkurt *et al.,* 2007; Withers *et al.,* 2015].

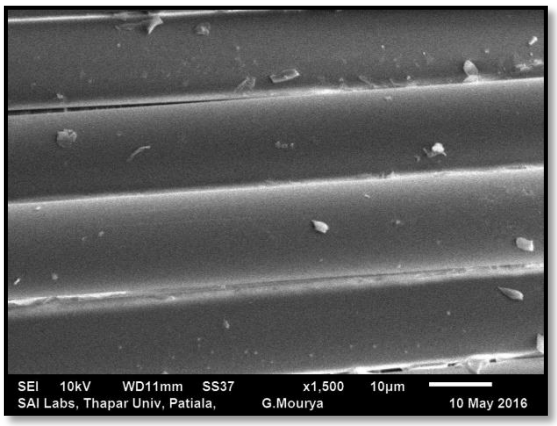

Figure 4.13: SEM micrograph of fractured surface of reference sample under flexural testing

Further as reported by Haque and Shamsuzzoha, (2003) also, it can be observed from Figure 4.13 that significant resin cracking and/or agglomeration were not observed at the interface region. Figure 4.14 shows the SEM micrographs of the fractured surface of flexural specimens of nanocomposites containing 1phr clay (compositions which showed best flexural properties). Figure 4.14 (a–b) is for NV1 and Figure 4.14 (c–d) is for NE1 specimens. The micrographs clearly show the presence of silicate platelets at the surface of glass fibre in the nanocomposites. As reported by Kornmann et al (2005), silicate layers are present at the surface of glass fibres because of the particular affinity of silicate platelets for the glass fibre surface. Both these constituents, i.e. clay and glass fibre are inorganic materials and

functionalized at the surface with organic molecules so that there may be polarity match between the respective surfaces.

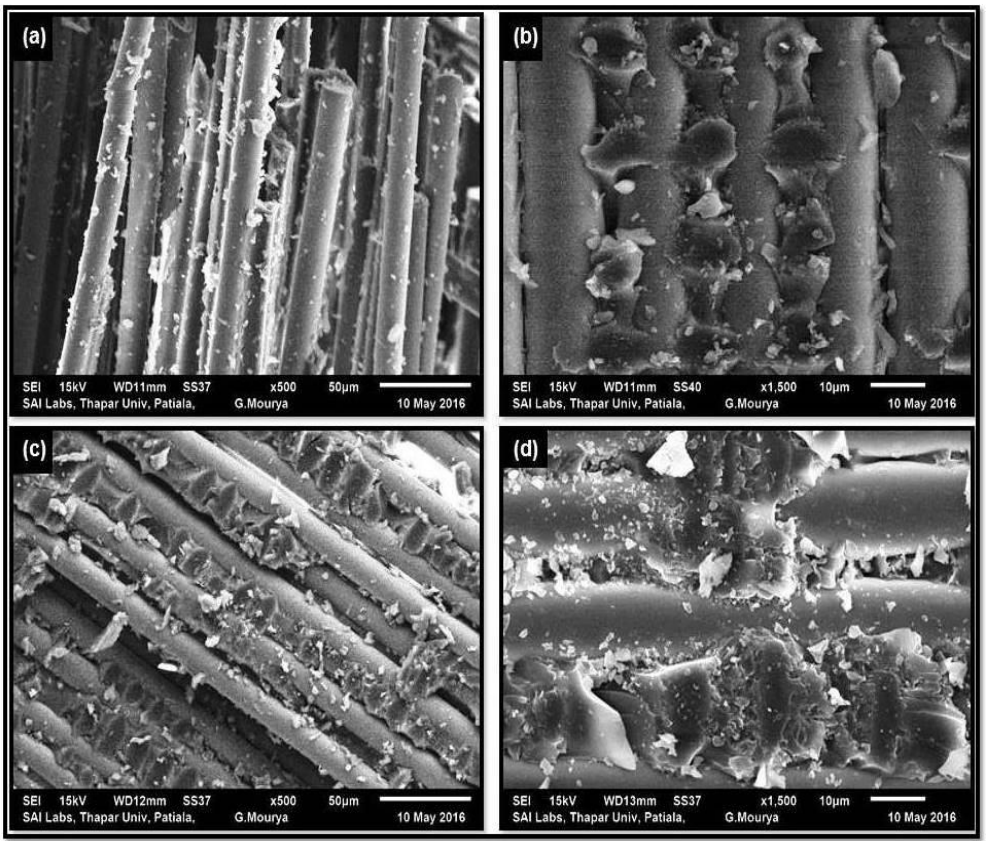

Figure 4.14: SEM micrographs of fractured surface of flexural specimens of nanocomposites with 1phr clay loading (a–b) NV1, and (c–d) NE1 formulations

The epoxy matrix for the nanocomposites (see Figure 4.14) looked more rough (i.e. toughened and ductile) as compared to the reference sample (see Figure 4.13). The fractured surface also indicated a strong interface bonding between the glass fibre and epoxy clay matrix. In the fractured surface of nanocomposites, the epoxy-resin can be observed to be present on the fibre surface indicating strong interfacial bonding among the constituents; see Figure 4.14. The nanocomposites also showed a significant resin cracking at the interface (see the rough appearance of fractured surface in Figure 4.14). Further, Figure 4.15 shows the SEM micrographs of the fractured surface of flexural specimens of nanocomposites containing 4 phr clay. Figure 4.15 (a–b) is for NV4 and Figure 4.15 (c–d) is for NE4 specimens. The micrographs clearly show poor dispersion of the silicate platelets in the epoxy matrix which resulted in formation of agglomerates. Agglomerates got formed because at high clay loading (here, 4 phr), the viscosity of resin increased and made uniform dispersion of clay and also degassing very difficult. Because of these reasons, the flexural properties of nanocomposites containing 4 phr clay deteriorated.

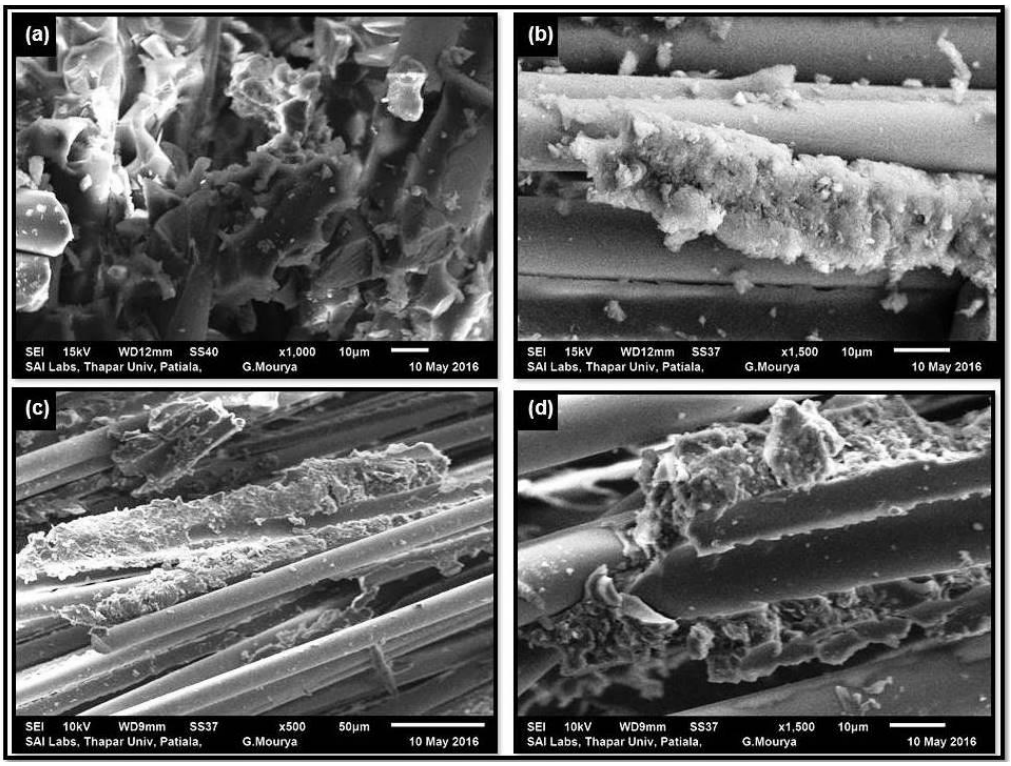

Figure 4.15: SEM micrographs of fractured surface of flexural specimens of nanocomposites with 4phr clay loading (a–b) NV4, and (c–d) NE4 formulations

SEM micrographs of fractured surfaces of the fracture toughness specimens at 2 phr with both nanoclays (NV and NE) are shown in Figure 4.16. Maximum improvement in fracture toughness properties was observed at 2 phr clay content.

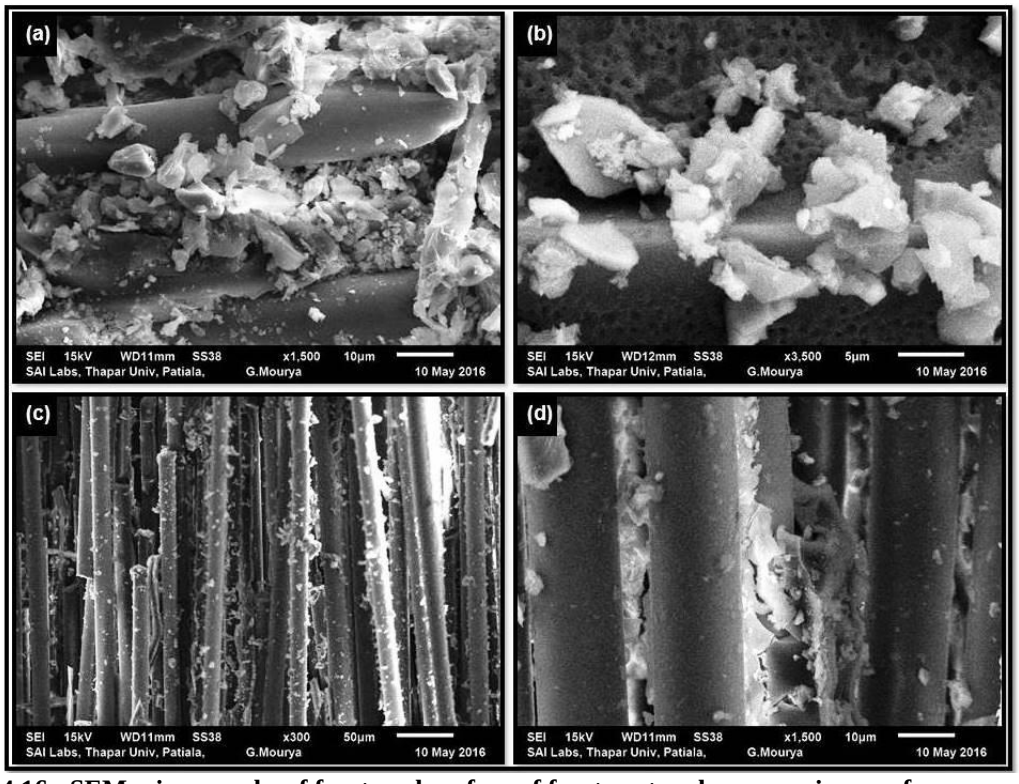

Figure 4.16: SEM micrographs of fractured surface of fracture toughness specimens of nanocomposites with 2phr clay loading (a–b) NV2, and (c–d) NE2 formulations

It is clearly visible from Figure 4.16 (b–c) that clay is uniformly distributed for nanocomposite formulations containing 2 phr clay. This uniformly distributed clay present at the surface of glass fibre in the fractured specimens indicated strong interfacial bonding between the glass fibre and the epoxy-clay matrix. These clay platelets also acted as crack stoppers and formed zig-zag path for propagation of crack which resulted in improved fracture toughness. However, clay addition beyond 2 phr resulted in decreased fracture toughness. SEM micrographs of fractured surfaces of fracture toughness specimens at 4 phr clay content are shown in Figure 4.17.

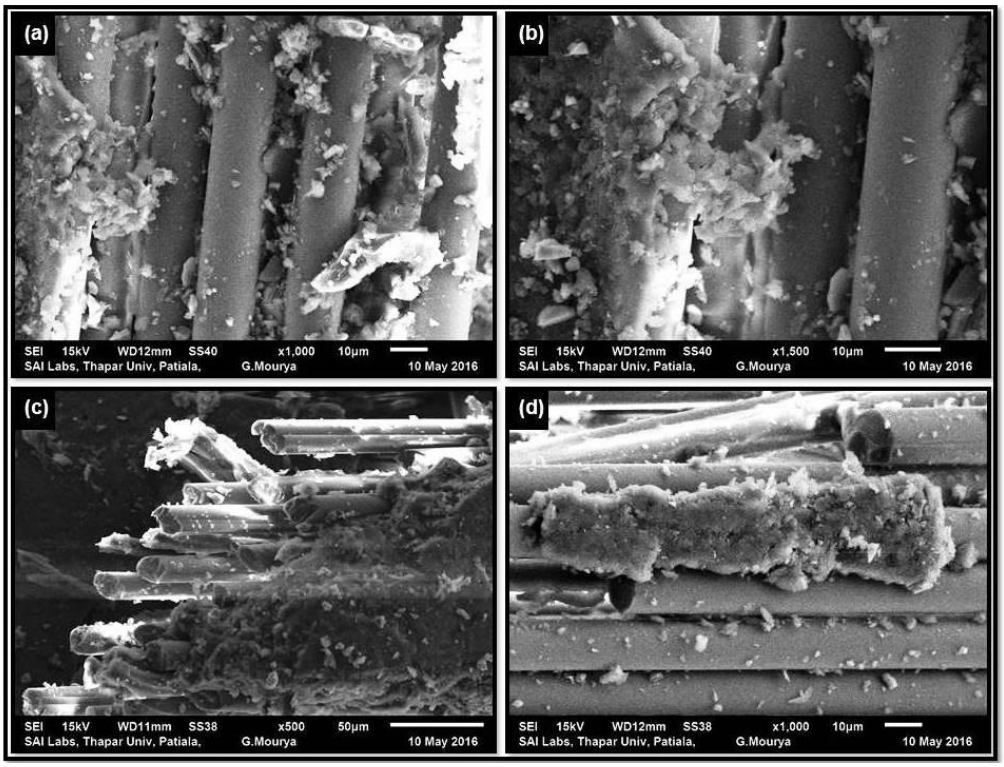

Figure 4.17: SEM micrographs of fractured surface of fracture toughness specimens of nanocomposites with 4phr clay loading (a–b) NV4, and (c–d) NE4 formulations

The agglomerated clay particles are clearly seen in Figure 4.17. These agglomerates of clay particles may have acted as crack initiating sites which may be the possible reason for decreased fracture toughness at this high clay loading value.

4.6 Summary of the Chapter

This chapter discussed the results of XRD and TEM characterization, mechanical testing (tensile, flexural, impact, and fracture toughness testing), and SEM fractographic analysis of some selected nanocomposite formulations. XRD revealed that nanocomposites containing 1 phr nanoclay showed complete or partial exfoliation, whereas an intercalated morphology

was observed for all other nanocomposite formulations. XRD results were also supported by the TEM analysis. The maximum improvement in tensile and flexural properties was observed in NV1 nanocomposite formulation. The maximum improvement in impact strength and fracture toughness properties was observed in NV2 nanocomposite formulation. SEM fractographic analysis of fractured surfaces showed that neat epoxy exhibited a smooth fractured surface, indicating brittle failure. However, for the nanocomposites, the epoxy matrix looked more rough (i.e. toughened and ductile) on addition of nanoclay into the matrix as compared to the reference sample. The fractured surfaces of nanocomposites containing 1 phr and 2 phr nanoclay indicated a strong interface bonding between glass fibre and epoxy clay matrix. The nanocomposites also showed a significant resin cracking at the interface. At higher clay loading (here, 4 phr), the SEM micrographs clearly showed poor dispersion of silicate platelets in the epoxy matrix, which resulted in formation of clay agglomerates (tactoids). Agglomerates got formed because at high clay loadings, degassing was very difficult. Because of this, the properties deteriorated beyond optimum clay content in the nanocomposites.

Chapter 5
Conclusions and Scope of Future Work

5.1 General

This chapter covers detailed information about the conclusions drawn from the present research work regarding mechanical properties (tensile, flexural, impact, and fracture toughness properties) of the glass fibre reinforced epoxy based nanocomposites. The chapter also discusses the type of morphology observed in different nanocomposite formulations and fractographic analysis of the various nanocomposites formulations. Finally, the research areas that can be explored for future researche have been discussed.

5.2 Conclusions

The various conclusions drawn from the present research work are discussed in the following sections.

5.2.1 Processing of Glass Fibre Reinforced Epoxy Based Nanocomposites

- The key feature for improvement in mechanical properties of glass fibre reinforced epoxy layered silicate nanocomposites is the type of morphology achieved during the processing of nanocomposites. The ability of epoxy monomers to diffuse into the basal spacing (interfacial galleries) is responsible for change in morphologies. The diffusion of epoxy monomer into the basal increases the interlamellar distance between silicate platelets and results in intercalated or exfoliated morphology.
- A definite sequence of steps is required during the processing of glass fibre reinforced epoxy nanocomposites. During processing of epoxy-clay mixture, different steps were followed viz. (i) hand mixing with the help of stirrer, (ii) homogenization at 20000 rpm for 10 min, and (iii) probe sonication at 80 % amplitude control for 10 min (pulse on time = 40 s, pulse off time = 20 s). After mixing the nanoclay, the curing agent was added to the epoxy-clay mixture and was mixed for 10 min with a mechanical stirrer. Finally, this mixture was infused in to the VARIM set-up. It was cured for 6 h at room temperature followed by post curing of 6 h at 60 ℃.

5.2.2 TEM/XRD Analysis

- XRD micrographs revealed that diffraction peak of nanoclay shifted either towards a lower angle or was absent in different nanocomposite formulations. Fully or partially exfoliated morphology was observed in NV1 and NE1 formulations, whereas, an intercalated morphology was observed for the remaining formulations (NV2, NE2, NV4, and NE4). TEM analysis validated the results obtained through XRD.
- TEM micrographs of the neat epoxy showed absolutely clear and smooth micrographs conforming absence of silicate platelets in the N0 composition.
- Nanocomposites containing 1 phr clay viz. NV1 and NE1 showed complete exfoliation and partial exfoliation respectively. For NV1, it was observed from TEM micrographs that the silicate platelets were not parallel to each other (randomly distributed) and the distance between the platelets was also not uniform. This indicated an exfoliated morphology. However for NE1, it was observed that morphology changed from one place to the other. In some regions, the clay platelets were still parallel to each other whereas in other regions, the clay layers were randomly distributed. This indicated a partially exfoliated morphology.
- Nanocomposite with 2 phr clay viz. NV2 and NE2 showed an intercalated morphology. Clay platelets were still parallel but with increased interlamellar spacing. It showed that the epoxy matrix was not able to exfoliate the silicate platelets.
- TEM micrographs for nanocomposite formulations with 4 phr nanoclay (NV4 and NE4) indicated a heterogeneous morphology and showed the presence of large clay agglomerates. These agglomerates were playing a major role in deteriorating the mechanical properties at higher clay content.

5.2.3 Tensile Properties Analysis

- For nanocomposites containing NV clay, the tensile modulus and strength showed an increasing trend with addition of nanoclay upto 1 phr (with improvement of 6 % and 10 % respectively over the reference sample). However, for nanocomposites with NE clay, the tensile modulus and strength remained almost unchanged with addition of clay upto 1 phr. Any clay addition beyond 1 phr resulted in a decreasing trend as compared to the reference sample.

- NV and NE nanoclay addition did not show significant effect on tensile properties of glass fibre reinforced epoxy composites due to the dominating effect of the glass fibre reinforcement.

5.2.4 Flexural Properties Analysis

- The flexural modulus and flexural strength showed an increasing trend with addition of both the nanoclays upto 1 phr. Beyond 1 phr addition, a decreasing trend was observed. For NV1 nanocomposite, the flexural modulus and strength increased by 31 % and 26 % respectively over the reference composite. Similarly for NE1 composition nanocomposite, flexural modulus and strength increased by 30 % and 17 % respectively over the reference sample.
- Flexural properties increased with addition of silicate plates due to the higher stiffness of silicate platelets. Higher stiffness improved the ability to reinforce the epoxy matrix. These silicate platelets improved the interfacial interaction upto optimal clay loading (here, 1 phr). At higher clay concentrations, viscosity of the resin increased and resulted in poor dispersion of silicate platelets. Consequently, formation of clay agglomerates resulted which decreased the flexural properties.

5.2.5 Impact Strength Analysis

- The addition of each nanoclay into the epoxy matrix improved the impact strength upto 2 phr clay loading and beyond this a decreasing trend was observed. For NV2 nanocomposite, the impact strength increased by 22 % over the reference sample. Similarly, for NE2 nanocomposite, the impact strength increased by 15 % over the reference sample.
- It was observed that intercalated morphology was best for improvement in impact strength. The intercalated silicate platelets acted as crack stoppers and formed a torturous crack propagation path, because of which the impact strength increased upto 2 phr clay loading. Beyond 2 phr addition, the impact strength decreased, may be due to the formation large clay agglomerates.

5.2.6 Fracture Toughness Analysis

- Fracture toughness increased with addition of both the nanoclays (NV and NE) upto 2 phr, and beyond this limit it deteriorated. It improved from 20.49 $MPa.m^{1/2}$ to 35.57 $MPa.m^{1/2}$ (an

improvement of 73 %) for the NV2 formulation. For NE2 composition, it increased from 20.49 MPa.$m^{1/2}$ to 32.24 MPa.$m^{1/2}$ (an improvement of 57 %).

- The addition of silicate platelets to the epoxy matrix improved the interfacial bonding (epoxy and glass fibre bonding). The major contributor towards toughening seems to be crack deflection due to presence of well dispersed silicate platelets in the epoxy matrix. At higher clay loadings (beyond 2 phr), formation of clay agglomerates took place and acted as stress concentration sites for crack propagation and also reduced the interfacial bonding between the epoxy matrix and glass fibre.

5.2.7 SEM Analysis of Fractured Surfaces

- The major improvements were observed in two mechanical properties viz. flexural properties and fracture toughness. The fractured surface of glass fibre reinforced epoxy nanocomposite (with no clay addition) under SEM micrographs appeared to be very smooth. This indicated a weak interfacial bonding between the glass fibre and the epoxy.
- The micrographs of nanocomposites with 1 phr clay loading (flexural samples) clearly showed the presence of silicate platelets at the surface of glass fibre in the nanocomposite. The epoxy matrix looked more rough (i.e. toughened and ductile) as compared to the glass fibre reinforced epoxy composite. The micrograph also indicated a strong interface bonding between glass fibre and epoxy clay matrix, and this was because of the addition of nanoclay.
- SEM micrographs of fractured surfaces of fracture toughness specimens at 2 phr with both nanoclays (NV and NE) showed that silicate platelets were uniformly distributed. The presence of uniformly distributed silicate platelets at the surface of glass fibre made the interfacial bonding between glass fibres and epoxy matrix stronger. These clay platelets also acted as crack stoppers and formed a zig-zag path for propagation of crack. This resulted in improved fracture toughness.
- SEM micrographs of the fractured surface, of both, the fracture toughness and flexural strength specimens of nanocomposites containing 4 phr clay clearly showed poor dispersion of silicate platelets which resulted in formation of tactoids (clay agglomerates). These tactoids got formed at such high clay loadings due to the increase in viscosity of the epoxy resin. Because of this increased viscosity, uniform dispersion of clay and degassing became very difficult. The tactoids of silicate platelets might have acted as crack initiating sites which decreased the properties.

5.3 Major Conclusions and Scope of Future Work

- The present research focussed on the synthesis, characterization, and evaluation of mechanical properties of glass fibre reinforced epoxy layered silicate nanocomposites. Maximum improvement in tensile strength/modulus and flexural strength/modulus were observed in nanocomposite with 1 phr clay. Impact strength, and fracture toughness showed best properties in nanocomposites containing 2 phr nanoclay. At higher clay loadings, all the four properties (tensile, flexural, impact, and fracture toughness) showed deteriorated properties due to presence of clay agglomerates or tactoids.
- TEM/XRD analysis confirmed that silicate platelets were able to exfoliate in the epoxy matrix of nanocomposites with 1 phr nanoclay. Beyond 1 phr, exfoliation of silicate platelets was impeded by the higher viscosity of the epoxy resin. An intercalated morphology was observed in nanocomposites with 2 phr clay loading. Clay tactoids or agglomerates were visible in nanocomposites with 4 phr clay.
- SEM analysis showed that fractured surface of glass fibre reinforced epoxy composite (reference sample) appeared to be very smooth and indicated a weak interfacial bonding between the glass fibre and the epoxy. But, the fractured surface of glass fibre reinforced epoxy layered silicate nanocomposites looked rougher as compared to the reference sample and indicated a strong interface bonding between glass fibre and epoxy clay matrix. At higher clay loading (here 4 phr) formation of clay tactoids (clay agglomerates) took place and resulted in weak interfacial bonding between epoxy matrix and glass fibre.
- The current research work can further be expanded to the areas of thermal property analysis like thermogravimetric analysis (TGA, used to quantify thermal stability and weight loss characteristics of different glass fibre reinforced epoxy based nanocomposite formulations) and differential scanning calorimetry (DSC, for obtaining glass transition temperature as well as to determine the extent of curing in different nanocomposite formulations).
- The barrier properties of glass fibre reinforced epoxy based nanocomposites could be analysed in terms of water, acetone, acid, base, or crude oil uptake. The presence of silicate platelets in the epoxy matrix hinders the diffusion of solvent molecules and increases the tortuosity path, making the diffusion of solvent molecules, a time consuming process consequently, the barrier properties improve.

- The epoxy matrix can be modified by incorporating thermoplastic like high-impact polystyrene (HIPS) and poly(methyl methacrylate) (PMMA), polyether polyol, or liquid rubber like poly(butadiene-co-acrylonitrile) (CTBN) for enhanced properties.

References

- Agubra VA, Owuar PS, Hosur MV. Influence of nanoclay dispersion methods on the mechanical behavior of E-glass/epoxy nanocomposites. Nanomaterials 2013; 3: 550–563.
- Alexandre M, Dubois P. Polymer-layered silicate nanocomposites: preparation, properties and uses of a new class of materials. Materials Science and Engineering 2000; 28: 1–63.
- Al-Qadhi M, Merah N, Gasem ZM, Abu-Dheir N, Aleem BJA. Effect of water and crude oil on mechanical and thermal properties of epoxy-clay nanocomposites. Polymer Composites 2014; 35: 318–326.
- Al-Qadhi M, Merah N, Gasem ZM. Mechanical properties and water uptake of epoxy-clay nanocomposites containing different clay loadings. Journal of Materials Science 2013; 48: 3798–3804.
- Azeez AA, Rhee KY, Park SJ, Hui D. Epoxy clay nanocomposites-processing, properties and applications: A review. Composites Part-B 2013; 45: 308–320.
- Bakar M, Białkowska A, Molenda J, Piasek J. Preparation and properties evaluation of thermoplastic modified epoxy nanocomposites. Journal of Macromolecular Science, Part B: Physics 2012; 51: 1159–1171.
- Basher M, Mertiny P, Sundararaj U. Effect of nanocomposite structures on fracture behaviour of epoxy-clay nanocomposites prepared by different dispersion methods. Journal of Nanomaterials 2014; 2014: 1–12.
- Bozkurt E, Kaya E, Tanoglu M. Mechanical and thermal behavior of non-crimp glass fiber reinforced layered clay/epoxy nanocomposites. Composites Science and Technology 2007; 67: 3394–3403.
- Callister W. Material science and engineering an introduction. 7th ed. USA: John Wiley & Sons; 2007.
- Camargo P, Satyanarayana K, Wypych F. Nanocomposites: synthesis, structure, properties and new application opportunities. Materials Research 2009; 12: 1–39.
- Campbell FC. Structural composite materials. ASM International; 2010.
- Chow WS. Water absorption of epoxy/glass fiber/organo-montmorillonite nanocomposites. eXPRESS Polymer Letters 2007; 1: 104–108.
- Composite Materials Handbook. 3rd vol. USA: Department of Defense; 2002.

- Das A, Stockelhuber KW, Jurk R, Jehnichen D, Heinrich G. A general approach to rubber-montmorillonite nanocomposites: intercalation of stearic acid. Applied Clay Science 2011; 51: 117–125.
- Haque A, Shamsuzzoha M. S2-glass/epoxy polymer nanocomposites: manufacturing, structures, thermal and mechanical properties. Journal of Composite Materials 2003; 37: 1821–1837.
- Harris B. Engineering composite materials. 2nd ed. Institute of Materials; 1999.
- Isik I, Yilmazer U, Bayram G. Impact modified epoxy/montmorillonite nanocomposites: synthesis and characterization. Polymer 2003; 44: 6371–6377.
- Kaushik A, Singh P, Kaushik J. The mechanical properties and chemical resistance of short glass-fiber-reinforced epoxy composites. International Journal of Polymeric Materials and Polymeric Biomaterials 2006; 55: 425–440.
- Kim JK, Mai YW. Engineered interfaces in fiber reinforced composites. 1st ed: Elsevier; 1998.
- Kornmann X, Rees M, Thomann Y, Necola A, Barbezat M, Thomann R. Epoxy-layered silicate nanocomposites as matrix in glass fibre-reinforced composites. Composites Science and Technology 2005; 65: 2259–2268.
- Kotsilkova R. Thermoset nanocomposites for engineering applications. United Kingdom: Smithers Rapra Technology Limited; 2007.
- Kumar MA, Reddy KH, Reddy YVM, Reddy GR, Naidu SV. Improvement of tensile and flexural properties in epoxy/clay nanocomposites reinforced with weave glass fiber reel. International Journal of Polymeric Materials 2010; 59:854–862.
- Kusmono, Wildan MW, Ishak ZAM. Preparation and properties of clay-reinforced Epoxy nanocomposites. International Journal of Polymer Science 2013; 2013: 1–7.
- Lam CK, Cheung H, Lau K, Zhou L, Ho M, Hui D. Cluster size effect in hardness of nanoclay/epoxy composites. Composites: Part B 2005; 36: 263–269.
- Lim SR, Chow WS. Fracture toughness enhancement of epoxy by organo-montmorillonite. Polymer-Plastics Technology and Engineering 2011; 50: 182–189.
- Lin LY, Lee JH, Hong CE, Yoo GH, Advani SG. Preparation and characterization of layered silicate/glass fiber/epoxy hybrid nanocomposites via vacuum-assisted resin transfer molding (VARTM). Composites Science and Technology 2006; 66: 2116–2125.

- Mallick PK. Fiber reinforced composites materials, Manufacturing and Design. 3rd ed. CRC Press; 2007.
- Mouloud A, Cherif R, Fellahi S, Grohens Y, Pillin I. Study of morphological and mechanical performance of amine-cured glassy epoxy-clay nanocomposites. Journal of Applied Polymer Science 2012; 124: 4729–4739.
- Park JH, Jana SC. Mechanism of exfoliation of nanoclay particles in epoxy-clay nanocomposites. Macromolecules 2003; 36: 2758–2768.
- Rafiq A, Al-qadhi M, Merah N, Ali Y. Mechanical behavior of hybrid glass fibre/epoxy clay nanocomposites. Advanced Materials Research 2014; 894: 336–341.
- Satishkumar TP, Satheeshkumar S, Naveen J. Glass fiber-reinforced polymer composites-a review. Journal of Reinforced Plastics and Composites 2014; 33: 1258–1275.
- Sharma B, Chhibber R, Mehta R. Effect of surface treatment of nanoclay on the mechanical properties of epoxy/glass fiber/clay nanocomposites. Composite Interfaces 2016; DOI: 10.1080/09276440.2016.1165522.
- Sharmila TKB, Ayswarya EP, Abraham BT, Begum PMS, Thachil ET. Fabrication of partially exfoliated and disordered intercalated cloisite epoxy nanocomposites via in situ polymerization: mechanical, dynamic mechanical, thermal and barrier properties. Applied Clay Science 2014; 102: 220–230.
- Smith WF, Hashemi J. Materials science and engineering. 4th ed. New Delhi: Tata McGraw Hill Education Private Limited; 2008.
- Thomas S, Joseph K, Malhotra SK, Goda K, Sreekala MS. Introduction to polymer composites: volume 1. Wiley-VCH Verlag GmbH & Co. KGaA; 2012.
- Vijayan PP, Harikrishnan MG, Puglia D, Vijayan PP, Kenny JM, Thomas S. Solvent uptake of liquid rubber toughened epoxy/clay nanocomposites. Advances in Polymer Technology 2015; 00: 1–7.
- Withers GJ, Yu Y, Khabashesku VN, Cercone L, Hadjiev VG, Souza JM, Davis DC. Improved mechanical properties of an epoxy glass-fiber composite reinforced with surface organomodified nanoclays. Composites: Part B 2015; 72: 175–182.
- Zunjarrao SC, Sriraman R, Singh RP. Effect of processing parameters and clay volume fraction on the mechanical properties of epoxy-clay nanocomposites. Journal of Materials Science 2006; 41: 2219–2228.

Web references

- http://nptel.ac.in/ (visited on 19th March, 2015)
- http://www.sigmaaldrich.com/ (downloaded on 19th October, 2015)
- http://www.ika.com/Dispersing_appl-5.html (visited on 28th November, 2015)
- http://www.sonicator.com/literature/how-it-works.shtml (visited on 23rd March, 2016)
- http://www.remilabworld.com/Direct_Drive_Stirrers.asp (visited on 23rd March, 2016)
- http://www.macroscientificworks.com/ovens-incubators8.html#ove8 (visited on 17th November, 2015)
- http://www.indutch.in/products.html (visited on 25th March, 2016)
- http://ipelican.com/en/131570 (visited on 11th April, 2016)
- http://senselektro.hu/wp-content/uploads/zwick/ProLine.pdf (downloaded on 30th January, 2016)
- http://www.atsfaar.it/ (visited on 24th December, 2015)
- http://www.panalytical.com/XPert3-Powder/Specifications.htm (visited on 19th January, 2016)
- http://www.hitachi.com/ (visited on 15th April,2016)
- http://www.jeol.com (visited on 15th November, 2015)